UNIVERSITY OF CALIFORNIA
RIVERSIDE

Purification and Processing of Graphitic Carbons

A Dissertation submitted in partial satisfaction
of the requirements for the degree of

Doctor of Philosophy

in

Chemistry

by

Kimberly Anne Worsley

December 2010

Dissertation Committee:
Dr. Robert C. Haddon, Chairperson
Dr. Pingyun Feng
Dr. Michael Marsella

The Dissertation of Kimberly Anne Worsley is approved:

_____

_____

_____

Committee Chairperson

University of California, Riverside

ACKNOWLEDGMENTS

I would like to acknowledge the support of my principle investigator, Dr. Robert Haddon. Through his guidance and knowledge I was able to achieve this life-long goal, while gaining experience unexpectedly in many fields of science. As well as organic chemistry, I studied physical chemistry, material processing, chemical engineering and physics. This is an extremely rare opportunity during a graduate career, and it enriched my knowledge of what it takes to be on the cutting edge of technology in academia, as well as in industry in this generation.

One of the greatest luxuries of working for Dr. Haddon is working with his group. His group, consisting mainly of post doctorates, travel from all over the world to work in his lab, bringing their expertise in various fields. As a graduate student I was able to benefit from their experience and hard work ethic. One day in lab, I received a call from someone that spoke Cantonese. Not understanding what was said, I was able to find someone in lab that could communicate. I realized at that time, that virtually anyone in the world could call our lab and would reach someone that would be able to speak with them. Besides English, our lab can communicate in French, Spanish, Russian, Bulgarian, Ukrainian, German, Cantonese, Mandarin, Japanese, as well as several Indian dialects. I consider myself to be extremely fortunate to have worked in such a wonderful environment. I would like to thank Elena Bekyarova and Misha Itkis who were always available when I needed them. They are wonderful people to work with and are the

backbone of the group. Ramesh Palanisamy was also a tremendous help. I could not have made it through without his guidance and knowledge. I would also like to express thanks to Irina Kalinina, Xiaobo Sun, Aiping Yu and Jason Tang for their support and friendly advice. Swadhin Mandal, Arindam Sarkar, Pradip Bag, and Sushanta Pal, as part of the Neutral Radical Group, assisted me on several occasions with questions in what I would consider to be true organic chemistry. I would also like to acknowledge the support of the staff of the Center for Nanoscale Science & Engineering (Nancy Jahr, Amanda Adame, Eva Barriga, Carla Reyes, Andrea Odio, and Nadine Okuns). Without them, I would have been without the essential tools to perform my research.

Within the Department of Chemistry, I would like to express gratitude towards my dissertation committee members, Dr. Pingyun Feng, and Dr. Michael Marsella. I appreciate the time taken to undergo the nessesary steps to complete my thesis and defense. Also, I would like to acknowledge the altruistic work preformed by the Chemistry Graduate Student Association, a group that I was apart of for most of my graduate career. I would like to recognise Stacie L. Eldridge, Theresa Massoud, Tony Ly, and Kayla Kaiser, who continually put in the extra effort and always leave their surroundings in a better condition than they found them.

Lastly, I would like to thank the publishers of the journals in which I've published for granting me permission to reprint material in my dissertation. Reprinted from Chemical Physics Letters, Vol. 445, by Kimberly A. Worsley,

Palanisamy Ramesh, Swadhin K. Mandal, Sandip Niyogi, Mikhail E. Itkis and Robert C. Haddon, “Soluble graphene derived from graphite fluoride.” pgs 51-56, Copyright 2007, with permission from Elsevier. Reproduced in part with permission from Kimberly A. Worsley, Irina Kalinina, Elena Bekyarova, Robert C. Haddon, “Functionalization and Dissolution of Nitric Acid Treated Single-Walled Carbon Nanotubes.” *Journal of the American Chemical Society,* **2009**, 131 (50), pp 18153–18158. Copyright 2009 American Chemical Society.

This research was made possible by the financial support of DOD/DMEA and partly by the National Science Foundation and the Environmental Protection Agency.

DEDICATIONS

I would like to dedicate this dissertation to Eli, James, Susan, John, Shelley and Mike. Thanks for your love and support.

ABSTRACT OF THE DISSERTATION

Purification and Processing of Graphitic Carbons

by

Kimberly Anne Worsley

Doctor of Philosophy, Graduate Program in Chemistry
University of California, Riverside, December 2010
Dr. Robert C. Haddon, Chairperson

Carbon materials exist in several forms and have a wide range of applications that are commonly encountered in everyday life. The more familiar applications range from car tires to cosmetics. The breadth of applications is solely due to the various graphitic and amorphous structures of carbon, which gives rise to a wide range of properties that can be engineered to obtain the desired feature or function. Allotropes of carbon include diamond, fullerenes, graphite (graphene) and carbon nanotubes. The latter two are the focus of this dissertation and their characterization, purification, and functionalization will be described in detail.

High solubility of purified single-walled carbon nanotubes (SWNTs) and graphene is desired for their utilization in various applications. In the case of SWNTs, concentrated nitric acid treatment is the most common form of purification currently used. It is highly effective in the removal of residual metal catalysts, but generates unwanted carbonaceous byproducts known as carboxylated carbons (CCs). Little is known about the nature of these species (CCs), and it is has been

suggested that because of their high carboxylic acid functionality and their adhesion to the SWNT side wall, that upon functionalization of an oxidized nanotube sample, the majority of the functionalization is occurring on the CCs and not the SWNTs, and that upon their removal, the SWNTs are rendered insoluble. Similar to SWNTs, soluble graphene is desirable to achieve facile manipulation of the material for device applications although the exfoliation of graphite to form a single layer has proven to be challenging.

In this dissertation, the characterization of the CCs will be discussed and upon their removal, it is demonstrated that solubility of the purified SWNTs is retained upon covalent functionalization with octadecylamine (ODA). Soluble graphene layers were formed by reacting graphite fluoride with alkyl lithium reagents. Functionalized graphene can be readily prepared by this technique and dispersed in organic solvent and upon annealing, the intrinsic properties can be partially restored. This dissertation serves to extend the achievements previously developed by the Haddon research group and adds to the continued progress in the advancement of carbon materials chemistry.

TABLE OF CONTENTS

LIST OF FIGURES AND TABLES

Figure *Page*

Table *Page*

LIST OF ACRONYMS

AC	Amorphous Carbon
AFM	Atomic Force Microscope
AP-SWNT	As-prepared Single-Walled Carbon Nanotube
CACs	Carboxylated Amorphous Carbons
CCFs	Carboxylated Carbonaceous Fragments
CCs	Carboxylated Carbons – CCFs and CACs combined
CNP	Carbon Nanoparticles
CVD	Chemical Vapor Deposition
DMF	N,N-Dimethylformamide
EA	Electric Arc-Discharge
HC	Hydrocarbon
HOPG	Highly Oriented Pyrolytic Graphite
HPLC	High Performance Liquid Chromatography
IR	Infrared
LA	Laser Ablation
MWNT	Multi-Walled Carbon Nanotube
ODA	Octadecylamine
SEM	Scanning Electron Microscopy
SWNT	Single-Walled Carbon Nanotube
SWNT-COOH	Nitric Acid Treated Single-Walled Carbon Nanotube
TEM	Transmission Electron Microscopy
TGA	Thermogravimetric Analyzer
XRD	X-Ray Diffraction

Chapter 1

Introduction to Graphitic Carbon Materials

There are a number of allotropes of carbon as a result of the three possible limiting hybridizations: sp, sp^2, and sp^3 together with various intermediate hybridizations which become important in distorted structures. Linear chain polymeric carbynes and tetrahedral diamond structures are formed from sp and sp^3 hybridization respectively. Of more interest and the focus of this work, sp^2 hybridization gives rise to planar structures that can exist in several different forms and are referred to as graphitic carbon materials. Such structures involve a hexagonal network of carbon atoms in a one atom thick graphene sheet molded into spherical, conical, tubular, or stacked arrangements.

Fullerenes,[1] nanohorns,[2] graphite (graphene),[3, 4] and carbon nanotubes[5] and their hexagonal, honey-comb framework are shown in Figure 1.1:

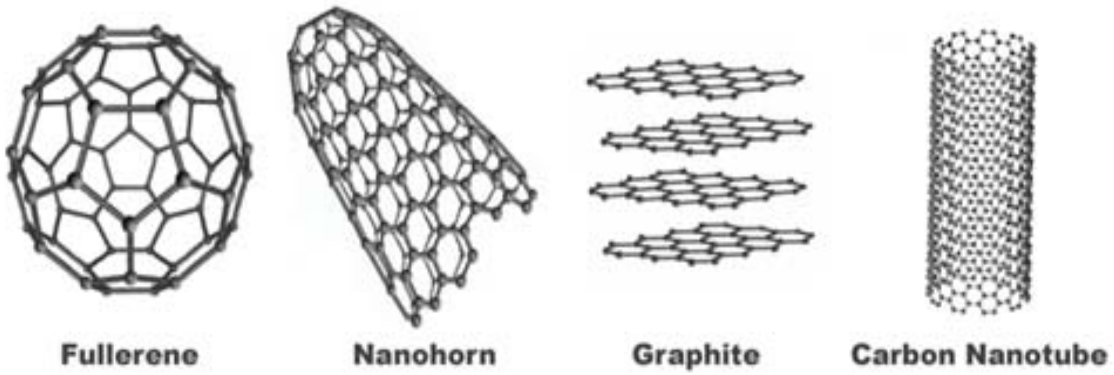

Figure 1.1: Graphitic Carbon Structures

The sp^2 lattice in each structure gives rise to unique electronic and thermal properties as well as high tensile strengths. It is the shape and electronic structure of these materials that distinguishes them for use in various applications. Fullerenes, being similar in structure to a soccer ball, can be doped with alkali metals to form a superconducting crystalline material.[6, 7] Nanohorns, resembling a cornucopia, have been utilized as an efficient gas-storing media.[8] Graphite, composed of sheets of graphene, have been exploited in composites yielding light-weight materials having exceptionally high thermal conductivity.[9] Carbon nanotubes are seamless cylinders of graphene, open at the termini or with half fullerene caps at each end (seen in Figure 1.3). They are sometimes referred to as "nanowires" and are used in various devises such as field effect transistors (FETs)[10-12] and gas sensors.[13, 14]

The preparation of various forms of carbon nanotubes and graphite has been the focus of my research. Optimization of the purification and processing of

these materials is essential in the development of useful applications for these materials as discussed earlier.

1.1 Single-Walled Carbon Nanotubes (SWNTs)

Carbon nanotubes have been observed as single- and multi-walled structures. As seen in Figure 1.2, multi-walled carbon nanotubes (MWNTs) are composed of over-lapping layers of single-walled carbon nanotubes (SWNTs) (depicted in Figure 1.1).

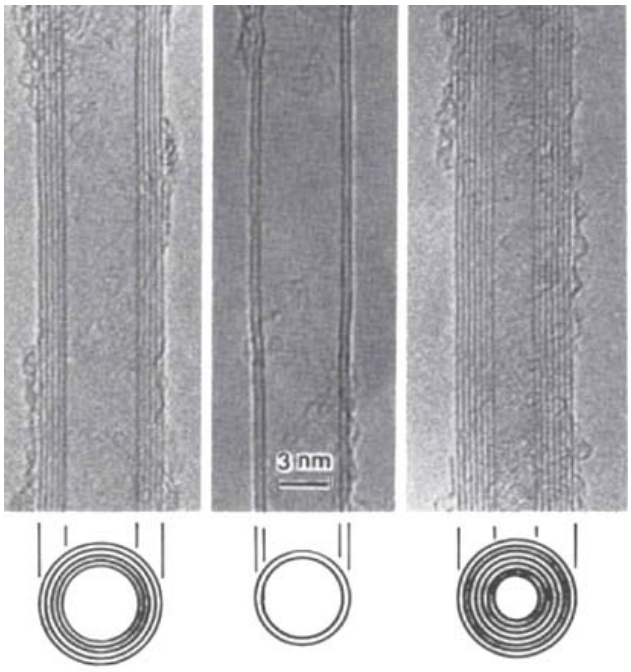

Figure 1.2: TEM images of MWNTs.[15] From left to right: 5, 2 and 7 walls.

Nanotube lengths can exceed 1 μm with typical diameters ranging from 1 to 2 nm and from 2 to 30 nm for SWNTs and MWNTs, respectively. Their electronic properties may be attributed to the diameter and chirality of the hexagonal lattice, which designates the way in which the graphene sheet is rolled into the tubular structure. Possible conformations include armchair, zigzag, and screw axis (chiral) SWNTs (Figure 1.3). Each chirality is denoted by a pair of integers (n,m), (Figure 1.4) which are related to a_1 and a_2, which are the 2D lattice unit vectors. An armchair tubule occurs when the value of n equals m. A zigzag tubule occurs when n or m equals zero. A screw axis tubule occurs for values of n and m that do not satisfy the requirements for the armchair and zigzag structures. The value of n and m can also indicate whether the nanotube is metallic ($n - m = 3q$, $q = 0, 1, 2, \ldots$) or semiconducting ($n - m = 3q \pm 1$, $q = 0, 1, 2, \ldots$).[16, 17] It is these characteristics that give carbon nanotubes their intrinsic properties and which ultimately determines the possible applications.

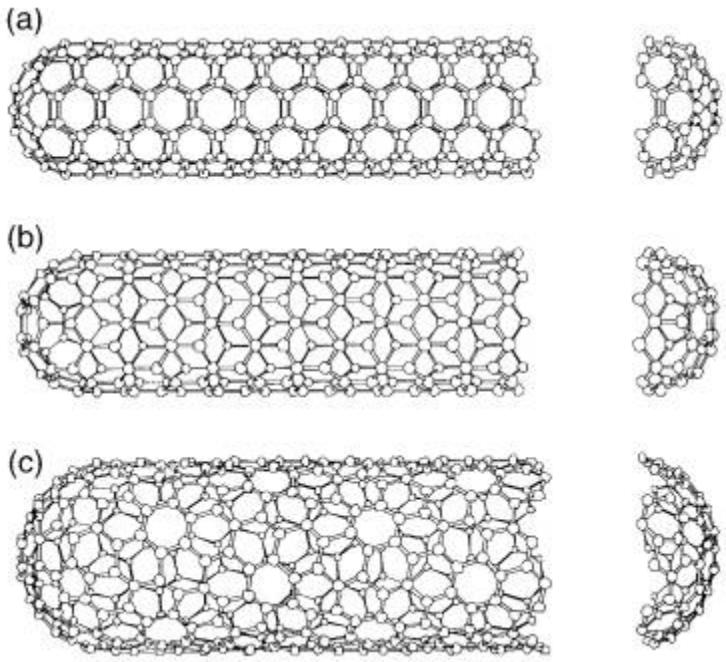

Figure 1.3: (a) Armchair, (b) zigzag, and (c) screw axis structures of SWNTs.[16]

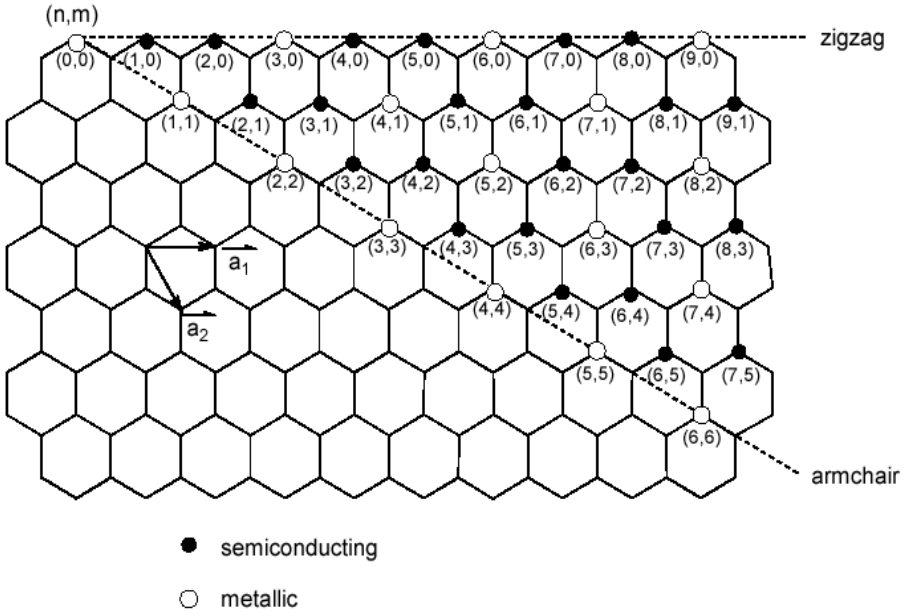

Figure 1.4: The lattice structure of a graphene sheet depicting the axes of the possible chiralities, their (*n,m*) integers and semiconducting or metallic behaviour.[16]

1.1.1 Synthesis

For the utilization of SWNTs in applications, it is important to optimize their production. Industry requires high quality nanotubes in bulk quantities hopefully by using cost effective, high yield simple growth methods. To date, the large-scale synthesis of defect free nanotubes with controlled chirality and macroscopic lengths has been unattainable. Current methods involve the exposure of a carbon source to a variety of environments which include high temperatures or pressures in an inert atmosphere and in the presence of metal catalysts. Such methods include electric arc-discharge (EA),[18, 19] laser ablation (LA),[19-22] and chemical vapor deposition (CVD).[23-25] The basic schematics of each technique is given in Figure 1.5:

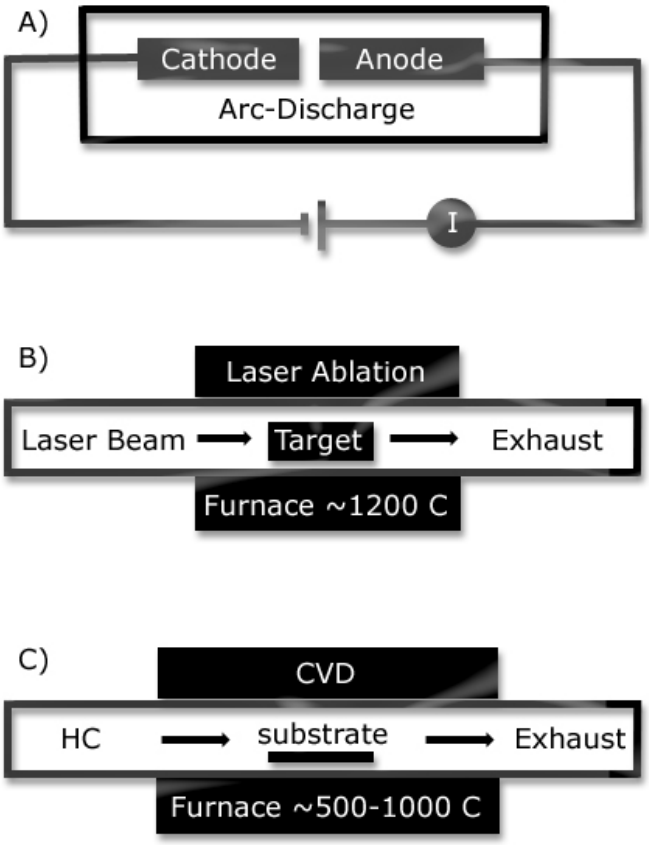

Figure 1.5: Schematic of A) Arc-discharge, B) laser ablation, and C) CVD apparatus for carbon nanotube synthesis.

Using the EA method (Figure 1.5a), carbon nanotubes are generated by evaporating a carbon anode in a helium plasma formed by high currents. This method produces high quality single- and multi-walled carbon nanotubes on a gram scale.[26, 27]

Similar to the EA method, LA (Figure 1.5b), also involves the condensation of carbon generated from the evaporation of a solid carbon source. In this case, a pulsed laser is used to irradiate a target containing both carbon and metal catalysts, such as cobalt and nickel, in a furnace at high

temperatures.[28] The carbon nanotubes that form are condensed as they exhaust through the apparatus. Laser-fabricated tubes are of the quite high quality, but in general, the yields are relatively low.

In CVD (Figure 1.5c), a hydrocarbon (HC) is passed through a furnace containing metal catalysts such as nickel, cobalt, and iron.[24, 29, 30] Some examples of the HCs used are methane, acetylene and carbon monoxide.[31, 32]

In all cases, unwanted by-products are formed. These include fullerenes, amorphous carbon, carbon nanoparticles, and metal catalysts enclosed in shelled carbon particles. Each technique can be optimized by varying the pressure, temperature, carbon source and catalysts to minimize these impurities, however, further processing is required to increase the purity.

1.1.2 Characterization

Due to the varying qualities of carbon nanotube samples and the presence of impurities, it is important to assess the purity. Techniques such as near-IR and Raman spectroscopy and thermogravimetric analysis (TGA) can give semi-quantitative measurements that compare the relative purities of the samples. Other techniques that give qualitative data include scanning electron microscopy (SEM), transmission electron microscopy (TEM) and atomic force microscopy (AFM).

Using solution phase near-IR spectroscopy, the relative purity of EA produced SWNT samples dispersed in N,N-dimethylformamide (DMF) can be

quantitatively measured.[33, 34] As seen in Figure 1.6, the absorption observed is due to the contribution of both the SWNTs and their carbonaceous impurities. It is the distinct interband transitions (seen in blue in Figure 1.6) that are characteristic of semiconducting and metallic SWNTs and the intensity of these peaks can provide a measure of the purity of the sample.

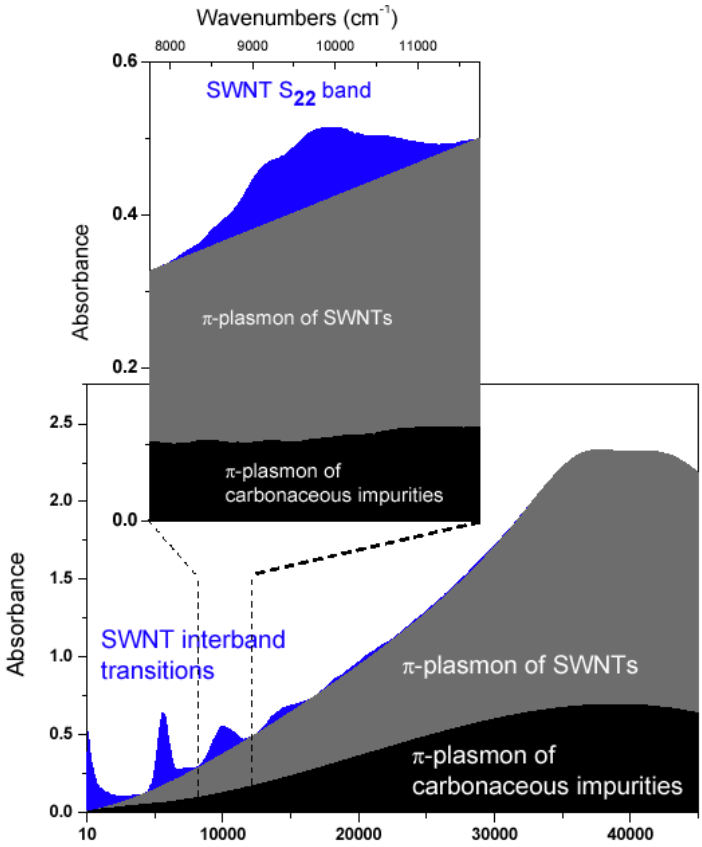

Figure 1.6: Schematic of a near-IR spectrum of EA produced SWNTs showing the interband transitions. Inset is a close-up of the S_{22} peak used to calculate the relative purity.[34]

In order to calculate the relative purity (*RP*), the ratio of the areal absorbance of the second semiconducting interband transition, denoted as S_{22} (with spectral

cutoffs = 7750 to 11 750 cm^{-1}),[35] is compared to that of reference sample in the following equation:

$$RP = \frac{AA(S,X)/AA(T,X)}{AA(S,R)/AA(T,R)} \quad (1)$$

where *AA(S,X)* is the areal absorbance of the S_{22} peak of sample *X* after baseline correction (blue area in inset of Figure 1.6), *AA(T,X)* is the total areal absorbance of the S_{22} peak (blue, gray and black area in the inset of Figure 1.6) of sample *X*, *AA(S,R)* is the areal absorbance of the S_{22} peak of the reference sample after baseline correction, and *AA(T,R)* is the total areal absorbance of the S_{22} peak of the reference sample. The value of *AA(S,R)/AA(T,R)* of reference sample R2 is 0.141, which is considered to be a material of high purity.[35] This method allows for a facile, quantitative analysis using material in solution phase that is representative of the total, bulk sample.

Raman scattering of SWNTs also is a useful tool in semi-quantitatively assessing the quality of a sample. Features observed are the low frequency radial breathing mode (RBM), and the high frequency D- and G-bands (Figure 1.7). The RBM is typically located in the range of 100 to 300 cm^{-1} and can be used to determine the diameter of the SWNTs present in the sample.[36] The D-band appears around 1300 cm^{-1}, is associated with disordered sp^3 hybridized carbon from defect sites and impurities and for this reason, is commonly referred to as the disorder band. The G-band, or graphitic band is associated with sp^2 hybridized carbon, and appears around 1600 cm^{-1}. The ratio of the intensities of

the D- and G-band, I_D/I_G, gives an alternative method for evaluating the purity of a SWNT sample.[37]

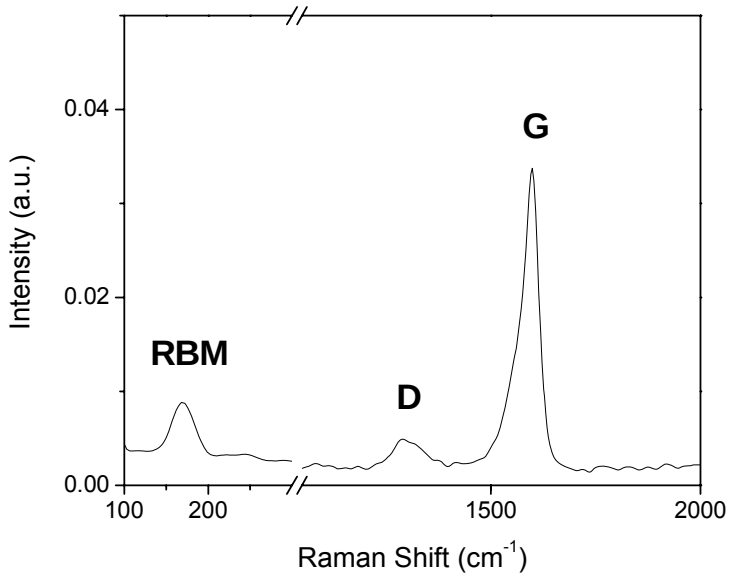

Figure 1.7: Typical Raman spectrum of EA produced SWNTs.

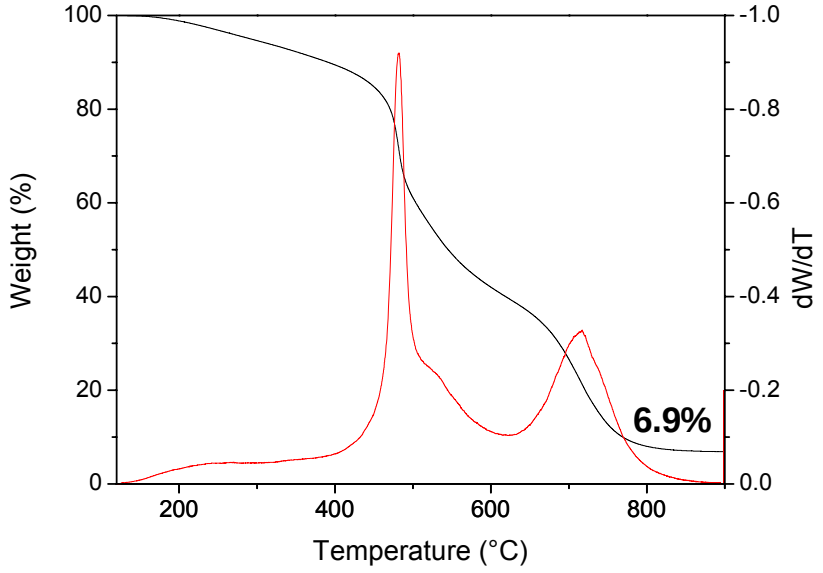

Figure 1.8: Typical TGA measurements showing weight change (black line) and its derivative (red), together with residual metal oxide (6.9%).

TGA (Figure 1.8) is a technique that directly gives a measure of the purity of the carbon sample. In this case, it is not the quality of the graphene lattice of the nanotubes that is observed, but the amount of metal catalyst residing in the sample. Typical measurements use around 5 mg of homogenized material and proceed at a heating rate of 5 ˚C/min in air.[38, 39] The derivative of the weight (red line in Figure 1.8) gives rise to peaks that are associated with the combustion temperatures of the various forms of carbon present. Lower burning temperatures are usually associated with amorphous carbon, while the larger graphitic structures oxidize at higher temperatures.[40] Quantitative data from this observation is not easily obtained, however, due to the magnitude of possible structures in the mult-component material and the overlap in peaks resulting in difficult deconvolution by Lorentzian or Gaussian fittings.[34] By reaching temperatures of 900 ˚C or more, the fraction of oxidized metal catalyst is found and is reduced by 20% to account for the amount of oxygen present in the pyrolized residue.

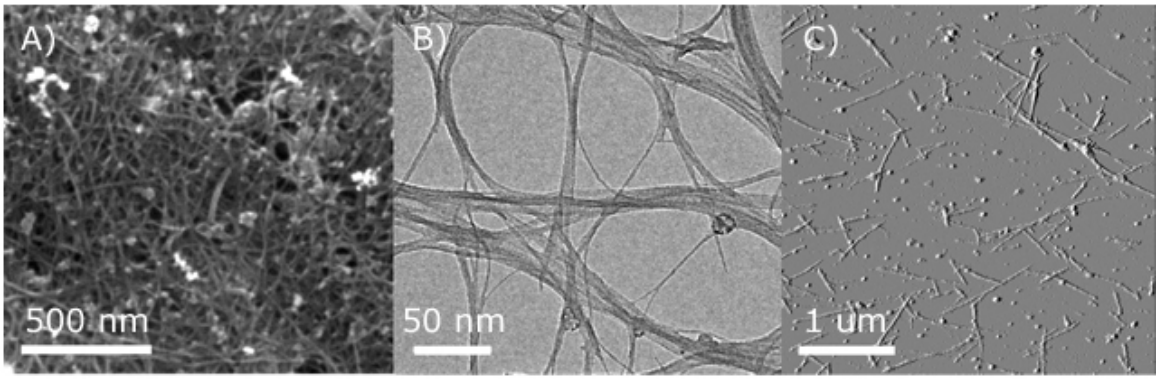

Figure 1.9: A) TEM, B) SEM, and C) tapping mode AFM images of purified SWNTs.

SEM, TEM and AFM are powerful tools that directly image the quality of carbon samples. As seen in Figure 1.9, images show long, interweaving tubes with clusters of amorphous particle impurities at different scan sizes. In industry, many companies that synthesize nanotubes erroneously offer these images as evidence of purity. Samples can be imaged to exclude carbon impurities and metal catalysts due the inhomogeneity of the material. Another serious drawback to microscopy is that these images are estimated to show less than 10^{-12} g of material, and are not representative of a 10 g batch of material.[34, 35]

1.1.3 Purification

All techniques described in Section 1.1.1 produce soot, which consists of SWNTs and impurities. These impurities in the as-prepared materials (AP-SWNTs) are comprised of fullerenes, residual metal catalysts and carbonaceous byproducts including amorphous carbon (AC) and graphitized carbon

nanoparticles (CNP). Several methods have been utilized to purify these materials, including oxidative procedures, and physical separation.

Some oxidative procedures include combining AP-SWNTs with combinations of reagents and concentrated acids such as H_2O_2,[41, 42] HCl,[42] H_2SO_4,[43, 44], and HNO_3[45] at various temperatures and for a wide array of reaction times. In some studies, microwave heating[46, 47] or sonication[48] is employed. These treatments effectively remove metal catalysts, and in the case of HNO_3, introduce acid functionality at termini and defect sites of the nanotube that can be further functionalized to improve solubility.[49]

Purification by physical separation of SWNTs from their impurities has been successfully employed after treatment with HNO_3 and other processing. These treatments include cross-flow filtration,[45, 50] high performance liquid chromatography (HPLC),[51, 52] and centrifugation.[53, 54] Although progress is seen by purity evaluations such as near-IR, Raman spectroscopy, and TGA, a pure SWNT sample has not been easily obtained on any useful scale.

1.1.4 Functionalization

As discussed earlier, carbon nanotubes exhibit many exceptional properties that make them an ideal material in various applications. However, their lack of solubility in aqueous and organic solvents limits their exploitation. Although SWNTs can be dispersed in solvents such as DMF, upon standing, precipitation occurs. Modifying the material by producing supramolecular

complexes is often an essential step in the preparation of workable material. Modifications include covalent or ionic functionalization on the termini or basal plane of the nanotube, and non-covalent adsorption by macromolecules or surfactants along the basal plane or inner cavity.

Covalent and ionic functionalization of carbon nanotubes has been widely explored and is often modeled after work that has been previously preformed on fullerenes. Functional groups are tailored to optimize the material for the intended application, and by converting from sp^2 to sp^3 hybridization, the electronic properties are altered leading to semiconducting material. Sidewall functionalization results in a high loading of functional groups, and examples include fluorination,[55, 56] carbene cycloadditions,[57-59] and radical reactions.[60, 61]

Nitric acid treatment of carbon nanotubes not only purifies the nanotube, but also provides oxygenated functionality at the termini and defect sites that can be used as anchors for further functionalization. As seen in Figure 1.10, the end cap of the nanotube is oxidized resulting in carboxylic acid functionalization. Amidation and esterification reactions are preformed directly on carboxylic acid groups or via the acyl chloride (Figure 1.10).[49, 62-64]

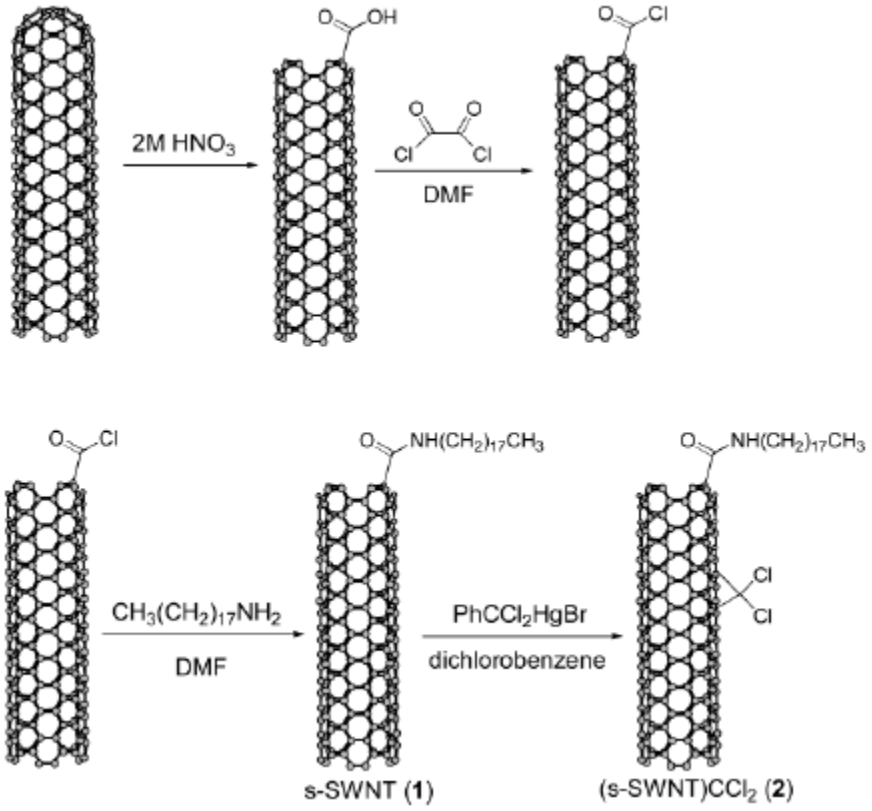

Figure 1.10: Schematic depicting: (1) ODA functionalization of termini via nitric acid purification followed by (2) sidewall functionalization of SWNTs by the addition of dichlorocarbene.[59]

Wrapping molecules and surfactants aid in the dispersion and exfoliation by providing a compatible interface between the nanotube wall and the solvent without altering the desired electronic properties. These macromolecules are ionic, polymeric or biological and are selected based on application and can be easily removed by simple washing or burning techniques if required. Some examples include sodium dodecyl sulfate (SDS),[65] poly(ethylene glycol),[66] and DNA.[67]

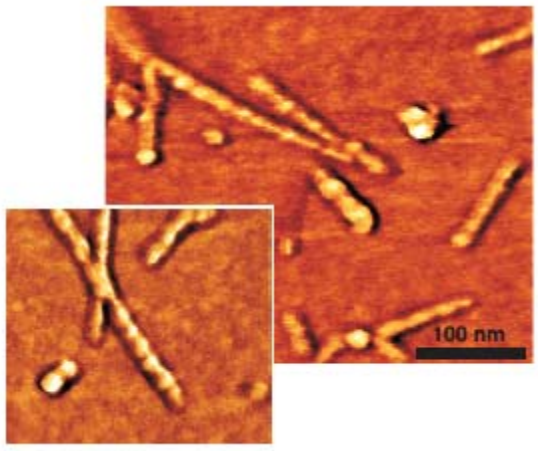

Figure 1.11: AFM of single stranded DNA-wrapped SWNTs.[67]

1.2 Graphite

Graphite is a 3-dimensional lattice consisting of layers of carbon atoms in aromatic, sp^2 hexagonal planar arrays. A single layer is separated from its neighbor by a distance of approximately 0.34 nm, and is commonly referred to as graphene. The cohesive properties of the graphene layers are due to weak van der Waals interactions. It is the structure of this carbon allotrope that gives graphene its high mechanical, thermal and chemical stability resulting in a wide range of possible device fabrication in microelectronics.[68-70]

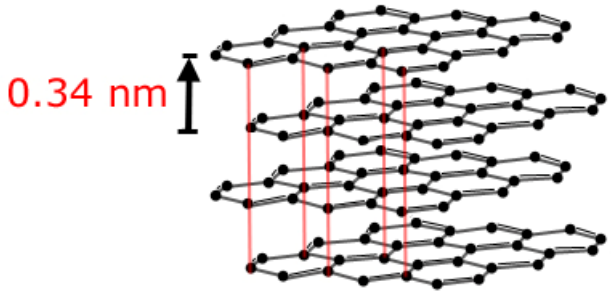

Figure 1.12: Schematic of the structure of graphite. Hexagonal ABAB stacking (indicated by the vertical lines) of graphene layers with an intermolecular spacing of 0.34 nm.

1.2.1 Production and Synthesis

Graphite is produced synthetically and is also a naturally occurring material. Depending on the origin, the lateral size and thickness as well as the crystallinity can vary. Natural graphite is mined in several parts of the world in the form of large flakes (> 1 mm) with superior crystallinity. Highly oriented pyrolytic graphite (HOPG) is a synthetic graphite that is produced by cracking a hydrocarbon at high temperature and pressures with subsequent heat treatment. It is undoubtedly the most common graphite utilized in research.[71] Another type of synthetic graphite is "kish" graphite. It is produced by the crystallization of carbon from molten steel during steel manufacturing and is generally larger than natural graphite flakes, although the crystallinity is not as high.[71]

1.2.2 Characterization

Two important instruments which used to characterize graphite are Raman scattering and X-ray diffraction (XRD). Raman scattering is used as described in Section 1.1.2 for assessing the purity of SWNTs. The I_D/I_G ratio is related to the magnitude of the disorder in the material. The frequency of the G-band also is an indication of the extent of sp^2 character. Higher Raman shifts are observed for more extended π-systems.[72]

XRD is a useful tool for determining the interlamellar space between graphene sheets. The typical distance is 0.34 nm for hexagonal ABAB graphite, but higher values are observed for disordered turbostratic or intercalated graphite.

1.2.3 Chemical Processing and Exfoliation

Exfoliation of the graphite layers is necessary to acquire low density, high aspect ratio (surface area to thickness) materials that are desirable for the fabrication of nanocomposites and in electronic devices. A one-atom thick graphene layer would be an ideal material due to its light weight, high strength and extensive surface area. Separation of the graphene layers may be accomplished by intercalation with alkali metals[73] or inorganic acids[74] followed by exfoliation at high temperatures. Typically, graphite is soaked in nitric or sulfuric acid and is allowed to stand for extended periods of time. During this time, the acid molecules penetrate the sample altering the distance between the layers,

and functionalizing the edges of the graphite. Alkali metals can also be used to intercalate the layers. Exfoliation occurs at high temperatures, or as recently reported by Viculis *et. al.*, in ethanol.[75] Aqueous solvents, such as ethanol react vigorously with alkali metals and will exfoliate the graphene layers at room temperature. As seen in Figure 1.13, addition of ethanol produces potassium ethoxide and hydrogen gas which aid in the separation of the graphene layers resulting in dispersed nanoplatelets of 2–10 nm in thickness.[75]

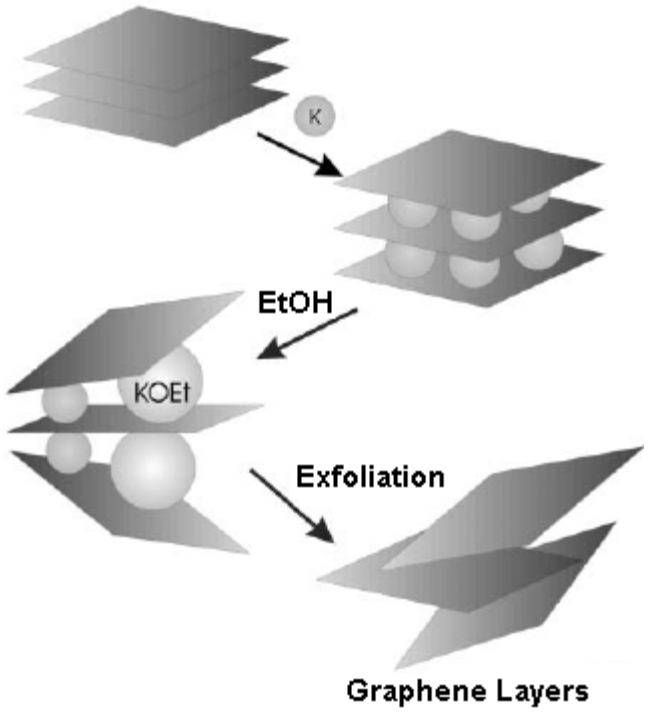

Figure 1.13: Exfoliation of graphite.[75]

1.2.4 Functionalization

Similar to carbon nanotubes, the solubility of exfoliated graphite is important. Due to the extensive sp^2 lattice the material is difficult to dissolve, and is therefore difficult to manipulate for direct application purposes. Solubility through a variety of functionalization procedures has been achieved for carbon nanotubes,[76, 77] and fullerenes,[78, 79] and therefore it is logically expected that the same procedures could be extended to single graphene sheets. Functionality can occur on the basal plane as seen in the formation of graphite oxide,[80] or along the periphery.[4] As well as improving the solubility of the material, both functionalization types prevent the re-aggregation and scrolling of the graphene layers.

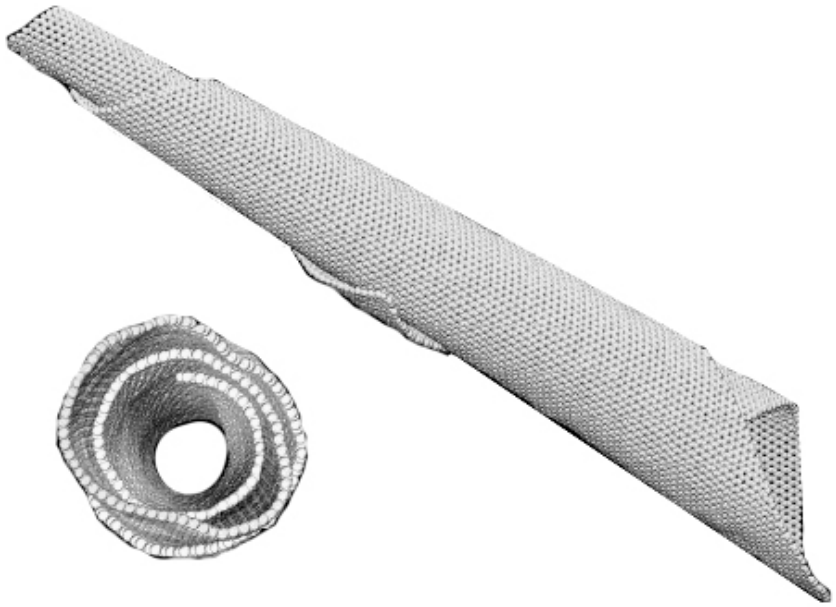

Figure 1.14: Graphene nanoscroll.[81]

1.3 Summary

Graphitic carbon materials, by definition, are carbon materials with varying contributions of the graphene structure. They share a sp^2 hybridized framework that gives rise to outstanding properties that can be exploited in many applications. The focus of this dissertation is the preparation and processing of carbon nanotubes and graphite for device application purposes. Although further progress is necessary for the utilization of these materials in an industrial manner, this study serves as an important contribution by my group in the advancement of this area of nanotechnology.

1.4 References

1. Kroto, H. W.; Heath, J. R.; O'Brien, S. C.; Curl, R. F.; Smalley, R. E., C60: Buckminsterfullerene. *Nature* **1985,** 318, 162-164.

2. Bekyarova, E.; Hanzawa, Y.; Kaneko, K.; Silvestre-Albero, J.; Sepulveda-Escribano, A.; Rodriguez-reinoso, F.; Kasuya, D.; Yudasaka, M.; Iijima, S., Cluster-Mediated Filling of Water Vapor in Intratube and Interstitial Nanospaces of Single-Wall Carbon Nanohorns. *Chem. Phys. Lett.* **2002,** 366, 463-468.

3. Geim, A. K.; S., K. N., The Rise of Graphene. *Nat. Mater.* **2007,** 6, 183-191.

4. Niyogi, S.; Bekyarova, E.; Itkis, M. E.; McWilliams, J. L.; Hamon, M. A.; Haddon, R. C., Solution Properties of Graphite and Graphene. *J. Am. Chem. Soc.* **2006,** 128, (24), 7720-7721.

5. Dresselhaus, M. S.; Dresselhaus, G.; Avouris, P., *Carbon Nanotubes: Synthesis, Structure, Properties and Applications*. Springer-Verlag: Berlin, 2001; Vol. 80.

6. Haddon, R. C., Electronic Structure, Conductivity and Superconductivity in Alkali Metal Doped C60. *Acc. Chem. Res* **1992,** 25, 127.

7. Murphy, D. W.; Hebard, A. F.; Haddon, R. C., Synthesis and Properties of Fullerene Superconductors. In *Processing and Properties of High-Tc Superconductors, Vol* World Scientific Press: 1992; p 409.

8. Bekyarova, E.; Kaneko, K.; Kasuya, D.; Takahashi, K.; Kokal, F.; Yudasaka, M.; Iijima, S., Pore Structure and Adsorption Properties of Single-Walled Carbon Nanohorn Bud-Like Aggregates Treated in Different Atmospheres. *Physica B* **2002,** 323, 143-145.

9. Yu, A.; Ramesh, P.; Sun, X.; Bekyarova, E.; Itkis, M. E.; Haddon, R., Enhanced Thermal Conductivity in a Hybrid Grpahite Nanoplatelet - Carbon Nanotube Filler for Epoxy Composites. *Adv. Mater.* **2008,** 20, 4740-4744.

10. Martel, R.; Schmidt, T.; Shea, H. R.; Hertel, T.; Avouris, P., Single- and Multi-Wall Carbon Nanotube Field-Effect Transistors. *Appl. Phys. Lett* **1998,** 73, 2447-9.

11. Javey, A.; Guo, J.; Wang, Q.; Lundstrom, M.; Dai, H., Ballistic Carbon Nanotube Field-Effect Transistors. *Nature* **2003,** 424, 654-657.

12. Star, A.; Gabriel, J.-C. P.; Bradley, K.; Gruner, G., Electronic Detection of Specific Protein Binding Using Nanotube FET Devices. *Nano Lett.* **2003,** 3, (4), 459-463.

13. Kong, J.; Franklin, N. R.; Zhou, C.; Chapline, M. G.; Peng, S.; Cho, K.; Dai, H., Nanotube Molecular Wires as Chemical Sensors. *Science* **2000,** 287, 622-625.

14. Modi, A.; Koratkar, N.; Lass, E.; Wei, B.; Ajayan, P. M., Miniaturized Gas Ionization Sensors Using Carbon Nanotubes. *Nature* **2003,** 424, 171-174.

15. Iijima, S., Helical Microtubules of Graphitic Carbon. *Nature* **1991,** 354, 56-58.

16. Dresselhaus, M. S.; Dresselhaus, G.; Eklund, P. C., *Science of Fullerenes and Carbon Nanotubes*. Academic: San Diego, 1996.

17. Saito, R.; Dresselhaus, G.; Dresselhaus, M. S., *Physical Properties of Carbon Nanotubes*. Imperial College Press: Singapore, 1998.

18. Iijima, S.; Ichihashi, T., Single-Shell Carbon Nanotubes of 1-nm Diameter. *Nature* **1993,** 363, 603-605.

19. Journet, C.; Maser, W. K.; Bernier, P.; Loiseau, A.; Lamy de la Chappelle, M.; Lefrant, S.; Deniard, P.; Lee, R.; Fischer, J. E., Large Scale Production of Single-Walled Carbon Nanotubes by the Electric-Arc Technique. *Nature* **1997,** 388, 756-758.

20. Guo, T.; Nikolaev, P.; Thess, A.; Colbert, D. T.; Smalley, R. E., Catalytic Growth of Single-Walled Nanotubes by Laser Vaporization. *Chem. Phys. Lett.* **1995,** 243, 49-54.

21. Zhang, Y.; Gu, H.; Iijima, S., Single-Wall Carbon Nanotubes Synthesized by Laser Ablation in a Nitrogen Atmosphere. *Appl. Phys. Lett.* **1998,** 73, (26), 3827-3829.

22. Arepalli, S., Laser Ablation Process for Single-Walled Carbon Nanotube Production. *J. Nanosci. Nanotechnol.* **2004,** 4, (4), 317-325.

23. Dai, H.; Rinzler, A. G.; Nikolaev, P.; Thess, A.; Colbert, D. T.; Smalley, R. E., Single-Wall Nanotubes Produced by Metal-Catalyzed Disproportionation of Carbon Monoxide. *Chem. Phys. Lett.* **1996,** 260, 471-475.

24. Cassel, A. M.; Raymakers, J. A.; Kong, J.; Dai, H., Large Scale CVD Synthesis of Single-Walled Carbon Nanotubes. *J. Phys. Chem. B* **1999,** 103, (31), 6484-6492.

25. Harutyunyan, A. R.; Pradhan, B. K.; Kim, U. J.; Chen, G.; Eklund, P. C., CVD Synthesis of Single Wall carbon nanotubes under "Soft" Conditions. *Nano Lett.* **2002,** 2, 525-530.

26. Ebbesen, T. W.; Ajayan, P. M., *Nature* **1992,** 358, 220.

27. Bethune, D. S.; Kiang, C. H.; de Vries, M. S.; Gorman, G.; Savoy, R.; Vazquez, J.; Bevers, R., Cobalt-Catalized Growth of Carbon Nanotubes with Single-Atomic-Layer Walls. *Nature* **1993,** 363, 605-607.

28. Thess, A.; Lee, R.; Nikolaev, P.; Dai, H.; Petit, P.; Robert, J.; Xu, C.; Lee, Y. H.; Kim, S. G.; Rinzler, A. G.; Colbert, D. T.; Scuseria, G. E.; Tomanek, D.; Fischer, J. E.; Smalley, R. E., Crystalline Ropes of Metallic Carbon Nanotubes. *Science* **1996,** 273, 483-487.

29. Kong, J.; Cassell, A. M.; Dai, H., Chemical Vapor Deposition of Methane for Single-Walled Carbon Nanotubes. *Chem. Phys. Lett.* **1998,** 292, 567-574.

30. Franklin, N. R.; Dai, H., An Enhanced CVD Approach to Extensive Nanotube Networks with Directionality. *Adv. Mater.* **2000,** 12, 890-894.

31. Hafner, J. H.; Bronikowski, M. J.; Azamian, B. R.; Nikolaev, P.; Rinzler, A. G.; Colber, D. T.; Smith, K. A.; Smalley, R. E., Catalytic Growth of Single-Wall Carbon Nanotubes from Metal Particles. *Chem. Phys. Lett.* **1998,** 296, 195-202.

32. Nikolaev, P.; Bronikowski, M. J.; Bradley, R. K.; Rohmund, F.; Colbert, D. T.; Smith, K. A.; Smalley, R. E., Gas-Phase Catalytic Growth of Single-Walled Carbon Nanotubes from Carbon Monoxide. *Chem. Phys. Lett.* **1999,** 313, 91-97.

33. Zhao, B.; Itkis, M. E.; Niyogi, S.; Hu, H.; Zhang, J.; Haddon, R. C., Study of the Extinction Coefficients of Single-Walled Carbon Nanotubes and Related Carbon Materials. *J. Phys. Chem. B* **2004,** 108, 8136-8141.

34. Itkis, M. E.; Perea, D.; Jung, R.; Niyogi, S.; Haddon, R. C., Comparison of Analytical Techniques for Purity Evaluation of Single-Walled Carbon Nanotubes. *J. Am. Chem. Soc.* **2005,** 127, 3439-3448.

35. Itkis, M. E.; Perea, D.; Niyogi, S.; Rickard, S.; Hamon, M.; Hu, H.; Zhao, B.; Haddon, R. C., Purity Evaluation of As-Prepared Single-Walled Carbon Nanotube Soot by Use of Solution Phase Near-IR Spectroscopy. *Nano Lett.* **2003,** 3, 309-314.

36. Rao, A. M.; Richter, E.; Bandow, S.; Chase, B.; Eklund, P. C.; Williams, K. A.; Fang, S.; Subbaswamy, K. R.; Menon, M.; Thess, A.; Smalley, R. E.;

Dresselhaus, G.; Dresselhaus, M., Diameter-Selective Raman Scattering from Vibrational Modes in Carbon Nanotubes. *Science* **1997,** 275, 187-191.

37. Dillon, A. C.; Yudasaka, M.; Dresselhaus, M. C., Employing Raman Spectroscopy to Qualitatively Evaluate the Purity of Carbon Single-Wall Nanotube Materials. *J. Nanosci. Nanotechnol.* **2004,** 4, (7), 691-703.

38. Arepalli, S.; Nikolaev, P.; Gorelik, O.; Hadjiev, V. G.; Bradlev, H. A.; Holmes, W.; Files, B.; Yowell, L., Protocol for the Characterization of Single-Wall Carbon Nanotube Material Quality. *Carbon* **2004,** 42, (8-9), 1783-1791.

39. Zhang, M.; Yudasaka, M.; Koshio, A.; Iijima, S., Thermogravimetric Analysis of Single-Wall Carbon Nanotubes Ultrasonicated in Monochlorobenzene. *Chem. Phys. Lett.* **2002,** 364, 420-426.

40. Trigueiro, J. P. C.; Silva, G. G.; Lavall, R. L.; Furtado, C. A.; Oliveira, S.; Ferlauto, A. S.; Lacerda, R. G.; Ladeira, L. O.; Liu, J. W.; Frost, R. L.; George, G. A., Purity Evaluation of Carbon Nanotube Materials by Thermogravimetric, TEM, and SEM Methods. *J. Nanosci. Nanotechnol.* **2007,** 7, (10), 3477-3486.

41. Miyata, Y.; Maniwa, Y.; Kataura, H., Selective oxidation of semiconducting single-wall carbon nanotubes by hydrogen peroxide. *J. of Physi. Chem. B* **2006,** 110, (1), 25-29.

42. Wang, Y. H.; Shan, H. W.; Hauge, R. H.; Pasquali, M.; Smalley, R. E., A Highly Selective, One-pot Purification Method for Single-walled Carbon Nanotubes. *J. Phys. Chem. B* **2007,** 111, (6), 1249-1252.

43. Yang, C. M.; Park, J. S.; An, K. H.; Lim, S. C.; Seo, K.; Kim, B.; Park, K. A.; Han, S.; Park, C. Y.; Lee, Y. H., Selective Removal of Metallic Single-Walled Carbon Nanotubes with Small Diameters by using Nitric and Sulfuric Acids. *J. Phys. Chem. B* **2005,** 109, (41), 19242-19248.

44. Sumanasekera, G. U.; Allen, J. L.; Fang, S. L.; Loper, A. L.; Rao, A. M.; Eklund, P. C., Electrochemical Oxidation of Single Wall Nanotube Bundles in Sulfuric Acid. *J. Phys. Chem. B* **1999,** 103, 4292-4297.

45. Liu, J.; Rinzler, A. G.; Dai, H.; Hafner, J. H.; Bradley, R. K.; Boul, P. J.; Lu, A.; Iverson, T.; Shelimov, K.; Huffman, C. B.; Rodriguez-Macias, F.; Shon, Y.-S.; Lee, T. R.; Colbert, D. T.; Smalley, R. E., Fullerene Pipes. *Science* **1998,** 280, 1253-1255.

46. Harutyunyan, A. R.; Pradhan, B. K.; Chang, J.; Chen, G.; Eklund, P. C., Purification of Single-Wall Carbon Nanotubes by Selective Microwave Heating of Catalyst Particles. *J. Phys. Chem. B* **2002,** 106, (34), 8671-8675.

47. Martinez, M. T.; Callejas, M. A.; Benito, A. M.; Maser, W. K.; Cochet, M.; Andres, J. M.; Schreiber, J.; Chauvet, O.; Fierro, L. G., Microwave Single Walled Carbon Nanotubes Purification. *Chem. Comm.* **2002**, (9), 1000-1001.

48. Tchoul, M. N.; Ford, W. T.; Lolli, G.; Resasco, D. E.; Arepalli, S., Effect of Mild Nitric Acid Oxidation on Dispersability, Size, and Structure of Single-Walled Carbon Nanotubes. *Chem. Mater.* **2007,** 19, (23), 5765-5772.

49. Hamon, M. A.; Hu, H.; Bhowmik, P.; Itkis, M. E.; Haddon, R. C., Ester-Functionalized Soluble Single-Walled Carbon Nanotubes. *Appl. Phys. A* **2002,** 74, 333-338.

50. Rinzler, A. G.; Liu, J.; Dai, H.; Nikolaev, P.; Huffman, C. B.; Rodriguez-Macias, F. J.; Boul, P. J.; Lu, A. H.; Heymann, D.; Colbert, D. T.; Lee, R. S.; Fischer, J. E.; Rao, A. M.; Eklund, P. C.; Smalley, R. E., Large-Scale Purification of Single-Wall Carbon Nanotubes: Process, Product and Characterization. *Appl. Phys. A* **1998,** 67, 29-37.

51. Niyogi, S.; Hu, H.; Hamon, M. A.; Bhowmik, P.; Zhao, B.; Rozenzhak, S. M.; Chen, J.; Itkis, M. E.; Meier, M. S.; Haddon, R. C., Chromatographic Purification of Soluble Single-Walled Carbon Nanotubes (s-SWNTs). *J. Am. Chem. Soc.* **2001,** 123, 733-734.

52. Zhao, B.; Hu, H.; Niyogi, S.; Itkis, M. E.; Hamon, M.; Bhowmik, P.; Meier, M. S.; Haddon, R. C., Chromatographic Purification and Properties of Soluble Single Walled Carbon Nanotubes. *J. Am. Chem. Soc.* **2001,** 123, 11673-11677.

53. Hu, H.; Yu, A.; Kim, E.; Zhao, B.; Itkis, M. E.; Bekyarova, E.; Haddon, R. C., Influence of the Zeta Potential on the Dispersability and Purification of

Single-Walled Carbon Nanotubes. *J. Phys. Chem. B* **2005,** 109, 11520-11524.

54. Yu, A.; Bekyarova, E.; Itkis, M. E.; Fakhrutdinov, D.; Webster, R.; Haddon, R. C., Application of Centrifugation to the Large-Scale Purification of Electric Arc Produced Single-Walled Carbon Nanotubes. *J. Am. Chem. Soc.* **2006,** 128, (30), 9902-9908.

55. Mickelson, E. T.; Huffman, C. B.; Rinzler, A. G.; Smalley, R. E.; Hauge, R. H.; Margrave, J. L., Fluorination of Single-Wall Carbon Nanotubes. *Chem. Phys. Lett.* **1998,** 296, 188-194.

56. Khabashesku, V. N.; Billups, E. W.; Margrave, J. L., Fluorination of Single-Wall Carbon Nanotubes and Subsequent Derivatization Reactions. *Acc. Chem. Res.* **2002,** 35, (12), 1087-1095.

57. Chen, J.; Hamon, M. A.; Hu, H.; Chen, Y.; Rao, A. M.; Eklund, P. C.; Haddon, R. C., Solution Properties of Single-Walled Carbon Nanotubes. *Science* **1998,** 282, 95-98.

58. Chen, Y.; Haddon, R. C.; Fang, S.; Rao, A. M.; Eklund, P. C.; Lee, W. H.; Dickey, E. C.; Grulke, E. A.; Pendergrass, J. C.; Chavan, A.; Haley, B. E.; Smalley, R. E., Chemical Attachment of Organic Functional Groups to Single-Walled Carbon Nanotube Material. *J. Mater. Res.* **1998,** 13, 2423-2431.

59. Hu, H.; Zhao, B.; Hamon, M. A.; Kamaras, K.; Itkis, M. E.; Haddon, R. C., Sidewall Functionalization of Single-Walled Carbon Nanotubes by Addition of Dichlorocarbene. *J. Am. Chem. Soc.* **2003,** 125, 14893-14900.

60. Ying, Y.; Saini, R. K.; Liang, F.; Sadana, A. K.; Billups, W. E., Functionalization of Carbon Nanotubes by Free Radicals. *Org. Lett.* **2003,** 5, (9), 1471-1473.

61. Bahr, J. L.; Yang, J.; Kosynkin, D. V.; Bronikowski, M. J.; Smalley, R. E.; Tour, J. M., Functionalization of Carbon Nanotubes by Electrochemical Reduction of Aryl Diazonium Salts: A Bucky Paper Electrode. *J. Am. Chem. Soc.* **2001,** 123, 6536-6542.

62. Bekyarova, E.; Davis, M.; Burch, T.; Itkis, M. E.; Zhao, B.; Sunshine, S.; Haddon, R. C., Chemically Functionalized Single-Walled Carbon

Nanotubes for Ammonia Sensors. *J. Phys. Chem. B* **2004,** 108, 19717-19720.

63. Hu, H.; Ni, Y.; Mandal, S. K.; Montana, V.; Zhao, B.; Haddon, R. C.; Parpura, V., Polyethyeneimine Functionalized Single-Walled Carbon Nanotubes as a Substrate for Neuronal Growth. *J. Phys. Chem. B* **2005,** 109, 4285-4289.

64. Zhao, B.; Hu, H.; Perea, D.; Haddon, R. C., Synthesis and Characterization of Water Soluble Single-Walled Carbon Nanotube Graft Copolymers. *J. Am. Chem. Soc.* **2005,** 127, 8197-8203.

65. Moore, V. C.; Strano, M. S.; Haroz, E. H.; Hauge, R. H.; Smalley, R. E.; Schmidt, J.; Talmon, Y., Individually Suspended Single-Walled Carbon Nanotubes in Various Surfactants. *Nano Lett.* **2003,** 3, 1379-1382.

66. Vaisman, L.; Marom, G.; Wagner, H. D., Dispersions of surface-modified carbon nanotubes in water-soluble and water-insoluble polymers. *Adv. Func, Mater.* **2006,** 16, (3), 357-363.

67. Zheng, M.; Jagota, A.; Strano, M. S.; Santos, A. P.; Barone, P.; Chou, S. G.; Diner, B. A.; Dresselhaus, M. S.; Mclean, R. S.; Onoa, G. B.; Samsonidze, G. G.; Semke, E. D.; Usrey, M. L.; Walls, D. J., Structure-Based Carbon Nanotube Sorting by Sequence-Dependent DNA Assembly. *Science* **2003,** 302, 1545-1548.

68. Novoselov, K. S.; Geim, A. K.; Morozov, S. V.; Jiang, D.; Zhang, Y.; Dubonos, S. V.; Grigorieva, I. V.; Firsov, A. A., Electric Field Effect in Atomically Thin Carbon Films. *Science* **2004,** 306, 666-669.

69. Berger, C.; Song, Z.; Li, T.; Li, X.; Ogbazghi, A. Y.; Feng, R.; Dai, Z.; Marchenkov, A. N.; Conrad, E. H.; First, P. N.; de Heer, W. A., Ultrathin Epitaxial Graphite: 2d Electron Gas Properties and a Route Toward Graphene-Based Nanoelectronics. *J. Phys. Chem. B* **2004,** 108, (52), 19912-19916.

70. Zhang, Y.; Small, J. P.; Pontius, W. V.; Kim, P., Fabrication and Electric-Field-Dependent Transport Measurements of Mesoscopic Graphite Devices. *Appl. Phys. Lett.* **2005,** 86, 073104.

71. Dresselhaus, M. S.; Dresselhaus, G., Intercalation compounds of graphite. *Advances in Physics* **2002,** 51, (1), 1-186.

72. Ferrari, A. C.; Robertson, J., Interpretation of Raman spectra of disordered and amorphous carbon. *Phys. Rev. B* **2000,** 61, (20), 14095-14107.

73. Chen, G. H.; Wu, D. J.; Weng, W. U.; Wu, C. L., Exfoliation of Graphite Flake and Its Nanocomposites. *Carbon* **2003,** 41, (3), 619-621.

74. Inagaki, M.; Tashiro, R.; Washino, Y.; Toyoda, M., Exfoliation Process of Graphite via Intercalation Compounds with Sulfuric Acid. *J. Phys. Chem. Solids* **2004,** 65, (2-3), 133-137.

75. Viculis, L. M.; Mack, J. J.; Mayer, O. M.; Hahn, T.; Kaner, R. B., Intercalation and Exfoliation Routes to Graphite Nanoplatelets. *J. Mater. Chem.* **2005,** 15, 974-978.

76. Niyogi, S.; Hamon, M. A.; Hu, H.; Zhao, B.; Bhowmik, P.; Sen, R.; Itkis, M. E.; Haddon, R. C., Chemistry of Single-Walled Carbon Nanotubes. *Acc. Chem. Res.* **2002,** 35, 1105-1113.

77. Tasis, D.; Tagmatarchis, N.; Bianco, A.; Prato, M., Chemistry of Carbon Nanotubes. *Chem. Rev.* **2006,** 106, (3), 1105-1136.

78. Hirsch, A., *The Chemistry of the Fullerenes*. Thieme: Stuttgart, 1994.

79. Diederich, F.; Thilgen, C., Covalent Fullerene Chemistry. *Science* **1996,** 271, 317-324.

80. Beckett, R. J.; Croft, R. C., The Structure of Graphite Oxide. *J. Phys. Chem.* **1952,** 56, (8), 929-935.

81. Braga, S. F.; Coluci, V. R.; Legoas, S. B.; Giro, R.; Galva, D. S.; Baughman, R. H., Structure and Dynamics of Carbon Nanoscrolls. *Nano Lett.* **2004,** 4, (5), 881-884.

Chapter 2

Isolation and Characterization of Carboxylated Carbons

2.1 Introduction

The development of single-walled carbon nanotubes (SWNTs) as a useful material has been highly dependent on their purification.[1-6] For most applications, a high-quality sample yielding reproducible results is desired. Upon formation by the various synthetic techniques (CVD, laser oven, electric arc) SWNT samples contain several contaminants, such as residual metal catalysts, amorphous carbon (AC) and graphitized carbon nanoparticles (CNP), and their removal has proven to be a strenuous and on-going challenge. A multitude of procedures involving combinations of prolonged stirring or sonication,[7] heat treatments,[8] and microwave radiation[5, 9, 10] in a variety of aqueous acidic solutions,[8, 11-14] have been successfully employed in the removal of some of these impurities. Other purification techniques utilize strong oxidative reactions that result in acid functionality on the SWNTs at the termini and defect sites - the most common of which, involves concentrated nitric acid at elevated

temperatures.[11, 15, 16] With the generation of acid functionality, it has been reported that the oxidation of SWNTs also leads to the formation of additional carbonaceous impurities.[1, 6, 11, 17-19] Techniques such as low and high speed centrifugation[6, 20] have been previously employed to remove some of the carbon impurities generated, but more recently, it has been suggested that impurities formed from nitric acid oxidation, referred to as carboxylated carbons (CCs), are absorbed onto the nanotube and are not readily removed by the traditional purification procedures previously described.[21] Their structure is reported to consist of polycyclic aromatic sheets with edge-terminated carboxylic acid functionality combined with larger, more cross-linked structures,[1] and their removal using various concentrations of aqueous NaOH followed by filtration techniques has been widely studied.[1, 11, 21-26] It is suggested that the absorption of the CCs onto the side-walls of the nanotube stems from the π–π interactions of the polycyclic structure, and under basic conditions, their dissolution occurs due to the presence of the deprotonated carboxylic acid residues.[1] Due to the difficulties in removing the NaCl salt after filtration and neutralization, a pure CC sample is not easily isolated and thus, previous studies have characterized this material in its de-protonated form.[21-24, 27] The remaining SWNTs are said to contain few acid sites for further functionalization which is essential in various applications as it increases their processability.[21-26] In this chapter, the purification of nitric acid treated SWNTs by washing with dilute NH_4OH is reported and shown to yield comparable results to that of base washing with

NaOH. The washed SWNTs are shown to still contain a significant amount of acid functionality and the collected CCs are isolated upon simple evaporation of the base. This allows for the full characterization of the CCs, verifying their composition as a bulk material consisting mainly of polycyclic aromatic carboxylic acids.

2.2 Experimental Methods

2.2.1 Starting materials

SWNTs prepared by electric arc-discharge were obtained from Carbon Solutions Inc. (www.carbonsolution.com). The SWNTs were refluxed in concentrated nitric acid for 1.5 h and then purified by low speed centrifugation.[6, 28] All other chemicals were purchased from Fisher Scientific and were used as received.

2.2.2 Characterization

Near-IR data was collected in a quartz cell of 1 cm path length on a Varian Cary 5000 spectrometer. Extinction coefficients where determined by measuring the absorbance at 550 nm of a series of aqueous solutions of known concentrations (0.005, 0.01, 0.02, and 0.04 mg/mL). These concentrations were prepared by diluting a 0.2 mg/mL stock solution and the mass of the material was corrected for metal and moisture content. Mid-IR spectra of the materials were

collected from a thin film on ZnSe using a Nicolet Nexus FT-IR spectrometer. Thermogravimetric analysis was preformed at a heating rate of 5 ºC/min in air using a Pyris Diamond thermogravimetric/differential thermal analyzer (TG/DTA). Images from a high resolution transmission electron microscope (TEM) were obtained from a Technai12 instrument operating at 120 kV accelerating voltage. Raman spectra of the starting material and products were collected from a Bruker RFS 100/S type FT-Raman spectrometer using a Nd-YAG laser excitation source with a wavelength of 1064 nm and a resolution of 8 cm^{-1}. XRD data was collected using a Bruker AXS D8 Advanced diffractometer using CuKα radiation (1.54 Å). The relative purity, as compared to a standard sample, was evaluated as described previously.[29-31] The conductivity of thin films prepared by spraying dilute aqueous solutions of each material was measured using a Keithley 2700 Multimeter/Data Acquisition System. The thickness of the films (*t*) was estimated from the measured absorption at 550 nm and the extinction coefficient (ε_{550nm}) of each material given in Table 2.1.

Table 2.1: Extinction coefficients determined from aqueous solutions of SWNT-COOH, w-SWNT-COOH and CC at 550 nm.

Material	**ε_{550nm} (L/g·cm)**
SWNT-COOH	25
w-SWNT-COOH	23
CC	15

2.2.3 Concentration Optimization Procedure

The concentration of the base in the washing procedure was determined by a series of experiments: 100 mg of SWNT-COOH was combined with 100 mL of a known concentration of NH_4OH (0.01, 0.1, 1, 3, 7, and 14 M), and was dispersed by sonication for 30 min in a polypropylene container. The samples were then stirred for 48 hrs under an argon atmosphere. Subsequently, the samples were filtered using a stainless steel frit through a 0.2 μm GV Millipore membrane and the filtrate was analyzed by near-IR spectroscopy to determine the amount of material removed using the appropriate extinction coefficient (given in Table 2.1). The data obtained was compared to values found using the same procedure with known concentrations of NaOH (0.001, 0.01, 0.1, and 1 M).

2.2.4 Base Washing Procedure

After the optimal concentration of NH_4OH was determined, the resulting base washing procedure was as follows: 100 mg of SWNT-COOH material was dispersed in 100 mL of 3 M NH_4OH in a Teflon beaker and was filtered using a stainless steel frit fitted with a 0.2 μm GV Millipore membrane. This was repeated several times until the filtrate was colorless. The SWNTs were then re-dispersed in 0.05 M HCl and were filtered using a 0.4 μm HTTP Millipore membrane and were further washed with water until the filtrate was pH neutral.

The CC solution collected was concentrated to dryness. The yields of w-SWNT-COOH and CCs collected by weight are roughly 70% and 30%, respectively.

2.2.5 Acid Neutralization Procedure

The acid content was determined by directly neutralizing each of the materials with NaOH.[32] Briefly, 100 mg of SWNT-COOH or w-SWNT-COOH, or 30 mg of CCs was combined with 25 mL of 0.0125 M NaOH in a sealed polyethylene container. After 48 hours of stirring under Ar, the pH was measured with a Corning pH meter 445, and this value was compared to a blank solution (without carbon material) that underwent the same process.

2.2.6 Acid Neutralization Calculation

The concentration of NaOH remaining, $[OH^-]$, in each mixture can be determined by measuring the pH and using the following equations:

$$14 - pH = pOH \quad (1)$$

$$pOH = - \log[OH^-] \quad (2)$$

The mmols of OH^- are then calculated by multiplying by the volume (0.025 L). The difference between the number of mmols of OH^- of the blank and that in the sample is assumed to be the number of mmols of OH^- that were needed to neutralize the acid functionality present in the sample.[32] This value is then divided by the starting mass (100 or 30 mg) to determine the acid content (given

in meq/g). In order to convert this result into mol%, the number of eq/g is multiplied by the atomic weight of carbon (C_{AW} = 12.01 g/mol).

For example:

The pH of a 0.1009 g sample of SWNT-COOH and the blank solution was measured to be 11.39 and 12.10, respectively.

Blank $[OH_B^-]$:

$$pOH = 14 - 12.10$$
$$pOH = 1.90$$
$$1.90 = -\log[OH_B^-]$$
$$[OH_B^-] = 0.01259\,M$$
$$0.025\,L \times [OH_B^-] = 0.3147\,mmols$$

SWNT-COOH $[OH^-]$:

$$pOH = 14 - 11.39$$
$$pOH = 2.61$$
$$2.61 = -\log[OH^-]$$
$$[OH^-] = 0.002455\,M$$
$$0.025\,L \times [OH^-] = 0.06137\,mmols$$

Acid Content:

$$\frac{0.3147\,mmols - 0.06137\,mmols}{0.1009\,g} = 2.511\,mmols/g \qquad 2.5\ meq/g$$

$$\frac{2.511\,mmols}{1\,g} \times \frac{12.01\,g}{1\,mol} \times \frac{1\,mol}{1000\,mmols} = 0.03015 \qquad 3.0\ mol\%$$

2.3 Results and Discussion

2.3.1 Concentration Optimization for NH_4OH Washing of SWNT-COOH

The formation of acid functionality on SWNTs by nitric acid oxidation has been briefly described in several publications.[11, 33-35] The aggressive acid treatment etches the defect sites and highly strained end caps forming several types of oxygen functionality such as carbonyl, carboxyl, alcohols, and lactones. Base washing de-protonates the acid sites which are reported to be mainly on the CCs,[21] resulting in their exfoliation and dissolution from the side-walls of the nanotube and allows for their full removal by repeated filtrations. The efficiency of the dissolution of the CCs is dependent on the concentration of the base, which presumably represents a compromise between a number of factors including the pK_a of the acid functionalities present in the CCs, the solution ionic strength, and the zeta potential.[36] To determine the appropriate concentration, various dilutions were used in a single washing experiment, and the amount of material removed in weight percent (wt%) was calculated from the absorbance using Beer's Law and the calculated extinction coefficient (ε) at 550 nm of an aqueous solution of CCs (Table 2.1, ε_{550nm} = 15 L/g·cm). It was found that 3 M NH_4OH (pK_b = 4.767)[37] and 0.01 M NaOH solutions were equally as effective in the removal of CCs in a single washing, removing around 17% of the total material (Figure 2.1). This corresponds to a pH of approximately 12 at 20 ºC in both cases. Previous studies have utilized Salzmann's protocol,[21, 23] which

involves heating in 8 M NaOH at 100 ºC for 48 hrs. This is a seemingly harsh treatment which may not be optimal for complete removal of the CCs.[24] A strongly basic solution of 8 M NaOH is an extreme excess with respect to the amount of acid sites in the sample and it has been previously shown for electric-arc produced SWNTs treated with various concentrations and durations of nitric acid, that the zeta potential is at a minimum (large negative value) when the pH of the aqueous SWNT dispersion is around neutral.[20, 28] This suggests that when SWNT-COOH are combined with a concentrated basic solution (at high pH), the mixture would have a high ionic strength and a small absolute zeta potential, leading to a relatively poor colloidal stability and thus, a poor dispersion and separation of the CCs.

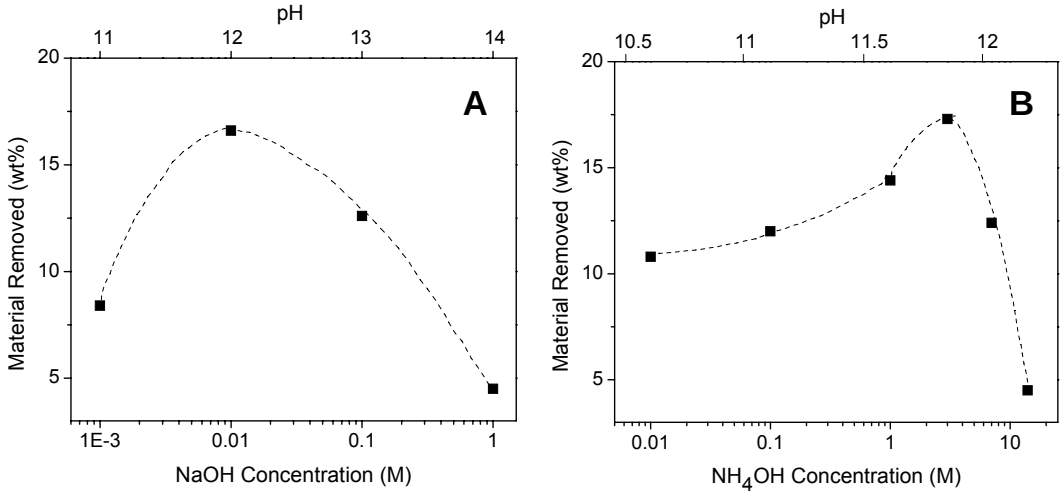

Figure 2.1: Amount of CC (wt %) removed from a single washing of A) SWNT-COOH with 0.001, 0.01, 0.1, and 1 M of NaOH, and B) 0.01, 0.1, 1, 3, 7, and 14 M NH_4OH.

2.3.2 FT-IR Spectra of Materials

After successive base washing using the optimized concentration, the starting material and isolated products were characterized by mid-IR spectroscopy (Figure 2.2). Upon comparison of the transmission spectra of SWNT-COOH and w-SWNT-COOH, the removal of carboxylic acid sites is apparent from the reduction in the intensity of the C=O stretch centered at 1741 cm^{-1}. However, these spectra are essentially featureless in comparison to the pronounced peaks exhibited by the transmittance spectra of the CCs indicating an increase in oxygen functionality with respect to the aromatic carbon framework. The broad band at ~3200 cm^{-1} and sharp peaks at 1734 cm^{-1} and 1591 cm^{-1} are features observed in the polycyclic aromatic spectra of fulvic acids[38] and are assigned to the O-H, C=O, and C=C stretching vibrations, respectively. Carboxylate ion peaks of CCs are reported to occur around 1620 cm^{-1} and 1450 cm^{-1},[24] and are not detected signifying that the NH_4OH was adequately removed upon evaporation. These observations are consistent with the proposal that the CCs contain a significant amount of acid functionality, although, some functionality still remains on the nanotubes after exhaustive washing with a NH_4OH.

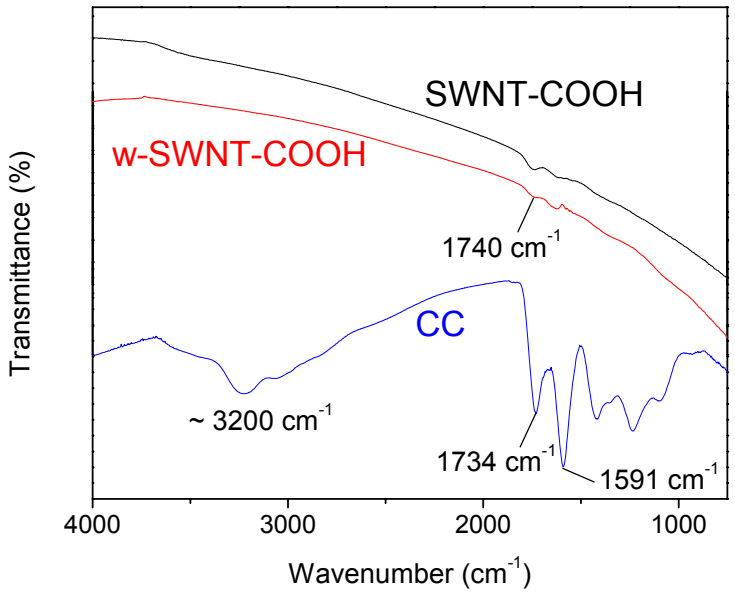

Figure 2.2: Mid-IR transmittance spectra collected from thin films of SWNT-COOH, w-SWNT-COOH, and CC on ZnSe.

2.3.3 Characterization of Materials by TGA

Identification of the burning temperatures of the individual components of carbon nanotube samples from a TG scan is known to be ambiguous.[31] The interaction between species in the multi-component material results in overlapping peaks that burn over a broad temperature range and are highly dependent on the nature and quantity of each individual component, such as the metal catalyst and carbon impurities.[39] The TGA data of each of the three materials are presented in Figure 2.3A-C. As seen in the derivative of Figure 2.3A, SWNT-COOH shows 3 peaks centered at 495, 540, and 705 ºC with a metal oxide residue of 7.5 wt%. After base washing of the SWNTs, the peak at

495 ºC is removed, and the metal oxide residue is increase to 9.4 wt% (Figure 2.3B). The carbon material removed is seen in Figure 2.3C, with a burning temperature of 560 ºC. This temperature is higher than expected and may be ascribed to the change in proportion of the components in the sample, such as the significantly lowered metal oxide content of 3.0 wt%. The peak centered at 220 ºC may be attributed to the high oxygen functionality present in the CC material.

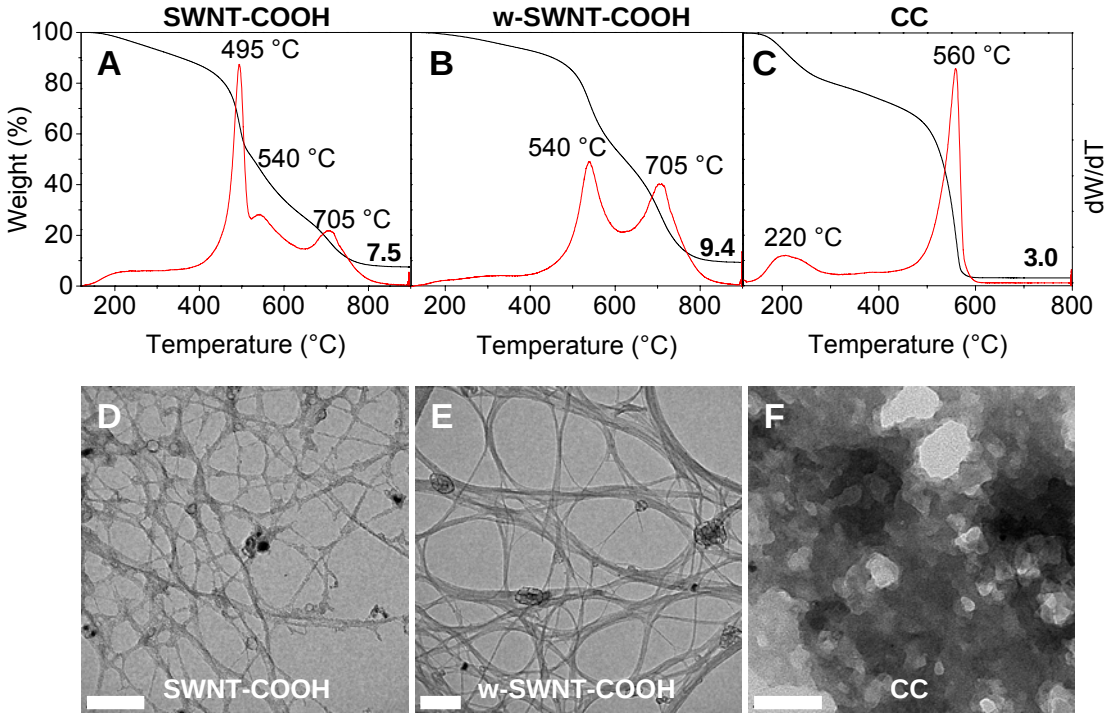

Figure 2.3: TGA weight change (black line) and its derivative (red line) for A) SWNT-COOH, B) w-SWNT-COOH, and C) CC. TEM images of D) SWNT-COOH, E) w-SWNT-COOH, and F) CC. Scale bar in each image represents 100 nm.

2.3.4 Analysis by TEM

TEM images verify the effectiveness of the purification procedure (Figure 2.3D-F). In Figure 2.3D, the nanotubes appear to have a web-like coating that is assigned the CCs along the side-walls. After base washing, the nanotubes appear free from this coating with smooth and well-defined walls (Figure 2.3E). The removed material (Figure 2.3F) appears amorphous, unlike the shell particles observed in TEM images of CNPs.[20] Also observed in the TEM images is a change in bundle size upon removal of the CCs. The base washed material, w-SWNT-COOH, is comprised of larger bundles than the SWNT-COOH starting material. Due to the loss of the CC coating, more surface area is exposed resulting in more $\pi-\pi$ interaction between nanotubes.

2.3.5 XRD Patterns of Bulk Powders

XRD patterns are shown in Figure 2.4A. A peak corresponding to a d-spacing of 0.34 nm is seen in SWNT-COOH and w-SWNT-COOH samples due to the intermolecular $\pi-\pi$ stacking within the bundles. This was not seen in the XRD pattern of the CCs, suggesting a composition of amorphous carbon particles or possibly a combination of smaller organic aromatic species with high acid functionality hindering $\pi-\pi$ stacking as would be expected in the case of highly functionalized polycyclic aromatic carboxylic acids.

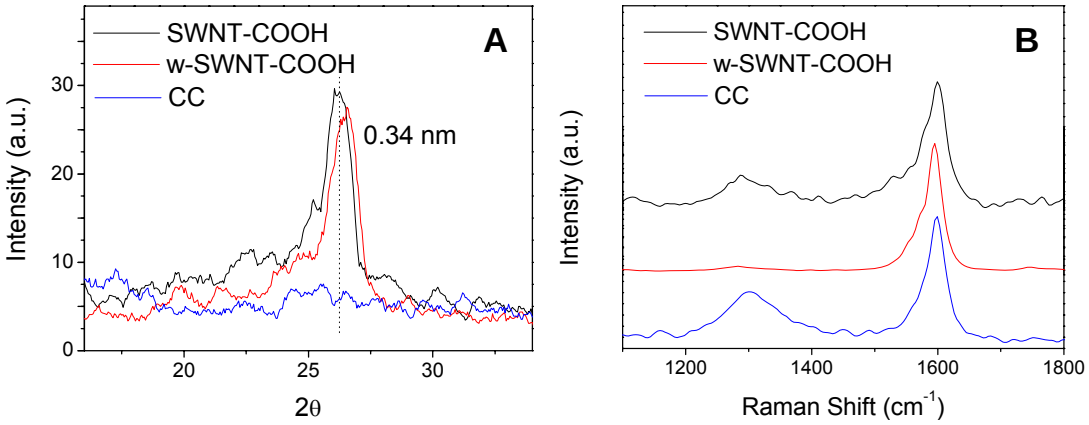

Figure 2.4: A) XRD patterns of bulk samples and B) Raman spectra of SWNT-COOH, w-SWNT-COOH, and CC. Raman spectra are normalized at the G-band and shifted vertically for clarity.

2.3.6 Purity Evaluation by NIR and Raman Scattering Characterization

Raman spectroscopy data was also used to characterize the materials and confirm their relative purities. As seen in Figure 2.4B, there is a significant decrease in the disordered D-band of w-SWNT-COOH when compared to SWNT-COOH. Although the D-band intensity is largest for CCs, a sizeable graphitic G-band is observed confirming the presence of polycyclic aromatic structure. The ratio of the intensities of the D-band to the G-band, I_D/I_G, is given in Table 2.2. Similar to previous studies, [21, 23, 24] the I_D/I_G ratio dramatically decreases from 0.23 to 0.04, as a result of the base purification, while the CCs, as expected, have the highest value of 0.40. The effectiveness of the base-washing is further confirmed by the relative purity values calculated from the

areal absorbance of the S_{22} transition in the near-IR.[29, 31] The purification technique resulted in a relative purity increase from 108% to 128% upon base-washing of the SWNT-COOH starting material, whereas CCs have no S_{22} transition resulting in a relative purity of 0%.

Table 2.2: Percent yield by mass, relative purity, I_D/I_G ratio, acid content data (given in mol% and meq/g) and the measured conductivity (σ) of SWNT-COOH, w-SWNT-COOH, and CC.

Material	Yield (%)	Relative Purity (%)	I_D/I_G	Acid Content (mol%)	Acid Content (meq/g)	σ (S/cm)
SWNT-COOH	-	108	0.23	3.0	2.5	200
w-SWNT-COOH	70	128	0.04	1.1	0.9	187
CC	30	0	0.40	7.3	6.1	0.0003

2.3.7 Assessment of Acid Content

In multi-walled carbon nanotubes (MWNTs), it was reported that CCs account for up to 43% of the total acid content.[25] In this study it was found that CCs account for over 70% of the total acid content of the SWNT-COOH starting sample (0.3 x 6.1 / 2.5). This difference may be explained by the relative stabilities of the single-walled compared to multi-walled tubes. MWNTs are structurally more stable than SWNTs, and are therefore more resistant to oxidation by nitric acid and subsequently, generate less CCs.[23] The nitric acid

treatment of SWNTs produces more CCs, and this can be seen in the color of the base washing solutions. Upon base washing of MWNTs, a yellow filtrate is observed,[23, 25] whereas, SWNTs give a brown-black solution.[21, 23, 24, 27] Although MWNTs may retain more acid functionality after base washing, approximately 30% of acid sites still remain on SWNTs for further functionalization after full removal of the CCs.

The quality of the nanotube can also be assessed by the acid content. For analysis, we assume that our SWNT sample is composed of (10,10) tubes in which the termini are cut perpendicular to the length of the tube; it has previously been calculated that the unit cell of a (10,10) SWNT contains 40 carbon atoms and that a 100 nm long nanotube would consist of ~ 16 000 carbon atoms, where 40 of those atoms are available for functionality at the termini (neglecting anhydrides).[17, 40] Thus, the expected acid content of a pristine SWNT is (40 x 1000)/(16 000 x 12.01 g/mol) = 0.2 meq/g. The measured value as seen in Table 2.2 is 0.9 meq/g, indicating a significant contribution of functionality located at defect sites. However, the total acid content of the starting material was found to be 2.5 meq/g, confirming the effectiveness of the purification procedure.

The mole ratio of acid functionality to carbon atoms of CCs can also be estimated by the acid content. The weight of acid functionality in 1 g of CC, assuming that all acid content is comprised of carboxylic acids, can be found by multiplying the acid content, 6.1 x 10^{-3} mol/g, by the molecular weight of a carboxylic acid group (-COOH = 45 g/mol). This gives 0.27 g of acid functionality

and therefore, 0.73 g of remaining carbon in the CC sample. This corresponds to a mol ratio of 0.0061 moles of acid functionality to 0.060 moles of carbon. Thus, there are approximately 10 carbon atoms per carboxylic acid functionality in the CC impurity corresponding to an average structure similar to that of naphthalene carboxylic acid.

2.3.8 Conductivity of Materials

Lastly, conductivity experiments were performed on thin films of each material. The conductivity (σ) of SWNT-COOH and w-SWNT-COOH were comparable at around 200 S/cm with films approximately 30 nm thick. Films of CCs with thicknesses above 400 nm exhibited extremely poor conductivity. This is not surprising, however, due to the high degree of functionality as confirmed by mid-IR, TGA, XRD, Raman and acid neutralization data.

2.4 Conclusions

Nitric acid purification of SWNTs results in the generation of oxygen functionality and CCs. A mild base treatment using dilute NH_4OH is an effective technique in the removal of CCs and gives comparable results to that of NaOH in a single washing. Unlike NaOH, NH_4OH can be readily evaporated allowing for characterization of a pure CC sample. Mid-IR, TGA, XRD, Raman and acid neutralization data indicate that the CCs are composed of a highly functionalized

polycyclic material, although some functionality is retained on the nanotubes after repeated base washing. TEM images show that the CCs are coated on the side-walls and their exfoliation is readily seen by comparing the base washed to the starting material. The effectiveness of the base washing procedure is verified by Raman scattering data and is confirmed by relative purity values measured by near-IR spectroscopy. Acid neutralization data show that approximately 70% of the acid functionality in SWNT-COOH resides on the CCs, which may explain the absence $\pi-\pi$ stacking observed in XRD data and the poor conductivity of thin films for this material. Further study of this material will lead to possible identification of some of the compounds that constitute the CC impurities.

2.5 References

1. Rinzler, A. G.; Liu, J.; Dai, H.; Nikolaev, P.; Huffman, C. B.; Rodriguez-Macias, F. J.; Boul, P. J.; Lu, A. H.; Heymann, D.; Colbert, D. T.; Lee, R. S.; Fischer, J. E.; Rao, A. M.; Eklund, P. C.; Smalley, R. E., Large-Scale Purification of Single-Wall Carbon Nanotubes: Process, Product and Characterization. *Appl. Phys. A* **1998,** 67, 29-37.

2. Shi, Z.; Lian, Y.; Liao, F. H.; Zhou, X.; Gu, Z.; Zhang, Y.; Iijima, S., Purification of Single-Wall Carbon Nanotubes. *Solid State Communications* **1999,** 112, 35-37.

3. Zimmerman, J. L.; Bradley, R. K.; Huffman, C. B.; Hauge, R. H.; Margrave, J. L., Gas-Phase Purification of Single-Wall Carbon Nanotubes. *Chem. Mater.* **2000,** 12, (5), 1361-1366.

4. Zheng, B.; Li, Y.; Liu, J., CVD Synthesis and Purification of Single-Walled Carbon Nanotubes on Aerogel-Supported Catalyst. *Appl. Phys. A (Materials Science Processing)* **2002,** A74, 345-348.

5. Harutyunyan, A. R.; Pradhan, B. K.; Chang, J.; Chen, G.; Eklund, P. C., Purification of Single-Wall Carbon Nanotubes by Selective Microwave Heating of Catalyst Particles. *J. Phys. Chem. B* **2002,** 106, (34), 8671-8675.

6. Hu, H.; Zhao, B.; Itkis, M. E.; Haddon, R. C., Nitric Acid Purification of Single-Walled Carbon Nanotubes. *J. Phys. Chem. B* **2003,** 107, 13838-13842.

7. Chiang, I. W.; Brinson, B. E.; Huang, A. Y.; Willis, P. A.; Bronikowski, M. J.; Margrave, J. L.; Smalley, R. E.; Hauge, R. H., Purification and Characterization of Single-Wall Carbon Nanotubes(SWNTs) Obtained From The Gas-Phase Decomposition of CO (HiPco Process). *J. Phys. Chem. B* **2001,** 105, 8297-8301.

8. Wang, Y. H.; Shan, H. W.; Hauge, R. H.; Pasquali, M.; Smalley, R. E., A Highly Selective, One-pot Purification Method for Single-walled Carbon Nanotubes. *J. Phys. Chem. B* **2007,** 111, (6), 1249-1252.

9. Esumi, K.; Ishigami, M.; Nakajima, A.; Sawada, K.; Honda, H., Chemical Treatment of Carbon Nanotubes. *Carbon* **1996,** 34, 279-281.

10. Martinez, M. T.; Callejas, M. A.; Benito, A. M.; Maser, W. K.; Cochet, M.; Andres, J. M.; Schreiber, J.; Chauvet, O.; Fierro, L. G., Microwave Single Walled Carbon Nanotubes Purification. *Chem. Comm.* **2002**, (9), 1000-1001.

11. Liu, J.; Rinzler, A. G.; Dai, H.; Hafner, J. H.; Bradley, R. K.; Boul, P. J.; Lu, A.; Iverson, T.; Shelimov, K.; Huffman, C. B.; Rodriguez-Macias, F.; Shon, Y.-S.; Lee, T. R.; Colbert, D. T.; Smalley, R. E., Fullerene Pipes. *Science* **1998,** 280, 1253-1255.

12. Sumanasekera, G. U.; Allen, J. L.; Fang, S. L.; Loper, A. L.; Rao, A. M.; Eklund, P. C., Electrochemical Oxidation of Single Wall Nanotube Bundles in Sulfuric Acid. *J. Phys. Chem. B* **1999,** 103, 4292-4297.

13. Yang, C. M.; Park, J. S.; An, K. H.; Lim, S. C.; Seo, K.; Kim, B.; Park, K. A.; Han, S.; Park, C. Y.; Lee, Y. H., Selective Removal of Metallic Single-Walled Carbon Nanotubes with Small Diameters by using Nitric and Sulfuric Acids. *J. Phys. Chem. B* **2005,** 109, (41), 19242-19248.

14. Miyata, Y.; Maniwa, Y.; Kataura, H., Selective oxidation of semiconducting single-wall carbon nanotubes by hydrogen peroxide. *J. of Physi. Chem. B* **2006,** 110, (1), 25-29.

15. Bower, C.; Kleinhammes, A.; Wu, Y.; Zhou, O., Intercalation and Partial Exfoliation of Single-Walled Carbon Nanotubes by Nitric Acid. *Chem. Phys. Lett.* **1998,** 288, 481-486.

16. Dillon, A. C.; Gennett, T.; Jones, K. M.; Alleman, J. L.; Parilla, P. A.; Heben, M. J., A Simple and Complete Purification of Single-Walled Carbon Nanotube Materials. *Adv. Mater.* **1999,** 11, (16), 1354-1358.

17. Hamon, M. A.; Hu, H.; Bhowmik, P.; Niyogi, S.; Zhao, B.; Itkis, M. E.; Haddon, R. C., End-Group and Defect Analysis of Soluble Single-Walled Carbon Nanotubes. *Chem. Phys. Lett.* **2001,** 347, (1-3), 8-12.

18. Hu, H.; Bhowmik, P.; Zhao, B.; Hamon, M. A.; Itkis, M. E.; Haddon, R. C., Determination of the Acidic Sites of Purified Single-Walled Carbon Nanotubes by Acid-Base Titration. *Chem. Phys. Lett.* **2001,** 345, 25-28.

19. Hamon, M. A.; Hu, H.; Bhowmik, P.; Itkis, M. E.; Haddon, R. C., Ester-Functionalized Soluble Single-Walled Carbon Nanotubes. *Appl. Phys. A* **2002,** 74, 333-338.

20. Yu, A.; Bekyarova, E.; Itkis, M. E.; Fakhrutdinov, D.; Webster, R.; Haddon, R. C., Application of Centrifugation to the Large-Scale Purification of Electric Arc Produced Single-Walled Carbon Nanotubes. *J. Am. Chem. Soc.* **2006,** 128, (30), 9902-9908.

21. Salzmann, C. G.; Llewellyn, S. A.; Tobias, G.; Ward, M. A. H.; Huh, Y.; Green, M. L. H., The Role of Carboxylated Carbonaceous Fragments in the Functionalization and Spectroscopy of a Single-Walled Carbon-Nanotube Material. *Adv. Mater.* **2007,** 19, (6), 883-887.

22. Verdejo, R.; Lamoriniere, S.; Cottam, B.; Bismarck, A.; Shaffer, M., Removal of Oxidation debris from Multi-walled Carbon Nanotubes. *Chemical Communications* **2007**, (5), 513-515.

23. Yu, H.; Jin, Y. G.; Peng, F.; Wang, H. J.; Yang, J., Kinetically Controlled Side-Wall Functionalization of Carbon Nanotubes by Nitric Acid Oxidation. *J. Phys. Chem. C* **2008,** 112, (17), 6758-6763.

24. Fogden, S.; Verdejo, R.; Cottam, B.; Shaffer, M., Purification of Single Walled Carbon Nanotubes: The Problem with Oxidation Debris. *Chem. Phys. Lett.* **2008,** 460, (1-3), 162-167.

25. Wang, Z.; Shirley, M. D.; Meikle, S. T.; Whitby, R. L. D.; Mikhalovsky, S., The Surface Acidity of Acid Oxidised Multi-walled Carbon Nanotubes and the Influence of In-situ Generated Fulvic Acids on their Stability in Aqueous Dispersions. *Carbon* **2009,** 47, (1), 73-79.

26. Shao, L.; Tobias, G.; Salzmann, C. G.; Ballesteros, B.; Hong, S. Y.; Crossley, A.; Davis, B. G.; Green, M. L. H., Removal of Amorphous Carbon for the Efficient Sidewall Functionalisation of Single-walled Carbon Nanotubes. *Chemical Communications* **2007**, (47), 5090-5092.

27. Price, B. K.; Lomeda, J. R.; Tour, J. M., Aggressively Oxidized Ultra-Short Single-Walled Carbon Nanotubes Having Oxidized Sidewalls. *Chem. Mater.* **2009,** 21, (17), 3917-3923.

28. Hu, H.; Yu, A.; Kim, E.; Zhao, B.; Itkis, M. E.; Bekyarova, E.; Haddon, R. C., Influence of the Zeta Potential on the Dispersability and Purification of Single-Walled Carbon Nanotubes. *J. Phys. Chem. B* **2005,** 109, 11520-11524.

29. Itkis, M. E.; Perea, D.; Niyogi, S.; Rickard, S.; Hamon, M.; Hu, H.; Zhao, B.; Haddon, R. C., Purity Evaluation of As-Prepared Single-Walled Carbon Nanotube Soot by Use of Solution Phase Near-IR Spectroscopy. *Nano Lett.* **2003,** 3, 309-314.

30. Zhao, B.; Itkis, M. E.; Niyogi, S.; Hu, H.; Perea, D.; Haddon, R. C., Extinction Coefficients and Purity of Single-Walled Carbon Nanotubes. *J. Nanosci. Nanotechnol.* **2004,** 4, 995-1004.

31. Itkis, M. E.; Perea, D.; Jung, R.; Niyogi, S.; Haddon, R. C., Comparison of Analytical Techniques for Purity Evaluation of Single-Walled Carbon Nanotubes. *J. Am. Chem. Soc.* **2005,** 127, 3439-3448.

32. Wu, Z. H.; Pittman, C. U.; Gardner, S. D., Nitric-Acid Oxidation of Carbon-Fibers and the Effects of Subsequent Treatment in Refluxing Aqueous NaOH. *Carbon* **1995,** 33, (5), 597-605.

33. Huang, H.; Kajiura, H.; Yamada, A.; Ata, M., Purification and Alignment of Arc-Synthesis Single-Walled Carbon Nanotube Bundles. *Chem. Phys. Lett.* **2002,** 356, 567-572.

34. Kuznetsova, A.; Popova, I.; Yates, J. T.; Bronikowski, M. J.; Huffman, C. B.; Liu, J.; Smalley, R. E.; Hwu, H. H.; Chen, J. G., Oxygen-Containing Functional Groups on Single Walled Carbon Nanotubes: NEXAFS and Vibrational Spectroscopic Studies. *J. Am. Chem. Soc.* **2001,** 123, (43), 10699-10704.

35. Chen, J.; Hamon, M. A.; Hu, H.; Chen, Y.; Rao, A. M.; Eklund, P. C.; Haddon, R. C., Solution Properties of Single-Walled Carbon Nanotubes. *Science* **1998,** 282, 95-98.

36. Worsley, K. A.; Kalinina, I.; Bekyarova, E.; Haddon, R. C., Functionalization and Dissolution of Nitric Acid Treated Single-Walled Carbon Nanotubes. *J. Am. Chem. Soc.* **2009,** 131, (50), 18153-18158.

37. Bates, R. G.; Pinching, G. D., Dissociation Constant of Aqueous Ammonia at 0 to 50°C from Emf Studies of the Ammonium Salt of a Weak Acid. *J. Am. Chem. Soc.* **1950,** 72, (3), 1393-1396.

38. Baigorri, R.; Fuentes, M.; Gonzalez-Gaitano, G.; Garcia-Mina, J. M.; Almendros, G.; Gonzalez-Vila, F. J., Complementary Multianalytical Approach To Study the Distinctive Structural Features of the Main Humic Fractions in Solution: Gray Humic Acid, Brown Humic Acid, and Fulvic Acid. *Journal of Agricultural and Food Chemistry* **2009,** 57, (8), 3266-3272.

39. Trigueiro, J. P. C.; Silva, G. G.; Lavall, R. L.; Furtado, C. A.; Oliveira, S.; Ferlauto, A. S.; Lacerda, R. G.; Ladeira, L. O.; Liu, J. W.; Frost, R. L.; George, G. A., Purity Evaluation of Carbon Nanotube Materials by

Thermogravimetric, TEM, and SEM Methods. *J. Nanosci. Nanotechnol.* **2007,** 7, (10), 3477-3486.

40. Hamon, M. A.; Itkis, M. E.; Niyogi, S.; Alvaraez, T.; Kuper, C.; Menon, M.; Haddon, R. C., Effect of Rehybridization on the Electronic Structure of Single-Walled Carbon Nanotubes. *J. Am. Chem. Soc.* **2001,** 123, 11292-11293.

Chapter 3

Isolation and Identification of Low Molecular Weight Carboxylated Carbons Derived from the Nitric Acid Treatment of Single-Walled Carbon Nanotubes

3.1 Introduction

Literature reports on the utilization of nitric acid in the oxidation of coal date to late 1800s.[1] This treatment was reported to form alkali-soluble material and has since been used on many forms of carbon including carbon fibers,[2, 3] petroleum asphaltenes,[4] carbon xerogels,[5] graphite,[6-8] and carbon nanotubes.[9-14] Although it is a well developed procedure, the mechanism of this reaction is generally described as complex due to the formation of several types of functionality resulting from the molecular rearrangements of chemisorbed oxygen. The severity of oxidation and type of functionality produced is known to be dependent on the extent of crystallinity and amount of surface area of the carbon material, and the conditions of the nitric acid treatment (temperature, pressure, concentration, reaction time).[15] IR spectroscopy[16] and acid-base

titrations[17] have been effective in monitoring the types and amounts of functionality, respectively, which have been shown to include carboxylic acids, ketones, alcohols, ethers, lactones, anhydrides and nitro groups.

The treatment of single-walled carbon nanotubes (SWNTs) with nitric acid is the most common oxidation reaction performed. Not only is it an effective method in the removal of residual metal catalysts, but it improves the processing of nanotubes by increasing the hydrophilicity and also provides carboxylic acid functionality which may be used for further functionalization of the nanotubes, improving the solubility in organic solvents.[18] It has also been observed that oxidation results in the generation of carboxylated carbons (CCs) that adhere to the surface of the nanotubes[9, 10, 13, 19-21] and which can be removed by filtration in under basic conditions.[10, 22-27] The structure of these molecules has been previously described as polycyclic aromatic sheets edge terminated with carboxylates (carboxylated carbon fragments, CCFs) together with cross-linked structures (carboxylated amorphous carbon, CAC).[9, 10]

Previous studies have isolated and identified the low molecular weight CCs formed from nitric acid oxidation of coal; these species include simple aliphatic dibasic acids (succinic, glutaric, and adipic), benzene carboxylic acids (benzene di-, tri-, tetra-, penta-carboxylic and mellitic acids), and picric acid.[15, 28-30] The yield of each species is reported to be dependant on the kind of coal, physical and chemical pretreatment, particle size, the presence of catalysts and the nitric acid reaction conditions.[28]

In this work, some of the low molecular weight CCs were isolated by Soxhlet extraction with tetrahydrofuran (THF) and were methylated using (trimethylsilyl)diazomethane ((TMS)CHN_2). The resulting species were separated by column chromatography and thin layer chromatography and identified by GC-MS and ^1H NMR.

3.2 Experimental Methods

3.2.1 Starting materials

SWNTs prepared by electric arc-discharge were obtained from Carbon Solutions Inc. (www.carbonsolution.com). The SWNTs were refluxed in concentrated nitric acid for 1 h and then purified by low speed centrifugation.[13, 31] All other chemicals were purchased from Aldrich and were used as received.

3.2.2 Extraction of CCs

The solvent was selected by first combining 10 mg of oxidized SWNT with 4 mL of various solvents. The mixtures were vigorously shaken and after precipitation, the absorption spectrum of the supernatant was measured. THF was selected based on the relative amount of material that dissolved.

A dry sample of SWNTs (4 g) was placed in a Saint-Gobain Alundum extraction thimble with pore size 5 μm and underwent extraction with THF for 4 days in a Soxhlet extractor. The filtrate collected was orange-brown in color and

was evaporated to dryness for further processing. The yield by mass of the remaining SWNTs was found to be approximately 98 %.

3.2.3 Functionalization and Separation

Approximately 75 mg (6.2 x 10^{-3} mol) of CC was dissolved in 40 mL of MeOH and the mixture was cooled to 0 ˚C in an ice bath. An excess of 2 M (TMS)CHN_2 (9 mL, 1.8 x 10^{-2} mol) in diethyl ether was added drop wise and the reaction mixture was allowed to warm to room temperature overnight. The crude product was evaporated to dryness on silica gel (400 mesh) and was separated into fractions by column chromatography using a hexane-ethyl acetate solution (4:1). The fractions were clear and colorless to pale yellow. Some fractions obtained contained several species and therefore, thin layer chromatography (TLC) was employed to further isolate these compounds. These separations occurred on silica gel aluminum foils with a 254 nm fluorescent indicator using hexane-ethyl acetate.

3.2.4 Characterization

The formation of methyl derivatives by (TMS)CHN_2 was verified by mid-IR transmission spectra obtained from thin films on a ZnSe substrate using a Nicolet Nexus FT-IR spectrometer at resolution of 8 cm^{-1}. The spectrometer chamber was purged with nitrogen during the spectra collection. The ^1H NMR spectra of the fractions collected were recorded at 300 MHz in $CDCl_3$ on a Bruker 300

spectrometer. The chemical shifts are given as δ values relative to tetramethylsilane as the internal standard.

GCMS analysis was performed at 70 eV with a Waters GCT instrument using a DB-5 capillary GC column. The mass spectrometer was set to acquire ions in the mass range 40 – 900 dalton. Each compound was identified by comparing the EI-MS data to known compounds in the National Institute of Standards and Technology (NIST) mass spectra database. The structures of compounds that were not identified in the NIST search were determined by using both ^{1}H NMR and FI-GCMS (field ionization - GCMS). FI was chosen because it is a very soft ionization process and ensures unambiguous identification of the parent ion, (M^{+}). ^{1}H NMR spectra were compared to data reported previously in literature.

3.3 Results and Discussion

3.3.1 Solvent Selection

The removal of CC from nitric acid treated carbon nanotube samples in the recent literature has usually employed strongly basic solutions such as aqueous NaOH.[10, 22-27] This is a tedious procedure which requires repeated filtration to remove all of the CC materials which are of a variety of compositions and molecular weights and is therefore restricted to analytical applications. In this study, facile removal of low molecular weight CC occurred by Soxhlet

extraction using THF. The solvent was selected based on the amount of material collected as compared to other solvents as seen in Figure 3.1.

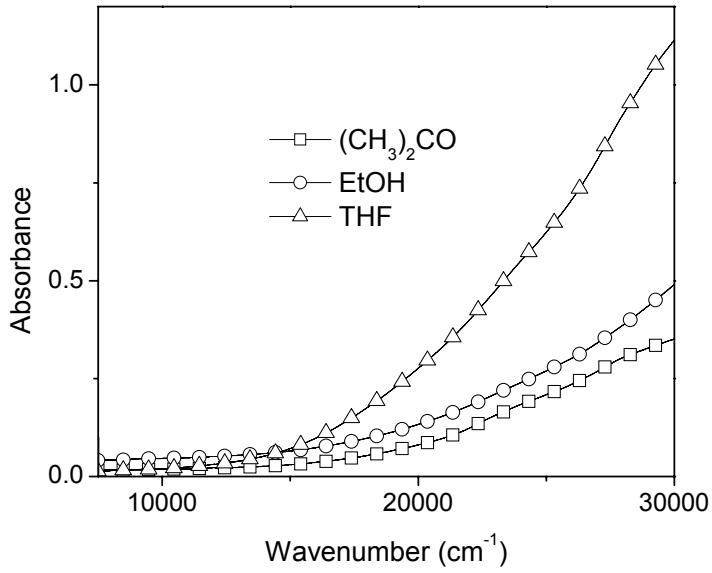

Figure 3.1: Near-IR absorbance spectra of CC removed from solvent washing with $(CH_3)_2CO$, EtOH and THF.

As noted by a number of authors, the color of the filtrate is an indication of the amount of material that is removed; the darker, and consequently, the higher the absorbance of the filtrate, the more concentrated the CC extract. It is presumed that THF is more effective than ethanol or acetone, as seen in the near-IR absorbance spectra of Figure 3.1, due to the relative basicities of each solvent (pK_a = -2.1, -2.3 and -7.2, respectively)[32-34] and its chemical compatibility.

3.3.2 Formation and Characterization of the Methyl Esters

The extracted material was isolated by evaporation, and underwent further processing with $(TMS)CHN_2$ according to the reaction scheme given below:

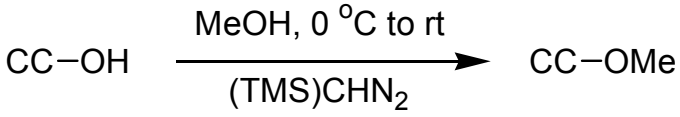

Figure 3.2: Reaction scheme.

Successful functionalization of the CC is supported by mid-IR spectroscopy (Figure 3.3). The small shift from 1735 cm^{-1} to 1740 $cm^{-1}$and the suppression of the broad band at 3200 cm^{-1}, which are assigned to the C=O and O-H stretching vibrations respectively, confirm the formation of the methylated material. Also present in both spectra are the 1550 cm^{-1} (asymmetric stretching) and 1360 cm^{-1} (symmetric stretching) bands attributed to $–NO_2$ functionality.

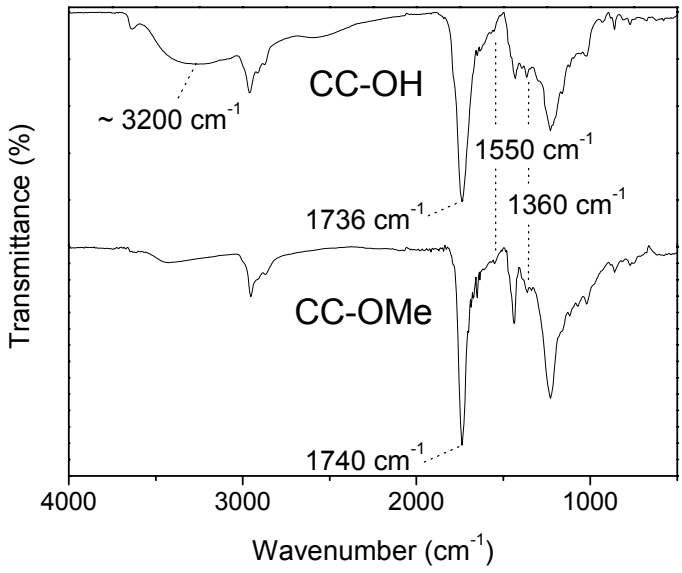

Figure 3.3: Baseline corrected mid-IR transmittance spectra of thin films of CCs in their acid form (CC-OH) and after methylation (CC-OMe) with (TMS)CHN_2.

3.3.3 Identification of the Methyl Esters

When analyzing the mass spectra of organic acids it is important to differentiate between the mass difference between carboxylic acid functionality (CO_2 = 43.9898 m/z) and that from polyethylene glycol (PEG, C_2H_4O = 44.0262 m/z). In this study, the resulting methyl derivatives were ideal for separation by chromatography in organic solvents and were unambiguously identified by GC-MS and ^1H NMR (given in the appendix). Table 3.1 gives the identified material and their methylated structures.

Table 3.1: The retention times, molecular weights (MW) and structures of the identified compounds.

Entry	Original Compound	Methylated Compound		
	Name	Retention Time (min)	Structure	MW (g/mol)
1	3,5-dinitrobenzoic acid	26.58	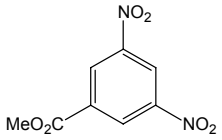	226
2	4-nitrophthalic acid	26.97	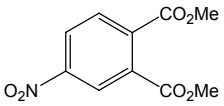	239
3	1,2-dihydroxy-4,5-dinitrobenzene	27.74	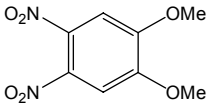	228
4	trimellitic acid	28.26	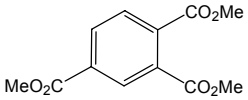	252
5	picric acid	29.20	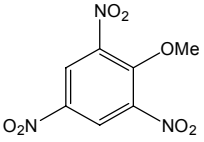	243
6	1,8-dinitronaphthalene	34.60	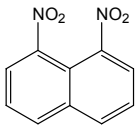	218
7	pyromellitic acid	34.72	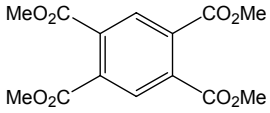	310

Table 3.1 continued:

Entry	Original Compound	Methylated Compound		
	Name	Retention Time (min)	Structure	MW (g/mol)
8	benzene pentacarboxylic acid	38.50	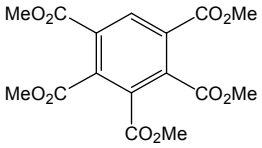	368
9	mellitic acid	41.81	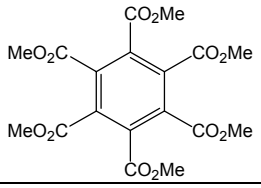	426

The CC material removed directly by THF extraction is comprised of small benzopolycarboxylic acids, alcohols and nitro compounds of low molecular weight (< 500 g/mol). These compounds are expected to be analogous to the larger polycyclic aromatic sheets and cross-linked structures that are generally referred to as humic acids.[29]

Due to the large scale of the extraction, the material removed could be fractionated to give an estimate of the yields of the individual compounds identified. Of the 75 mg of material collected after Soxhlet extraction, around half of the material remained on the column and with further separation by TLC, some of the isolated material was identified as contaminants that are not directly attributed to the synthesis or purification of the nanotubes. Contaminants include several common phthalates, THF stabilizers such as butylhydroxytoluene (BHT), and $(TMS)CHN_2$ reaction byproducts. The most abundant ester compounds

isolated from the reaction mixture were mellitic (~10 mg) and picric acids (~2 mg), followed by benzene pentacarboxylic and pyromellitic acids (~1 mg each). The remaining compounds constituted only a relatively small proportion of the isolated compounds (> 1 mg each).

3.4 Conclusions

The extracted methylated CCs of nitric acid purified SWNTs were identified using GC-MS and ^{1}H NMR and are found to be comprised of small benzopolycarboxyl acids and organic nitro compounds. The majority of the identified material has been seen in previous literature reports on the material isolated after the treatment of coal with similar oxidation treatments. The yield of each compound is roughly estimated, and as in the case of coal, is highly dependent on the starting SWNT sample, the nitric acid reaction conditions and overall processing of the material.

3.5 References

1. Friswill, D., *Proc. Chem. Soc.* **1892**, 9.

2. Wu, Z. H.; Pittman, C. U.; Gardner, S. D., Nitric-Acid Oxidation of Carbon-Fibers and the Effects of Subsequent Treatment in Refluxing Aqueous NaOH. *Carbon* **1995,** 33, (5), 597-605.

3. Lakshminarayanan, P. V.; Toghiani, H.; Pittman, C. U., Nitric Acid Oxidation of Vapor Grown Carbon Nanofibers. *Carbon* **2004,** 42, (12-13), 2433-2442.

4. Al-Samarraie, M. F.; Steedman, W., A Study of the Nitric Acid Oxidation of Petroleum Asphaltenes. *Liq. Fuels Tech.* **1985,** 3, (1), 55-71.

5. Silva, A. M. T.; Machado, B. F.; Figueiredo, J. L.; Faria, J. L., Controlling the Surface Chemistry of Carbon Xerogels using HNO3-hydrothermal Oxidation. *Carbon* **2009,** 47, (7), 1670-1679.

6. Scharff, P.; Xu, Z. Y.; Stumpp, E.; Barteczko, K., Reversibility of the Intercalation of Nitric-Acid into Graphite. *Carbon* **1991,** 29, (1), 31-37.

7. Sorokina, N. E.; Maksimova, N. V.; Avdeev, V. V., Anodic Oxidation of Graphite in 10 to 98% HNO3. *Inorg. Mater.* **2001,** 37, (4), 360-365.

8. Dreyer, D. R.; Park, S.; Bielawski, C. W.; Ruoff, R. S., The Chemistry of Graphene Oxide. *Chem. Soc. Rev.* **2010,** 39, (1), 228-240.

9. Liu, J.; Rinzler, A. G.; Dai, H.; Hafner, J. H.; Bradley, R. K.; Boul, P. J.; Lu, A.; Iverson, T.; Shelimov, K.; Huffman, C. B.; Rodriguez-Macias, F.; Shon, Y.-S.; Lee, T. R.; Colbert, D. T.; Smalley, R. E., Fullerene Pipes. *Science* **1998,** 280, 1253-1255.

10. Rinzler, A. G.; Liu, J.; Dai, H.; Nikolaev, P.; Huffman, C. B.; Rodriguez-Macias, F. J.; Boul, P. J.; Lu, A. H.; Heymann, D.; Colbert, D. T.; Lee, R. S.; Fischer, J. E.; Rao, A. M.; Eklund, P. C.; Smalley, R. E., Large-Scale Purification of Single-Wall Carbon Nanotubes: Process, Product and Characterization. *Appl. Phys. A* **1998,** 67, 29-37.

11. Vaccarini, L.; Goze, C.; Aznar, R.; Micholet, V.; Journet, C.; Bernier, P., Purification Procedure of Carbon Nanotubes. *Synth. Met.* **1999,** 103, 2492-2493.

12. Nagasawa, S.; Yudasaka, M.; Hirahara, K.; Ichihashi, T.; Iijima, S., Effect of Oxidation on Single-Walled Carbon Nanotubes. *Chem. Phys. Lett.* **2000,** 328, (4,5,6), 374-380.

13. Hu, H.; Zhao, B.; Itkis, M. E.; Haddon, R. C., Nitric Acid Purification of Single-Walled Carbon Nanotubes. *J. Phys. Chem. B* **2003,** 107, 13838-13842.

14. Tchoul, M. N.; Ford, W. T.; Lolli, G.; Resasco, D. E.; Arepalli, S., Effect of Mild Nitric Acid Oxidation on Dispersability, Size, and Structure of Single-Walled Carbon Nanotubes. *Chem. Mater.* **2007,** 19, (23), 5765-5772.

15. Krevelen, D. W., *Coal; Typology, Chemistry, Physics and Constitution*. Elsevier Pub. Co.: Amsterdam. New York, 1961; Vol. Coal: Typology, Chemistry, Physics, Constitution.

16. Zawadzki, J., IR Spectroscopic Investigations of the Mechanism of Oxidation of Carbonaceous Films with Nitric Acid Solution. *Carbon* **1980,** 18, (4), 281-285.

17. Boehm, H. P., *Chemical Identification of Surface Groups*. 1966; Vol. 16, p 179-264.

18. Hamon, M. A.; Chen, J.; Hu, H.; Chen, Y.; Itkis, M. E.; Rao, A. M.; Eklund, P. C.; Haddon, R. C., Dissolution of Single-Walled Carbon Nanotubes. *Adv. Mater.* **1999,** 11, 834-840.

19. Hamon, M. A.; Hu, H.; Bhowmik, P.; Niyogi, S.; Zhao, B.; Itkis, M. E.; Haddon, R. C., End-Group and Defect Analysis of Soluble Single-Walled Carbon Nanotubes. *Chem. Phys. Lett.* **2001,** 347, (1-3), 8-12.

20. Hu, H.; Bhowmik, P.; Zhao, B.; Hamon, M. A.; Itkis, M. E.; Haddon, R. C., Determination of the Acidic Sites of Purified Single-Walled Carbon Nanotubes by Acid-Base Titration. *Chem. Phys. Lett.* **2001,** 345, 25-28.

21. Hamon, M. A.; Hu, H.; Bhowmik, P.; Itkis, M. E.; Haddon, R. C., Ester-Functionalized Soluble Single-Walled Carbon Nanotubes. *Appl. Phys. A* **2002,** 74, 333-338.

22. Salzmann, C. G.; Llewellyn, S. A.; Tobias, G.; Ward, M. A. H.; Huh, Y.; Green, M. L. H., The Role of Carboxylated Carbonaceous Fragments in the Functionalization and Spectroscopy of a Single-Walled Carbon-Nanotube Material. *Adv. Mater.* **2007,** 19, (6), 883-887.

23. Yu, H.; Jin, Y. G.; Peng, F.; Wang, H. J.; Yang, J., Kinetically Controlled Side-Wall Functionalization of Carbon Nanotubes by Nitric Acid Oxidation. *J. Phys. Chem. C* **2008,** 112, (17), 6758-6763.

24. Fogden, S.; Verdejo, R.; Cottam, B.; Shaffer, M., Purification of Single Walled Carbon Nanotubes: The Problem with Oxidation Debris. *Chem. Phys. Lett.* **2008,** 460, (1-3), 162-167.

25. Wang, Z.; Shirley, M. D.; Meikle, S. T.; Whitby, R. L. D.; Mikhalovsky, S., The Surface Acidity of Acid Oxidised Multi-walled Carbon Nanotubes and the Influence of In-situ Generated Fulvic Acids on their Stability in Aqueous Dispersions. *Carbon* **2009,** 47, (1), 73-79.

26. Price, B. K.; Lomeda, J. R.; Tour, J. M., Aggressively Oxidized Ultra-Short Single-Walled Carbon Nanotubes Having Oxidized Sidewalls. *Chem. Mater.* **2009,** 21, (17), 3917-3923.

27. Worsley, K. A.; Kalinina, I.; Bekyarova, E.; Haddon, R. C., Functionalization and Dissolution of Nitric Acid Treated Single-Walled Carbon Nanotubes. *J. Am. Chem. Soc.* **2009,** 131, (50), 18153-18158.

28. Grosskinsky, O., Oxidation of Coal with Nitric Acid. *Glueckauf* **1952,** 88, 376-9.

29. Franke, N. W.; Kiebler, M. W.; Ruof, C. H.; Savich, T. R.; Howard, H. C., Water-Soluble Polycarboxylic Acids by Oxidation of Coal. *Ind. Eng. Chem.* **1952,** 44, (11), 2784-2792.

30. Benning, A., The Importance of Nitric Acid Oxidation in Clarification of the Constitution of Coal. *Brennstoff-Chemie* **1955,** 36, 38-43.

31. Hu, H.; Yu, A.; Kim, E.; Zhao, B.; Itkis, M. E.; Bekyarova, E.; Haddon, R. C., Influence of the Zeta Potential on the Dispersability and Purification of Single-Walled Carbon Nanotubes. *J. Phys. Chem. B* **2005,** 109, 11520-11524.

32. Arnett, E. M.; Wu, C. Y., Stereoelectronic Effects on Organic Bases .3. The Basicities of Some Saturated Ethers in Aqueous Sulfuric Acid. *J. Am. Chem. Soc.* **1960,** 82, (18), 4999-5000.

33. Newall, C. E.; Eastham, A. M., Relative Basicities of Water, Methanol, and Ethanol. *Can. J. Chem.* **1961,** 39, (9), 1752-6.

34. Campbell, H. J.; Edward, J. T., Ionization of Organic Compounds in Acid .1. Aliphatic Ketones. *Can. J. Chem.* **1960,** 38, (11), 2109-2116.

3.6 Appendix

Methyl 3,5-dinitrobenzoate (1):

EI-MS (70 eV): m/z (%): 226 (M^+, 15), 196 (66), 195 (86), 181 (19), 149 (38), 133 (19), 102 (14), 75 (100), 74 (52), 44 (20). NIST similarity index: 92.4 %.

4-Nitrophthalic acid dimethyl ester (2):

EI-MS (70 eV): m/z (%): 239 (M^+, 3), 209 (11), 208 (100), 162 (40), 161 (7), 103 (12), 76 (12), 75 (26), 74 (14), 44 (13). NIST similarity index: 96.2 %.

1,2-Dinitro-4,5-dimethoxybenzene (3):

EI-MS (70 eV): m/z (%): 228 (M^+, 100), 181 (41), 137 (29), 93 (29), 92 (29), 78 (29), 76 (52), 75 (41), 50 (38), 44 (68). NIST similarity index: 91.5 %.

Trimellitic acid trimethyl ester (4):

EI-MS (70 eV): m/z (%): 252 (M^+, 6), 222 (14), 221 (100), 162 (26), 119 (8), 103 (21), 76 (8), 75 (19), 74 (9), 44 (10). NIST similarity index: 95.1 %.

Methyl picrate (5):

EI-MS (70 eV): m/z (%): 243 (M^+, 23), 214 (7), 213 (100), 196 (10), 166 (12), 120 (7), 93 (17), 80 (9), 75 (42), 62 (19). ^{1}H NMR ($CDCl_3$, 300 MHz): δ (ppm) 4.19 (s, 3H), 8.91 (s, 2H).

1,8-dinitronaphthalene (6):

EI-MS (70 eV): m/z (%): 218 (M^+, 9), 172 (65), 142 (18), 116 (13), 115 (14), 114 (100), 113 (28), 88 (21), 63 (13), 44 (12). NIST similarity index: 97.5 %.

Pyromellitic acid tetramethyl ester (7):

EI-MS (70 eV): m/z (%): 310 (M^+, 1), 280 (14), 279 (100), 233 (33), 162 (29), 161 (14), 103 (13), 75 (21), 74 (13), 44 (20). NIST similarity index: 79.1 %.

Benzenepentacarboxylic acid pentamethyl ester (8):

EI-MS (70 eV): m/z (%): 368 (M^+, 1), 338 (18), 337 (100), 291 (25), 220 (14), 162 (23), 161 (11), 104 (13), 75 (11), 44 (80). ^{1}H NMR ($CDCl_3$, 300 MHz): δ (ppm) 3.89 (s, 3H), 3.96 (s, 12H), 8.68 (s,1H).

Mellitic acid hexamethyl ester (9):

EI-MS (70 eV): m/z (%): 426 (M^+, 1), 396 (21), 395 (100), 364 (5), 349 (20), 293 (5), 220 (8), 162 (13), 104 (10), 44 (14). NIST similarity index: 97.2 %.

Chapter 4

Functionalization and Dissolution of Nitric Acid Treated Single-Walled Carbon Nanotubes

4.1 Introduction

While there has been substantial progress in the purification of SWNTs,[1-18] outstanding questions remain and the resolution of this issue constitutes one of the most serious obstacles to the realization of high quality SWNT specialty chemicals and to the exploitation of the unique properties of this material.[19-21] The contaminants in the as-prepared materials (AP-SWNTs) are comprised of residual metal catalysts and carbonaceous byproducts including amorphous carbon (AC) and graphitized carbon nanoparticles (CNPs), which are generated by the various preparative techniques (electric arc, CVD, laser oven). Oxidative procedures are often employed as a first step in the removal of these impurities,[13, 20] and the most common technique involves a reflux of the AP-SWNTs in nitric acid.[1, 2, 22] This treatment reduces the metal content, but it is known to consume some of the SWNTs and to produce additional carbonaceous

impurities, commonly referred to as carboxylated carbons (CCs).[1, 2, 22-25] The nature of this problem was first recognized by the Smalley group who identified the CCs as polycyclic aromatic sheets, edge terminated with carboxylates (carboxylated carbon fragments, CCFs) together with cross-linked structures (carboxylated amorphous carbon, CAC).[1, 2] While filter washing with mildly basic solution was shown to be effective in removing the CCs on a small scale, these workers noted that the process could not be scaled due to the tendency of the retained SWNTs to pack together and inhibit the filtration process as they accumulate deposited CCs.[2] The large scale purification of the nitric acid treated SWNTs utilized centrifugation followed by cross-flow filtration and an additional "polishing" step.[1, 2]

Shortly thereafter the Haddon group introduced soluble SWNTs by chemically functionalizing the carboxylic acid groups that are introduced by nitric acid treatment with octadecylamine to produce SWNTs terminated with long chain amides (SWNT-CONH$(CH_2)_{17}CH_3$).[26] Given the presence of CCs, the nature of the soluble SWNTs was of interest and the Haddon research group undertook a number of studies to clarify the role of carboxylated impurities in the dissolution process. The amount of end-group and defect sites present in nitric acid treated SWNT samples was analyzed;[23, 27] this was accomplished by converting the carboxylic acid groups to octadecylamide (SWNT-CONH$(CH_2)_{17}CH_3$) and octadecylester (SWNT-COO$(CH_2)_{17}CH_3$) groups via the acylchloride. It was reported that the loading of octadecylamino (ODA) and

octadecyloxy (ODO) groups present in the sample was higher than the expected value of 0.25 mol percent functionality which would be characteristic of a perfect 100 nm long (10,10) SWNT, which is cut perpendicular to the nanotube axis and terminated with carboxylic acid groups.[23, 27] This result indicated that contaminating CCs could be retained in the samples that were produced during the nitric acid treatment, together with end- and defect-functionalized SWNTs.

The presence of highly carboxylated contaminants in the nitric acid treated SWNTs was further supported by the high acid content determined by acid–base titrations also reported by the Haddon group, which exceeded the theoretical value (above) by an order of magnitude in some cases.[24] The titration experiments were carried out in two steps: (1) a forward titration with base in which the conjugate base of the SWNT-COOH material was isolated by filtration, (2) a reverse titration step with acid neutralization of the conjugate base (SWNT-COO^- Na^+) isolated in the first step. In general it was found that the acid content determined in the forward step (1) was higher than that in the reverse step (2), and the difference was attributed to the partial purification which is achieved in the basic titration as a result of dissolution of the CCs in step (1).[24]

The Haddon group then utilized chromatography to investigate the nature of the material that was taken into solution by the ODA functionalization; due to the high solubility of ODA functionalized SWNTs, this material could be separated on HPLC columns resulting in fractions of SWNT-ODA and CC-ODA that were characterized by AFM, UV–vis absorption and emission, near-IR, and

Raman spectroscopy.[28, 29] The fact that the SWNT-CONH$(CH_2)_{17}CH_3$ fraction which separated on the column was recovered in high yield from the HPLC experiment suggested that this material maintained its solubility in the absence of functionalized CCs.

Recently there has been a resurgence of interest in this issue, and several groups have reported the removal of CCFs by washing nitric acid treated CNTs with NaOH.[30-34] In some cases it was found that the majority of the carboxylic acid functionality was present on the CCFs and that this contaminant must be removed prior to chemical functionalization.

Surfactants[2] and side-wall functionalization[35-40] have been extensively employed to disperse SWNTs, but noncovalent interactions and π-stacking routes for the dissolution of SWNTs have also become well developed.[41-48] It is therefore plausible that it is the absorption of the functionalized CCFs on the SWNT surface that is responsible for the dissolution of materials such as SWNT-CONH$(CH_2)_{17}CH_3$.[30-33]

There have been substantial advances in the analysis and postprocessing of nitric acid treated SWNTs so that it is now possible to contemplate the essentially complete removal of the CCs which is considered to be comprised of CAC and CCFs.[1-3, 13, 20, 22, 49-51] Thus it seemed worthwhile to revisit this issue, and consequently, base washed nitric acid treated electric arc SWNTs (SWNT-COOH) that had been purified by low speed centrifugation,[22, 50] were functionalized with octadecylamine (ODA) and fully characterized (both starting

material, SWNT-COOH and products, SWNT-CONH$(CH_2)_{17}CH_3$). It is the purpose of this chapter to investigate the removal of the CCs and the role of this contaminant in the dissolution of SWNTs chemically functionalized with long chain amides (SWNT-CONH$(CH_2)_{17}CH_3$). The results lead to a consistent picture of the effect of base washing on SWNTs, the presence of residual carboxylic acid functionality, and the role of CCs in the solubility of functionalized SWNTs.

4.2 Experimental Methods

4.2.1 Starting Materials and Characterization

As prepared SWNTs, produced by electric arc discharge, were obtained from Carbon Solutions, Inc. (www.carbonsolution.com). The SWNTs were refluxed in concentrated nitric acid for 1.5 h and then purified by low speed centrifugation.[22, 50] Other chemicals were purchased from Aldrich and used without further treatment. The sonication of samples was performed in a VWR Ultrasonic Bath sonicator (model 550HT). Solution phase near-IR data was collected in a quartz cell of 1 cm path length on a Varian Cary 5000 spectrophotometer. The mid-IR spectra of the materials reported in Figure 4.5, were obtained from thin films on a ZnSe substrate using a Nicolet Nexus FT-IR spectrometer at resolution of 8 cm^{-1} and the spectrometer chamber was purged with nitrogen during the spectra collection. TGA was preformed at a heating rate

of 5 ºC/min in air using a Pyris 1 thermogravimetric analyzer (Perkin-Elmer). Raman spectra of the starting material and products were collected from a Bruker RFS 100/S type FT-Raman spectrometer using a Nd:YAG laser excitation source with a wavelength of 1064 nm and a resolution of 8 cm^{-1}. Images from a high resolution transmission electron microscope (TEM) were obtained from a Technai 12 instrument operating at a 120 kV accelerating voltage.

4.2.2 Concentration Optimization Procedure

The optimal concentration of the NaOH solution for base washing the SWNT-COOH material were determined by conducting a series of experiments to measure the amount of CCs that were removed in a single wash. For these experiments, 100 mg of purified, nitric acid treated SWNT-COOH (0W) was dispersed in 100 mL of 0.001, 0.01, 0.1, or 1 M NaOH by sonication (~30 min) in a polyethylene container; this mixture was allowed to stir for 48 h under argon. The black mixture was filtered through a Millipore Durapore membrane with a pore size of 0.22 μm and a diameter of 90 mm supported on a stainless steel frit. The filtrate was then diluted to 500 mL, and the absorbance at 550 nm was measured and normalized by the concentration (A × 0.5 L/0.1 g).

4.2.3 Base Washing Procedure

Once the concentration of the base was optimized, successive base washings were performed in a Teflon beaker: 500 mg of 0W SWNT-COOH were

dispersed in 500 mL of 0.01 M NaOH by sonication for 30 min followed by stirring for 1 h. To facilitate the filtration, which is very slow in the presence of high concentrations of CCs,[2, 20] the mixture was divided into two equal portions which were processed in separate filtering stations comprised of a Millipore Durapore membrane with a pore size of 0.22 μm and a diameter of 90 mm supported on a stainless steel frit. The material was recombined, and either the solid was neutralized (1W) or the previous steps were repeated two more times (3W) or until the filtrate was colorless (FW). All samples were neutralized by addition of 500 mL of 0.01 M HCl. These mixtures were filtered using 0.4 μm polycarbonate membranes and were washed with DDI water until the filtrate was pH neutral. Each material was collected, dried, and fully characterized before undergoing functionalization.

4.2.4 Acid Neutralization Procedure

The acid content was determined by directly neutralizing each of the materials with NaOH.[52] Briefly, 100 mg of SWNT-COOH material were combined with 25 mL of 0.0125 M NaOH in a sealed polyethylene container. After 48 hours of stirring under Ar, the pH was measured with a Corning pH meter 445, and this value was compared to a blank solution (without SWNT material) that underwent the same process.

4.2.5 Synthesis of SWNT-CONH(CH_2)$_{17}$$CH_3$

Functionalization of the carboxylic acid groups of the washed samples (1W, 3W, and FW) and the starting material (0W) was achieved by use of the 1,3-dicyclohexylcarbodiimide (DCC) coupling reaction. Approximately 100 mg (8.3 mmols) of material were sonicated in 100 mL of anhydrous *N,N*-dimethylformamide (DMF, DrySolv) for 10 h. In an argon atmosphere, the homogeneous suspension was then combined with 1 g (4.8 mmols) of DCC and was stirred for 30 min at room temperature. Then 1 g (3.7 mmols) of octadecylamine (ODA) was added, and the reaction temperature was raised to 120 ˚C. After 6 days, the resulting solution was cooled to room temperature and filtered on a 0.2 µm Millipore Fluoropore membrane. The material was then redispersed in DMF and filtered repeatedly until the filtrate was colorless; this step was then repeated with ethanol. The resulting black solid was dried at room temperature under vacuum in a desiccator (yield by weight was 100–110%).

4.2.6 ODA Loading Calculation by Mid-IR

By using the *v*(C-H) stretching vibrations that originate from the alkyl chains of the ODA in the mid-IR range, one can calculate the loading of ODA in the functionalized material based on a series of standard solutions of ODA in CCl_4.[23]

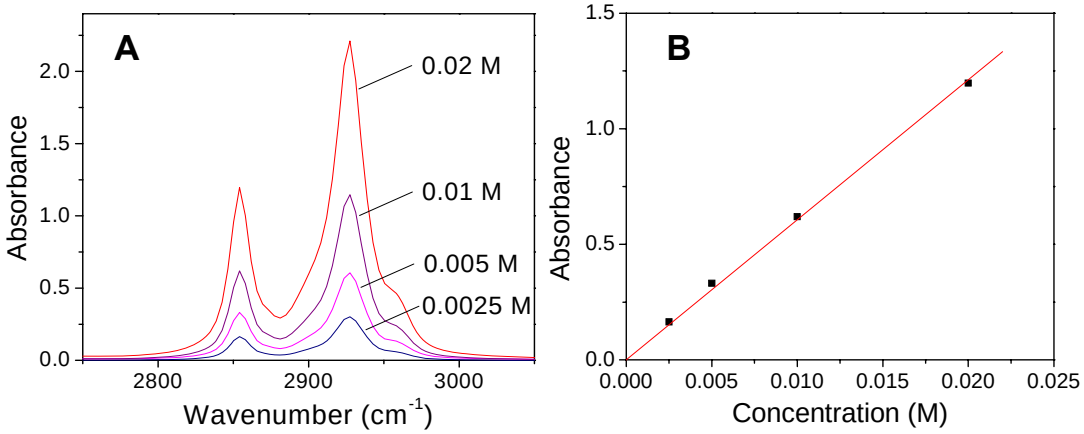

Figure 4.1: (A) Absorbance spectra showing the *v*(C-H) stretching vibrations of the ODA standard solutions in CCl_4 using a quartz cell with path length of 1 mm. (B) Absorbance at 2854 cm^{-1} versus concentration for the ODA standard solutions. Slope = 61 L/mol, R^2 = 0.9996

Figure 4.1A shows the absorbance spectra of standard concentrations of ODA in CCl_4. The absorbance is then measured for each standard at 2854 cm^{-1}, and is plotted against the concentration and fitted with a straight line passing through zero (Figure 4.1B). By measuring the absorbance of a known weight of material, the concentration of the ODA in the sample can be determined. This is then multiplied by the molecular weight of ODA (ODA_{MW} = 269.51 g/mol) and divided by the original sample weight to give the weight percent loading of ODA.

4.2.7 ODA Loading Calculation by Acid Neutralization

The concentration of NaOH remaining, $[OH^-]$, in each solution of ~0.1 g of SWNT-COOH in 25 mL of 0.0125 M NaOH, can be determined by measuring the pH and using the following equations:

$$14 - pH = pOH \quad (1)$$

$$pOH = - \log[OH^-] \quad (2)$$

The number of mmols of OH^- are then calculated by multiplying by the volume (0.025 L). The difference between the number of mmols of OH^- of the blank and that in the sample is assumed to be the number of mmols of OH^- that were needed to neutralize the acid functionality present in the sample.[52] This value is then divided by the starting mass (0.1 g) to determine the acid content (given in meq/g). In order to convert this result into mol%, the number of eq/g is multiplied by the atomic weight of carbon (C_{AW} = 12.01 g/mol).

For example:

The pH of a 0.1024 g sample of 0W SWNT-COOH and that of the blank solution was measured to be 11.45 and 12.10, respectively.

Blank $[OH^-_B]$: Moles of base in blank

$$pOH = 14 - 12.10$$
$$pOH = 1.90$$
$$1.90 = - \log[OH^-_B]$$
$$[OH^-_B] = 0.01259\ M$$
$$0.025\ L \times [OH^-_B] = 0.3147\ mmols\ OH^-_B$$

0W SWNT-COOH $[OH^-_{0W}]$:

$$pOH = 14 - 11.45$$
$$pOH = 2.55$$
$$2.55 = -\log[OH^-_{0W}]$$
$$[OH^-_{0W}] = 0.002818\ M$$
$$0.025\ L \times [OH^-_{0W}] = 0.07046\ mmols$$

Acid Content:

$$\frac{0.3147\ mmols - 0.07046\ mmols}{0.1024\ g} = 2.385\ mmols/g$$ 2.4 meq/g

$$\frac{2.385\ mmols}{1\ g} \times \frac{12.01\ g}{1\ mol} \times \frac{1\ mol}{1000\ mmols} = 0.02864$$ 2.9 mol%

If one gram of SWNT-COOH was reacted with ODA, the theoretical ODA loading can be estimated by multiplying the acid content (in eq/g) by the molecular weight of ODA (ODA_{MW} = 269.51 g/mol). This value is the maximum mass of ODA that can be gained in the product, assuming that all acid sites are functionalized. This value divided by the total mass of the product (one gram plus the ODA mass) gives the theoretical ODA loading.

$$\frac{2.385\ mmols}{1\ g} \times \frac{1\ mol}{1000\ mmols} \times \frac{269.51\ g}{1\ mol} = 0.6428$$
$$\frac{0.6428}{0.6428 + 1} = 0.3913$$ 39%

4.2.8 Determination of the Solubility of SWNT-CONH(CH_2)$_{17}$$CH_3$

The solubility of the functionalized material in tetrahydrofuran (THF) was estimated from a saturated dispersion: 50 mg of the functionalized material and 5 mL THF were sonicated for 6 h, and the resulting suspension was allowed to stand overnight at room temperature. Then 50 µL of the upper layer were carefully removed by syringe and further diluted to 25 mL with THF. The concentration of the dispersions was calculated by estimation of the extinction coefficient at 550 nm, using a previously described procedure.[53]

4.3 Results and Discussion

4.3.1 Concentration Optimization for NaOH Washing of SWNT-COOH

The optimum pH for the extraction of the CCs by base washing nitric acid treated electric arc SWNTs (SWNT-COOH) that had been purified by low speed centrifugation[22, 50] was determined, while recognizing that this was unlikely to lead to a single step process for removal of the CCs (at least on any useful scale).[2, 20] Thus, the effect of a single base washing step over a range of pH values using aqueous solutions of NaOH with concentrations from 0.001 to 1 M was examined. As noted by a number of authors, the color of the filtrate is an indication of the amount of material that is being removed in the washing step; the darker and, consequently, the higher the absorbance of the filtrate, the more concentrated the CC extract.[30-32] Thus, the efficiency of the process was

monitored by spectroscopy (experimental section), by measuring the normalized absorbance of the extract at 550 nm. As may be seen from Figure 4.2A, the maximum absorbance of the filtrate from a single NaOH extraction occurred in the vicinity of pH 12 and presumably represents a compromise between a number of factors including the pK_a of the acid functionalities present in the CCs, the solution ionic strength, zeta potentials, and the filtration process. As explained below, this latter factor is the most important in determining the efficiency of the process.[2]

The removal of CCs by serial base washings (NaOH solution, pH=12) was performed to investigate the convergence of this technique. By using spectroscopic techniques the continued removal of CCs was detected until washing number 15 (Figure 4.2B). As noted previously, simple base washing is not a practical technique for the large scale purification of nitric acid treated SWNTs,[2, 20] because the SWNTs pack together as the volume of the dispersion is reduced in the filter funnel resulting in a nanotube cake that acts as a second membrane which hinders the separation of the CCs and dramatically slows the permeation rate of the NaOH solution; thus the area of the filter membrane is the critical parameter.[2]

The base washed SWNT-COOH material was characterized at various stages of the procedure: 0 washings, 1 washing, 3 washings, and full (15) washings (when no more material was observed to be removed), hereafter referred to as 0W, 1W, 3W, and FW, respectively. The acid content of each of

these samples was determined, the purity assessed by near-IR absorption spectroscopy, and the Raman spectrum obtained. Samples of each material were then functionalized with ODA and the ODA loading in the SWNT-$CONH(CH_2)_{17}CH_3$ product was estimated by mid-IR absorption.[23]

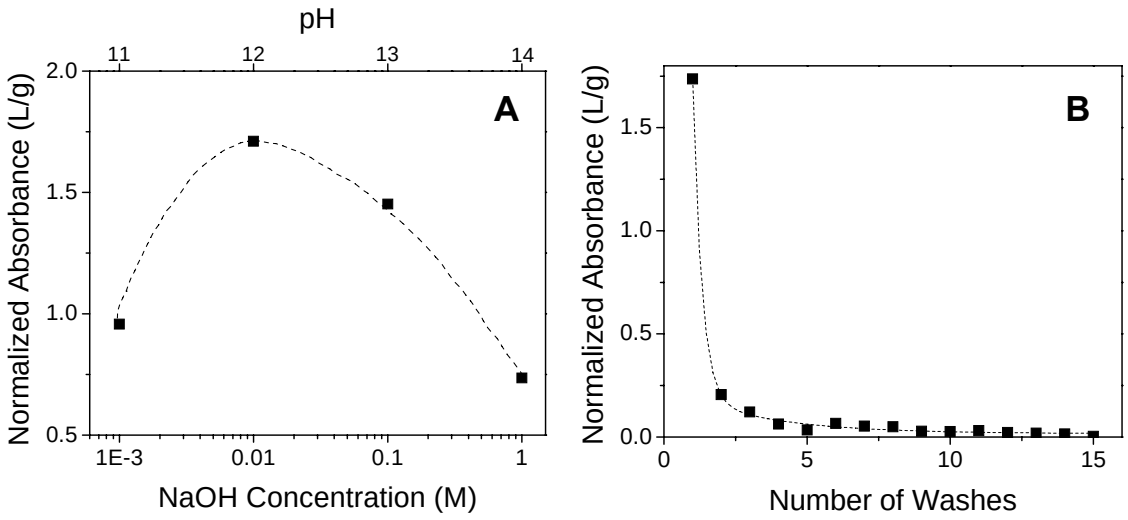

Figure 4.2: Normalized absorbance at 550 nm of the filtrate after base washing of nitric acid treated SWNTs. A) Single washing with 0.001, 0.01, 0.1, and 1 M NaOH; B) serial washing with 0.01 M NaOH.

4.3.2 Near-IR and Raman Scattering Characterization

The relative carbonaceous purity of each sample of the base washed SWNT-COOH materials was characterized by use of near-IR spectroscopy;[21, 54] the relative purity of the SWNTs increased monotonically with the number of base washing cycles performed on the starting material (Figure 4.3A) presumably because the removal of the CCs decreases the background absorption of the carbonaceous impurities which underlies the S_{22} interband

transition.[53, 55] The higher relative carbonaceous purity with increasing base wash cycles measured by near-IR analysis is supported by Raman spectroscopy (Figure 4.3B). As seen in previous studies,[30-32] the intensity ratio, I_D/I_G, is reduced upon base washing and the evolution toward an increasingly pure product from 0W to FW is observed.

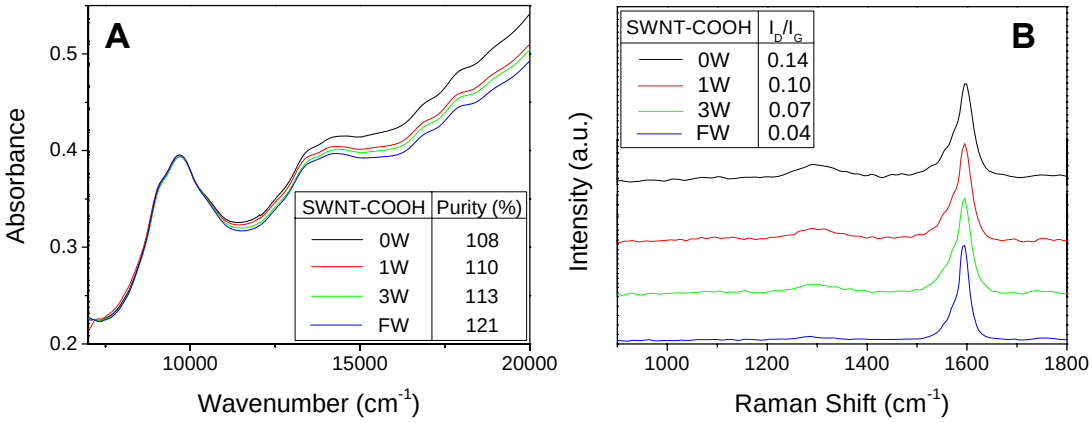

Figure 4.3: A) Near-IR spectra and relative carbonaceous purities, B) Raman spectra and I_D/I_G values of SWNT-COOH materials (0W, 1W, 3W, and FW correspond to 0, 1, 3, and full washes). Raman spectra are normalized at the G-band and shifted vertically for clarity.

4.3.3 Based Washed SWNT-COOH Functionalization

Functionalization of each material (0W, 1W, 3W, and FW) was accomplished by a DCC coupling reaction that resulted in the attachment of ODA through an amide linkage to give SWNT-CONH$(CH_2)_{17}CH_3$,[23, 25, 26, 56-58] as seen in the reaction scheme given below:

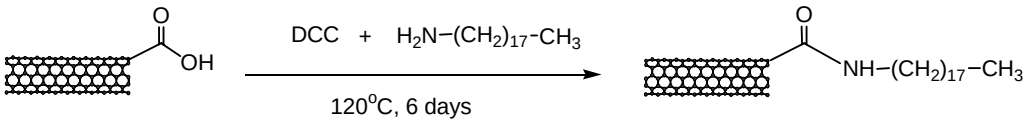

Figure 4.4: Schematic of reaction pathway.

Prior to functionalization, it is important to achieve a well dispersed mixture of SWNTs in DMF. For the reactions, a 10 h sonication treatment was employed to ensure that the material was fully dispersed within the solvent. Poor dispersions inhibit access of the reagents to the SWNT-COOH acid sites, which ultimately results in incomplete functionalization. After completion of the functionalization reaction, initial filtration of the reaction mixture gave rise to a dark filtrate which may be assigned to the functionalized impurities previously isolated by chromatography.[28, 29]

4.3.4 Mid-IR Characterization

The removal of acid sites and the occurrence of the functionalization reactions are supported by mid-IR spectroscopy. The broad peak centered at 1741 cm^{-1}, which is assigned to the C=O stretch of the carboxylic acid groups, decreases with base washing (Figure 4.5A). Upon formation of the amide linkage, well-defined peaks are observed (Figure 4.5B); the prominent bands at 2920 and 2850 cm^{-1} are due to the symmetric and asymmetric vibrations of the C-H groups, and the shift of the C=O stretch to 1655 cm^{-1} supports the

conversion of the carboxylic acid group to an amide.[23] The peaks at 1590 and 1465 cm^{-1} may be attributed to the C=C stretching of the polyaromatic backbone of the nanotubes. The peak at 1720 cm^{-1} may be assigned to the presence of residual lactones or anhydrides[59] that remain after functionalization.

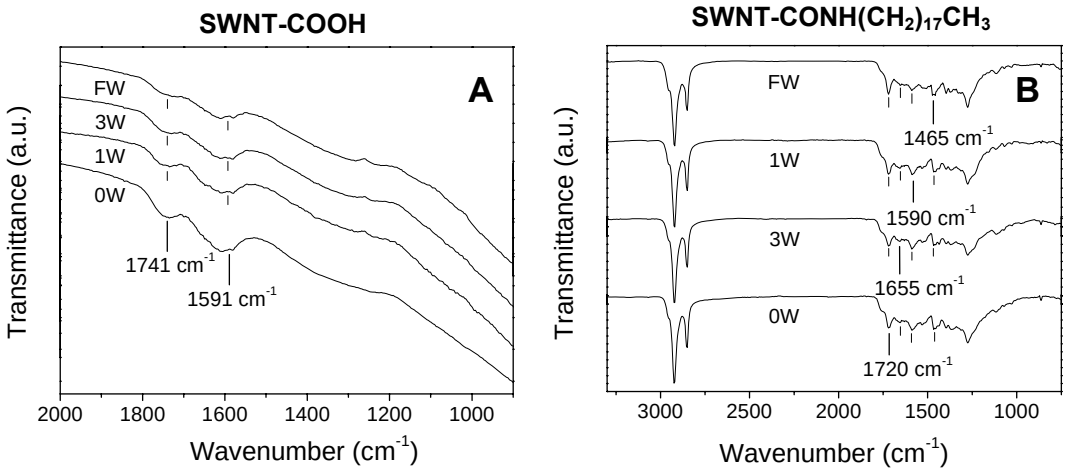

Figure 4.5: Mid-IR transmittance spectra of thin films of A) unfunctionalized SWNT-COOH material and B) SWNT-CONH$(CH_2)_{17}CH_3$ material (baseline corrected spectrum) deposited on a ZnSe substrate (0W, 1W, 3W, and FW correspond to 0, 1, 3, and full washes).

4.3.5 Characterization of Base Washed and Functionalized Materials by TGA

Identifying the burning temperatures of the individual components of carbon nanotube materials from a TGA scan is complicated by the interaction between the components – particularly the nature and quantity of metallic catalyst impurities. Due to the interaction between the components, the TGA usually consists of overlapping peaks that burn over a broad temperature range

as shown in the TG derivative data.[60] In Figure 4.6, the sharp peak at 480 ºC for the unwashed SWNT-COOH materials is evidently associated with the CCs due to its gradual disappearance with base washing. While this peak is prominent in the 0W material, it is estimated to be associated with no more than 17% of the total starting material by weight; this is comparable to the total weight of CCs removed at FW. The CC peak has an overlapping peak at about 515 ºC seen in the 0W SWNT-COOH material. With continual base washing, the burning temperature of this peak gradually shifts to 535 ºC as the CCs are completely removed. This peak and a broad peak at 700 ºC may be attributed to residual SWNTs and other large graphitic structures such as CNPs. When functionalized, a peak at 345 ºC appears, indicating the presence of the ODA in the samples. This peak is observed to be the largest in the 0W SWNT-CONH$(CH_2)_{17}CH_3$ material, indicating a higher loading when compared to the other functionalized material.

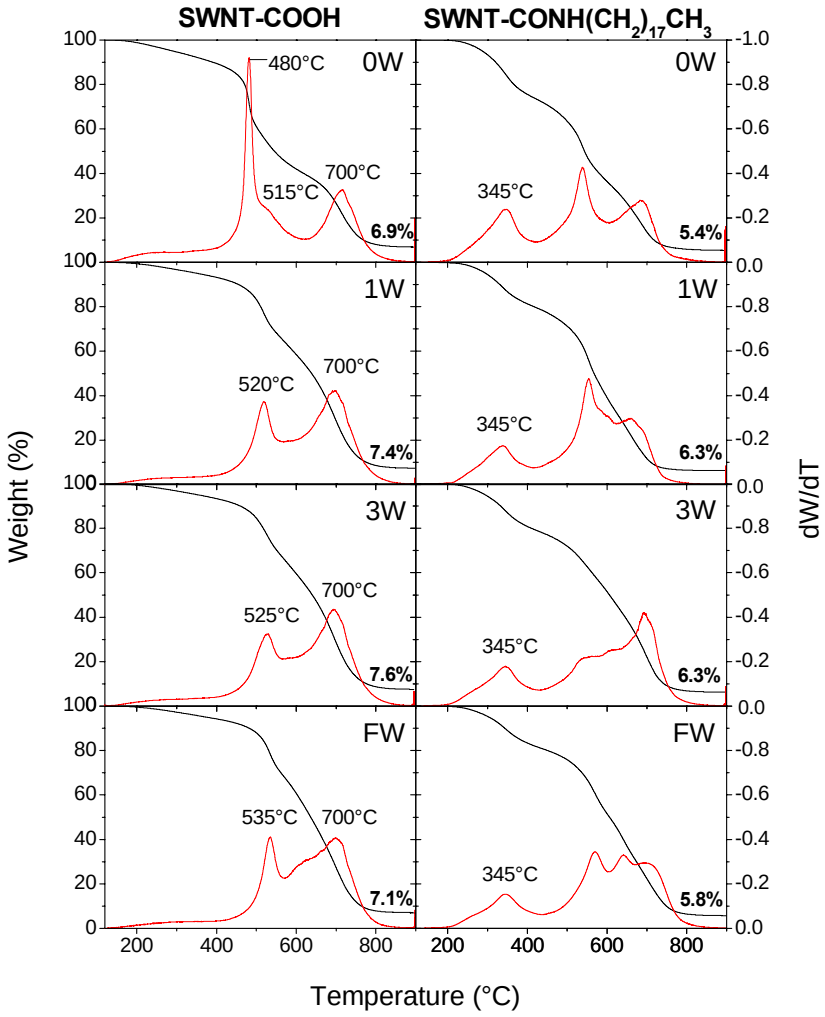

Figure 4.6: TGA measurements showing weight change (black line) and its derivative (red), together with residual metal oxide: base washed samples (left column, SWNT-COOH) and functionalized samples (right column, SWNT-$CONH(CH_2)_{17}CH_3$) (0W, 1W, 3W, and FW correspond to 0, 1, 3, and full washes).

4.3.6 ODA Loading by Mid-IR Spectroscopy and Acid Neutralization Techniques

It was previously shown that solution phase mid-IR spectroscopy may be used to determine the loading of the ODA functionality present in the SWNT-$CONH(CH_2)_{17}CH_3$ material based upon the measured absorbance of the C-H stretch at a known sample concentration.[23] The reduction in the degree of functionalization of the SWNT-$CONH(CH_2)_{17}CH_3$ material with base washing of the starting material suggests that under standard washing conditions some of the CCs become functionalized and are retained in the final product. In a previous determination of the acid content of the SWNT-COOH material an acid–base titration sequence was utilized as discussed above.[24, 61] However this method involves the filtration of a basic dispersion of the SWNT-COOH material, and it was previously reported that it removes CCs in the first step of the procedure;[24] thus in the present work, direct base titration experiments were employed to determine the acid content.[52] If none of the CCs were removed during functionalization, the loading of ODA determined for the SWNT-$CONH(CH_2)_{17}CH_3$ material would be identical to the values obtained from the acid content data in the SWNT-COOH starting material; the fact that the degree of functionalization is always less than the acid content data suggests that the filtration with DMF and then ethanol during the workup of the reaction is partially effective in removing the functionalized CCs.

Table 4.1: Estimated ODA loading (Weight Percent) in SWNT-$CONH(CH_2)_{17}CH_3$.[a]

Sample	Mid-IR Data			Acid Content Data		
	Sample Weight (mg)	ODA Weight (mg)	ODA Loading (%)	Acid Content of Starting Material (mol %)	Acid Content of Starting Material (meq/g)	Theoretical ODA Loading (%)
0W	1.0	0.33	33	2.9	2.4	39
1W	0.9	0.22	25	1.9	1.6	30
3W	1.0	0.24	24	1.6	1.4	27
FW	1.0	0.20	20	1.2	1.0	21

[a]Materials calculated from solution phase mid-IR and acid content data. 0W, 1W, 3W, and FW correspond to 0, 1, 3, and full washes.

As seen in Table 4.1, there is a gradual decrease in the degree of functionality for both the starting material and functionalized samples as a function of the number of base wash cycles. The analysis shows that the amount of acid sites is reduced from 2.4 to 1.0 meq/g; this is still higher than the value of 0.25 mol percent functionality (0.21 meq/g), which would be characteristic of a perfect 100 nm long (10,10) SWNT, which is cut perpendicular to the nanotube axis.[23, 27] Nevertheless this value represents a theoretical minimum for SWNTs of this length, and given the damage that is apparent after nitric acid treatment,[57, 62] it may be that this result is characteristic of such samples.

4.3.7 TEM Comparison of Base Washed and Functionalized Materials

TEM images verify the effectiveness of functionalization and the base wash in purifying nitric acid treated SWNTs (Figure 4.7). In the SWNT-COOH starting material (0W), the nanotubes have a web-like coating along the side walls which presumably corresponds to the CCs. After several washes with dilute NaOH, the material is freed from this coating and well-defined side-walls become visible (FW). Upon functionalization the final SWNT-CONH$(CH_2)_{17}CH_3$ materials are indistinguishable, and it is apparent that the careful workup of functionalized SWNTs and exhaustive base washing of the starting SWNT-COOH material are effective in producing high quality materials.

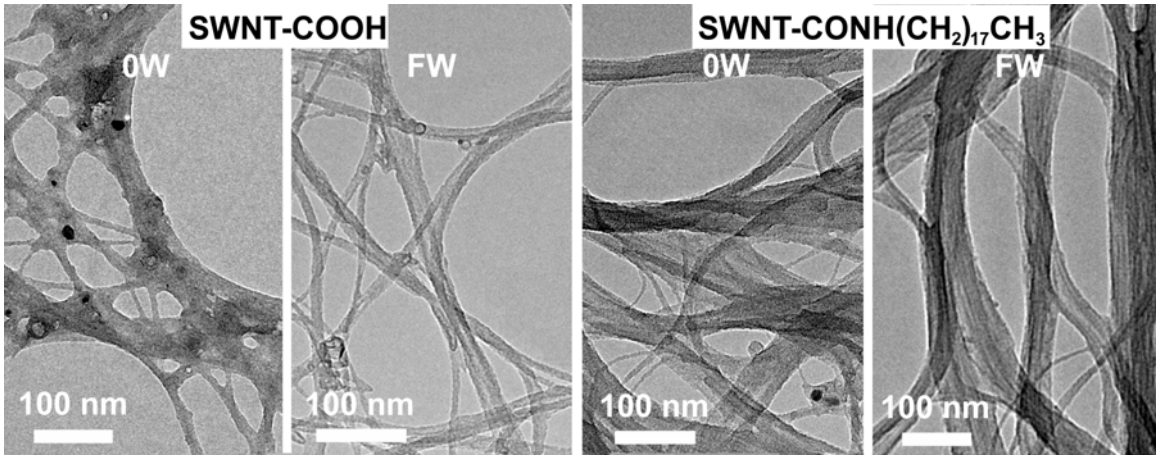

Figure 4.7: TEM images of unfunctionalized (SWNT-COOH) and functionalized SWNT-CONH$(CH_2)_{17}CH_3$ samples (0W and FW correspond to 0 and full washes).

4.3.8 Solubility of Functionalized Materials

Finally, the solubility of each of the functionalized materials was evaluated by using the extinction coefficients calculated for each material at 550 nm. The solubility of SWNT-CONH$(CH_2)_{17}CH_3$ was found to be approximately constant at 7 g/L (Table 4.2), and thus the CCs retained in the samples exert a relatively minor effect on the dissolution of this material. These SWNT derivatives dissolve in organic solvents in much the same way as high polymers to give extremely viscous solutions. This result serves to emphasize the ability of chemical functionalization to modify and enhance the properties of single-walled carbon nanotubes and encourages the view that SWNT specialty chemicals are within reach.

Table 4.2: Solubility data of functionalized material calculated from the respective extinction coefficient.[a]

SWNT-CONH$(CH_2)_{17}CH_3$	**ε (L/g·cm)**	**solubility (g/L)**
0W	19	7.6
1W	21	7.6
3W	21	7.0
FW	20	6.6

[a]0W, 1W, 3W, and FW correspond to 0, 1, 3, and full washes.

4.4 Conclusions

Nitric acid purification of SWNTs generates carboxylic acid functionalized carbon nanotubes and carbon fragments. The degree of functionalization and the concentration of the carboxylated carbons in the final product are dependent on the nature of the acid treatment and the postprocessing of the SWNT product. However, even after exhaustive base washing, the SWNTs contain detectable amounts of acid functionality which are susceptible to covalent chemical functionalization reactions in quantities that are sufficient to modify the material properties and, in the case of octadecylamine functionalization, to produce compounds that are soluble in organic solvents.

4.5 References

1. Liu, J.; Rinzler, A. G.; Dai, H.; Hafner, J. H.; Bradley, R. K.; Boul, P. J.; Lu, A.; Iverson, T.; Shelimov, K.; Huffman, C. B.; Rodriguez-Macias, F.; Shon, Y.-S.; Lee, T. R.; Colbert, D. T.; Smalley, R. E., Fullerene Pipes. *Science* **1998,** 280, 1253-1255.

2. Rinzler, A. G.; Liu, J.; Dai, H.; Nikolaev, P.; Huffman, C. B.; Rodriguez-Macias, F. J.; Boul, P. J.; Lu, A. H.; Heymann, D.; Colbert, D. T.; Lee, R. S.; Fischer, J. E.; Rao, A. M.; Eklund, P. C.; Smalley, R. E., Large-Scale Purification of Single-Wall Carbon Nanotubes: Process, Product and Characterization. *Appl. Phys. A* **1998,** 67, 29-37.

3. Dillon, A. C.; Gennett, T.; Jones, K. M.; Alleman, J. L.; Parilla, P. A.; Heben, M. J., A Simple and Complete Purification of Single-Walled Carbon Nanotube Materials. *Adv. Mater.* **1999,** 11, (16), 1354-1358.

4. Zimmerman, J. L.; Bradley, R. K.; Huffman, C. B.; Hauge, R. H.; Margrave, J. L., Gas-Phase Purification of Single-Wall Carbon Nanotubes. *Chem. Mater.* **2000,** 12, (5), 1361-1366.

5. Monthioux, M.; Smith, B. W.; Burteaux, B.; Claye, A.; Fischer, J. E.; Luzzi, D. E., Sensitivity of Single-Wall Carbon Nanotubes to Chemical Processing: An Electron Microscopy Investigation. *Carbon* **2001,** 39, 1251-1272.

6. Arepalli, S.; Nikolaev, P.; Gorelik, O. P.; Nadjiev, V. G.; Holmes, W.; Files, B.; Yowell, L., Protocol for the Characterization of Single-Wall Carbon Nanotube Material Quality. *Carbon* **2004,** 42, (8-9), 1783-1791.

7. Arepalli, S.; Nikolaev, P.; Gorelik, O.; Hadjiev, V. G.; Bradlev, H. A.; Holmes, W.; Files, B.; Yowell, L., Protocol for the Characterization of Single-Wall Carbon Nanotube Material Quality. *Carbon* **2004,** 42, (8-9), 1783-1791.

8. Lian, Y.; Maeda, Y.; Wakahara, T.; Akasaka, T.; Kazaoui, S.; Minami, N.; Shimizu, T.; Choi, N.; Tokumoto, H., Nondestructive and High-Recovery-Yield Purification of Single-Walled Carbon Nanotubes by Chemical Functionalization. *J. Phys. Chem. B* **2004,** 108, (26), 8848-8854.

9. Fang, H. T.; Liu, C. G.; Chang, L.; Feng, L.; Min, L.; Cheng, H. M., Purification of Single-Wall Carbon Nanotubes by Electrochemical Oxidation. *Chem. Mater.* **2004,** 16, (26), 5744-5750.

10. Kim, Y.; Luzzi, D. E., Purification of Pulsed Laser Synthesized Single Wall Carbon Nanotubes by Magnetic Filtration. *J. Phys. Chem. B* **2005,** 109, (35), 16636-16643.

11. Vivekchand, S. R. C.; Jayakanth, R.; Govindaraj, A.; Rao, C. N. R., The problem of Purifying Single-Walled Carbon Nanotubes. *Small* **2005,** 1, (10), 920-923.

12. Yang, C. M.; Park, J. S.; An, K. H.; Lim, S. C.; Seo, K.; Kim, B.; Park, K. A.; Han, S.; Park, C. Y.; Lee, Y. H., Selective Removal of Metallic Single-Walled Carbon Nanotubes with Small Diameters by using Nitric and Sulfuric Acids. *J. Phys. Chem. B* **2005,** 109, (41), 19242-19248.

13. Park, T. J.; Banerjee, S.; Hemraj-Benny, T.; Wong, S. S., Purification Strategies and Purity Visualization Techniques for Single-Walled Carbon Nanotubes. *J. Mater. Chem.* **2006,** 16, (2), 141-154.

14. Tobias, G.; Shao, L. D.; Salzmann, C. G.; Huh, Y.; Green, M. L. H., Purification and Opening of Carbon Nanotubes using Steam. *J. Phys. Chem. B* **2006,** 110, (45), 22318-22322.

15. Chen, Y. H.; Iqbal, Z.; Mitra, S., Microwave-Induced Controlled Purification of Single-Walled Carbon Nanotubes Without Sidewall Functionalization. *Adv. Mater.* **2007,** 17, (18), 3946-3951.

16. Tchoul, M. N.; Ford, W. T.; Lolli, G.; Resasco, D. E.; Arepalli, S., Effect of Mild Nitric Acid Oxidation on Dispersability, Size, and Structure of Single-Walled Carbon Nanotubes. *Chem. Mater.* **2007,** 19, (23), 5765-5772.

17. Nikolaev, P.; Gorelik, O.; Allada, R. K.; Sosa, E.; Arepalli, S.; Yowell, L., Soft-Bake Purification of Single-Walled Carbon Nanotubes Produced by Pulsed Laser Vaporizationt. *J. Phys. Chem. C* **2007,** 111, (48), 17678-17683.

18. Wang, Y. H.; Shan, H. W.; Hauge, R. H.; Pasquali, M.; Smalley, R. E., A Highly Selective, One-pot Purification Method for Single-walled Carbon Nanotubes. *J. Phys. Chem. B* **2007,** 111, (6), 1249-1252.

19. Giles, J., Growing Nanotech Trade Hit by Questions Over Quality. *Nature* **2005,** 432, 791.

20. Haddon, R. C.; Sippel, J.; Rinzler, A. G.; Papadimitrakopoulos, F., Purification and Separation of Carbon Nanotubes. *MRS Bull.* **2004,** 29, 252-259.

21. Itkis, M. E.; Perea, D.; Jung, R.; Niyogi, S.; Haddon, R. C., Comparison of Analytical Techniques for Purity Evaluation of Single-Walled Carbon Nanotubes. *J. Am. Chem. Soc.* **2005,** 127, 3439-3448.

22. Hu, H.; Zhao, B.; Itkis, M. E.; Haddon, R. C., Nitric Acid Purification of Single-Walled Carbon Nanotubes. *J. Phys. Chem. B* **2003,** 107, 13838-13842.

23. Hamon, M. A.; Hu, H.; Bhowmik, P.; Niyogi, S.; Zhao, B.; Itkis, M. E.; Haddon, R. C., End-Group and Defect Analysis of Soluble Single-Walled Carbon Nanotubes. *Chem. Phys. Lett.* **2001,** 347, (1-3), 8-12.

24. Hu, H.; Bhowmik, P.; Zhao, B.; Hamon, M. A.; Itkis, M. E.; Haddon, R. C., Determination of the Acidic Sites of Purified Single-Walled Carbon Nanotubes by Acid-Base Titration. *Chem. Phys. Lett.* **2001,** 345, 25-28.

25. Hamon, M. A.; Hu, H.; Bhowmik, P.; Itkis, M. E.; Haddon, R. C., Ester-Functionalized Soluble Single-Walled Carbon Nanotubes. *Appl. Phys. A* **2002,** 74, 333-338.

26. Chen, J.; Hamon, M. A.; Hu, H.; Chen, Y.; Rao, A. M.; Eklund, P. C.; Haddon, R. C., Solution Properties of Single-Walled Carbon Nanotubes. *Science* **1998,** 282, 95-98.

27. Hamon, M. A.; Itkis, M. E.; Niyogi, S.; Alvaraez, T.; Kuper, C.; Menon, M.; Haddon, R. C., Effect of Rehybridization on the Electronic Structure of Single-Walled Carbon Nanotubes. *J. Am. Chem. Soc.* **2001,** 123, 11292-11293.

28. Niyogi, S.; Hu, H.; Hamon, M. A.; Bhowmik, P.; Zhao, B.; Rozenzhak, S. M.; Chen, J.; Itkis, M. E.; Meier, M. S.; Haddon, R. C., Chromatographic Purification of Soluble Single-Walled Carbon Nanotubes (s-SWNTs). *J. Am. Chem. Soc.* **2001,** 123, 733-734.

29. Zhao, B.; Hu, H.; Niyogi, S.; Itkis, M. E.; Hamon, M.; Bhowmik, P.; Meier, M. S.; Haddon, R. C., Chromatographic Purification and Properties of Soluble Single Walled Carbon Nanotubes. *J. Am. Chem. Soc.* **2001,** 123, 11673-11677.

30. Salzmann, C. G.; Llewellyn, S. A.; Tobias, G.; Ward, M. A. H.; Huh, Y.; Green, M. L. H., The Role of Carboxylated Carbonaceous Fragments in the Functionalization and Spectroscopy of a Single-Walled Carbon-Nanotube Material. *Adv. Mater.* **2007,** 19, (6), 883-887.

31. Yu, H.; Jin, Y. G.; Peng, F.; Wang, H. J.; Yang, J., Kinetically Controlled Side-Wall Functionalization of Carbon Nanotubes by Nitric Acid Oxidation. *J. Phys. Chem. C* **2008,** 112, (17), 6758-6763.

32. Fogden, S.; Verdejo, R.; Cottam, B.; Shaffer, M., Purification of Single Walled Carbon Nanotubes: The Problem with Oxidation Debris. *Chem. Phys. Lett.* **2008,** 460, (1-3), 162-167.

33. Wang, Z.; Shirley, M. D.; Meikle, S. T.; Whitby, R. L. D.; Mikhalovsky, S., The Surface Acidity of Acid Oxidised Multi-walled Carbon Nanotubes and the Influence of In-situ Generated Fulvic Acids on their Stability in Aqueous Dispersions. *Carbon* **2009,** 47, (1), 73-79.

34. Price, B. K.; Lomeda, J. R.; Tour, J. M., Aggressively Oxidized Ultra-Short Single-Walled Carbon Nanotubes Having Oxidized Sidewalls. *Chem. Mater.* **2009,** 21, (17), 3917-3923.

35. Georgakilas, V.; Kordatos, K.; Prato, M.; Guldi, D. M.; Holzinger, M.; Hirsch, A., Organic Functionalization of Carbon Nanotubes. *J. Am. Chem. Soc.* **2002,** 124, (5), 760-761.

36. Sun, Y. P.; Fu, K.; Huang, W., Functionalized Carbon Nanotubes: Properties and Applications. *Acc. Chem. Res.* **2002,** 35, 1096-1104.

37. Saini, R. K.; Chiang, I. W.; Peng, H.; Smalley, R. E.; Billups, W. E.; Hauge, R. H.; Margrave, J. L., Covalent Sidewall Functionalization of Single Wall Carbon Nanotubes. *J. Am. Chem. Soc.* **2003,** 125, 3617-3621.

38. Dyke, C. A.; Tour, J. M., Covalent Functionalization of Single-Walled Carbon Nanotubes for Materials Applications. *J. Phys. Chem. A* **2004,** 108, (51), 11151-11159.

39. Chattopadhyay, J.; de Jesus Cortez, F.; Chakraborty, S.; Slater, N. K. H.; Billups, W. E., Synthesis of Water-Soluble PEGylated Single-Walled Carbon Nanotubes. *Chem. Mater.* **2006,** 18, (25), 5864-5868.

40. Tasis, D.; Tagmatarchis, N.; Bianco, A.; Prato, M., Chemistry of Carbon Nanotubes. *Chem. Rev.* **2006,** 106, (3), 1105-1136.

41. Chen, R. J.; Zhang, Y. G.; Wang, D. W.; Dai, H. J., Noncovalent Sidewall Functionalization of Single-Walled Carbon Nanotubes for Protein Immobilization. *J. Am. Chem. Soc.* **2001,** 123, (16), 3838-3839.

42. Chen, J.; Liu, H.; Weimer, W. A.; Halls, M. D.; Waldeck, D. H.; Walker, G. C., Noncovalent Engineering of Carbon Nanotube Surfaces by Rigid,

Functional Conjugated Polymers. *J. Am. Chem. Soc.* **2002,** 124, (31), 9034-9035.

43. Zheng, M.; Jagota, A.; Semke, E. D.; Diner, B. A.; McLean, R. S.; Lustig, S. R.; Richardson, R. E.; Tassi, N. G., DNA-Assisted Dispersion and Separation of Carbon Nanotubes. *Nat. Mater.* **2003,** 2, 338-342.

44. Zheng, M.; Jagota, A.; Strano, M. S.; Santos, A. P.; Barone, P.; Chou, S. G.; Diner, B. A.; Dresselhaus, M. S.; Mclean, R. S.; Onoa, G. B.; Samsonidze, G. G.; Semke, E. D.; Usrey, M. L.; Walls, D. J., Structure-Based Carbon Nanotube Sorting by Sequence-Dependent DNA Assembly. *Science* **2003,** 302, 1545-1548.

45. Chattopadhyay, D.; Galeska, I.; Papadimitrakopoulos, F., A Route for Bulk Separation of Semiconducting from Metallic Single-Wall Carbon Nanotubes. *J. Am. Chem. Soc.* **2003,** 125, (11), 3370-3375.

46. Strano, M. S.; Zheng, M.; Jagota, A.; Onoa, G. B.; Heller, D. A.; Barone, P. W.; Usrey, M. L., Understanding the Nature of the DNA-Assisted Separation of Single-Walled Carbon Nanotubes Using Fluorescence and Raman Spectroscopy. *Nano Lett.* **2004,** 4, (4), 543-550.

47. Li, H. P.; Zhou, B.; Lin, Y.; Gu, L. R.; Wang, W.; Fernando, K. A. S.; Kumar, S.; Allard, L. F.; Sun, Y. P., Selective interactions of porphyrins with semiconducting single-walled carbon nanotubes. *J. Am. Chem. Soc.* **2004,** 126, (4), 1014-1015.

48. Ju, S. Y.; Utz, M.; Papadimitrakopoulos, F., Enrichment Mechanism of Semiconducting Single-Walled Carbon Nanotubes by Surfactant Amines. *J. Am. Chem. Soc.* **2009,** 131, (19), 6775-6784.

49. Bower, C.; Kleinhammes, A.; Wu, Y.; Zhou, O., Intercalation and Partial Exfoliation of Single-Walled Carbon Nanotubes by Nitric Acid. *Chem. Phys. Lett.* **1998,** 288, 481-486.

50. Hu, H.; Yu, A.; Kim, E.; Zhao, B.; Itkis, M. E.; Bekyarova, E.; Haddon, R. C., Influence of the Zeta Potential on the Dispersability and Purification of Single-Walled Carbon Nanotubes. *J. Phys. Chem. B* **2005,** 109, 11520-11524.

51. Yu, A.; Bekyarova, E.; Itkis, M. E.; Fakhrutdinov, D.; Webster, R.; Haddon, R. C., Application of Centrifugation to the Large-Scale Purification of Electric Arc Produced Single-Walled Carbon Nanotubes. *J. Am. Chem. Soc.* **2006,** 128, (30), 9902-9908.

52. Wu, Z. H.; Pittman, C. U.; Gardner, S. D., Nitric-Acid Oxidation of Carbon-Fibers and the Effects of Subsequent Treatment in Refluxing Aqueous NaOH. *Carbon* **1995,** 33, (5), 597-605.

53. Zhao, B.; Itkis, M. E.; Niyogi, S.; Hu, H.; Perea, D.; Haddon, R. C., Extinction Coefficients and Purity of Single-Walled Carbon Nanotubes. *J. Nanosci. Nanotechnol.* **2004,** 4, 995-1004.

54. Itkis, M. E.; Perea, D.; Niyogi, S.; Rickard, S.; Hamon, M.; Hu, H.; Zhao, B.; Haddon, R. C., Purity Evaluation of As-Prepared Single-Walled Carbon Nanotube Soot by Use of Solution Phase Near-IR Spectroscopy. *Nano Lett.* **2003,** 3, 309-314.

55. Zhao, B.; Itkis, M. E.; Niyogi, S.; Hu, H.; Zhang, J.; Haddon, R. C., Study of the Extinction Coefficients of Single-Walled Carbon Nanotubes and Related Carbon Materials. *J. Phys. Chem. B* **2004,** 108, 8136-8141.

56. Hamon, M. A.; Chen, J.; Hu, H.; Chen, Y.; Itkis, M. E.; Rao, A. M.; Eklund, P. C.; Haddon, R. C., Dissolution of Single-Walled Carbon Nanotubes. *Adv. Mater.* **1999,** 11, 834-840.

57. Hu, H.; Zhao, B.; Hamon, M. A.; Kamaras, K.; Itkis, M. E.; Haddon, R. C., Sidewall Functionalization of Single-Walled Carbon Nanotubes by Addition of Dichlorocarbene. *J. Am. Chem. Soc.* **2003,** 125, 14893-14900.

58. Niyogi, S.; Hamon, M. A.; Hu, H.; Zhao, B.; Bhowmik, P.; Sen, R.; Itkis, M. E.; Haddon, R. C., Chemistry of Single-Walled Carbon Nanotubes. *Acc. Chem. Res.* **2002,** 35, 1105-1113.

59. Fuente, E.; Menendez, J. A.; Diez, M. A.; Suarez, D.; Montes-Moran, M. A., Infrared Spectroscopy of Carbon Materials: A Quantum Chemical Study of Model Compounds. *J. Phys. Chem. B* **2003,** 107, (26), 6350-6359.

60. Trigueiro, J. P. C.; Silva, G. G.; Lavall, R. L.; Furtado, C. A.; Oliveira, S.; Ferlauto, A. S.; Lacerda, R. G.; Ladeira, L. O.; Liu, J. W.; Frost, R. L.;

George, G. A., Purity Evaluation of Carbon Nanotube Materials by Thermogravimetric, TEM, and SEM Methods. *J. Nanosci. Nanotechnol.* **2007,** 7, (10), 3477-3486.

61. Boehm, H. P., Some Apects of the Surface Chemistry of Carbon Blacks and Other Carbons. *Carbon* **1994,** 32, 759-769.

62. Bonifazi, D.; Nacci, C.; Marega, R.; Campidelli, S.; Ceballos, G.; Modesti, S.; Meneghetti, M.; Prato, M., Microscopic and Spectroscopic Characterization of Paintbrush-like Single-Walled Carbon Nanotubes. *Nano Lett.* **2006,** 6, (7), 1408-1414.

Chapter 5

Soluble Graphene Derived from Graphite Fluoride

5.1 Introduction

The unique sp^2 structure of covalent carbon-carbon lattice, graphene, serves as the building block for several forms of carbon materials including graphite, and multi- and single-walled carbon nanotubes. The strong covalent bonds between carbon atoms provide graphene with high mechanical, thermal and chemical stability. It is considered to be one of the strongest known materials per unit weight with a theoretical Young's modulus of 1060 GPa[1] and also conducts electricity through the π-electron cloud resulting in a wide range of applications with great promise for quantum electronics.[2-5]

In the normal 3-D form of graphite the graphene sheets stack to produce an insoluble material that is difficult to process; solution phase manipulation of carbon based materials such as carbon nanotubes,[6-11] have already been demonstrated through chemical functionalization reactions. Recently, similar

chemical functionalization reactions of graphene layers have been attempted by several research groups in order to solubilize graphene sheets.[12, 13]

Exfoliation of graphite is necessary for the production of graphene sheets that are desirable for the fabrication of nanocomposites and electronic devices. Separation of the graphene layers is currently accomplished by intercalation of graphite with acid or alkali metals followed by an exfoliation step,[14, 15] but exfoliated graphite does not disperse in organic solvents and re-aggregates readily. Functionalization of the basal plane is necessary to increase the solubility and prevent the formation of $\pi-\pi$ interactions and scrolling.[15] Such functionalization can also result in the loss of the intrinsic electronic properties upon the formation of sp^3 carbon centers, although in some cases the electronic properties of the functionalized graphene could be recovered by simple reduction or annealing.[13] Covalent intercalation compounds of graphite such as graphite oxide and graphite fluoride are appropriate starting materials for this approach and recently, the potential of graphite oxide has been demonstrated in several reports.[16-18] This chapter will discuss the production of functionalized graphene layers starting from an alternate precursor: graphite fluoride. Characterization by use of spectroscopic and microscopic techniques will give evidence for production of the structures given below.

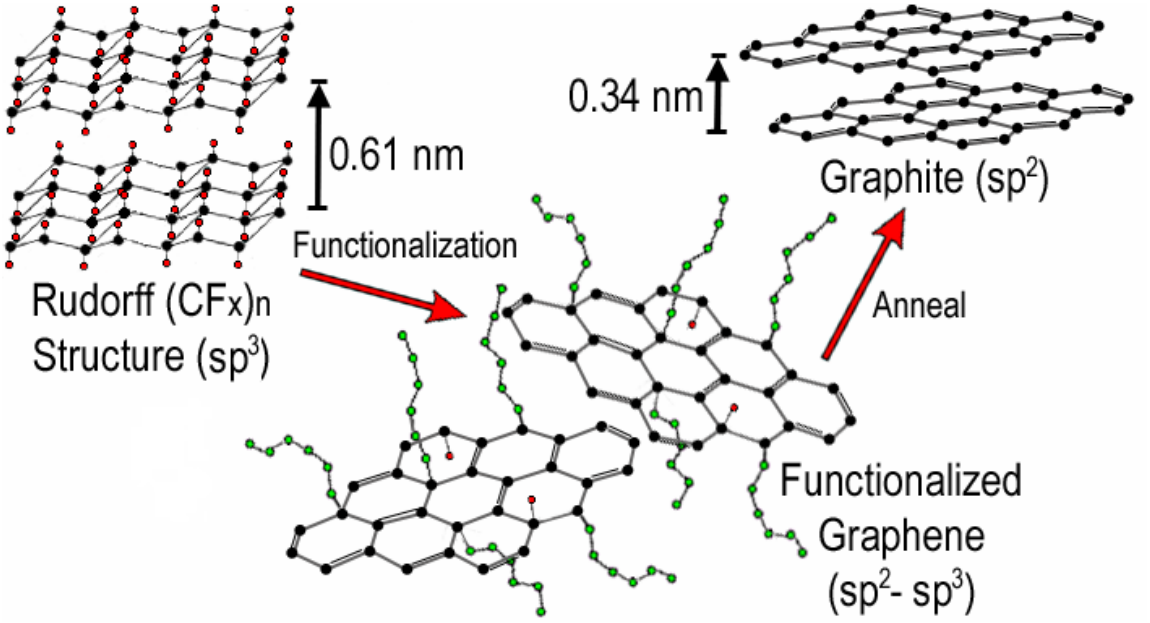

Figure 5.1: Schematic of reaction pathway.

5.2 Experimental Methods

5.2.1 Synthesis of Functionalized Graphene

Graphite fluorides and the alkyl lithium reagents were purchased from Alfa Aesar and were used as received. Tetramethylethylenediamine (TMEDA) (Aldrich) was distilled from KOH and stored in a glove box. All reactions were carried out in an oven-dried, two-necked round bottom flask, fitted with a reflux condenser under argon atmosphere. Before each reaction, 100 mg (2.3, 3.2, 3.4 mmols of F in $(CF_x)_n$, where x = 0.5, 1.0, 1.2, respectively) of graphite fluoride, was placed under vacuum for three hours in a round bottom flask and heated to remove moisture. A mixture of TMEDA (2.5 equiv.; 5.8, 8.1, 8.6 mmols) in 30 mL

hexane was added and the resulting black solution was stirred for one hour. The reaction temperature was lowered to 0 ºC with an ice bath and the alkyl-lithium reagent (1.25 equiv; 2.9, 4.0, 4.3 mmols) added drop wise; after stirring for 1 hour the reaction was allowed to come to room temperature. After stirring for 3 days the reaction was quenched with 5 mL of isopropanol, and then diluted to 100 mL with ethanol. The product was filtered using a 0.2 μm GTTP millipore filter paper giving a solid black powder which was dispersed by sonication in 100 mL of ethanol and then filtered two more times. The reaction scheme[19] for the various graphite fluorides is given below; the products are denoted as R-CF_x, where x corresponds to the composition of the starting graphite fluoride and R to the alkyl group in the R-Li reagent used for functionalization. The reaction proceeds by two reaction pathways (Figure 5.2): the alkyl lithium reagent both replaces fluorine by alkyl groups and introduces additional double bonds by eliminating molecular fluorine; thus in general $z < x - y$.

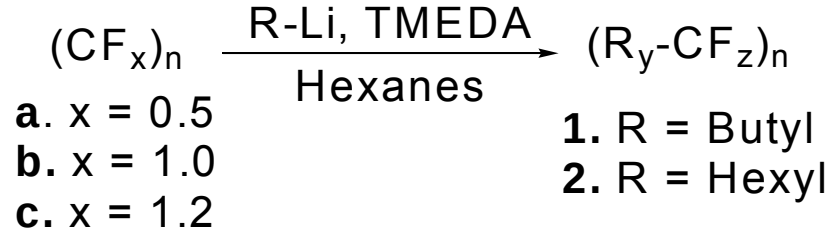

Figure 5.2: Reaction procedure of the formation of functionalized graphene.

5.2.2 Characterization

AFM images of freshly prepared samples were obtained on a Digital Instruments Nanoscope (IIIA), operating in tapping mode. Solutions of each product in acetone were evaporated on freshly cleaved mica substrates in air. Mid-IR spectra of the starting materials and the products were collected from a thin film on ZnSe using a Nicolet Nexus FT-IR spectrometer. Near-IR data was collected in a quartz cell of 1 cm path length on a Varian Cary 5000 spectrometer. In determining the extinction coefficient, dispersions of each product at various concentrations (0.1, 0.05, 0.025, and 0.00125 mg/mL) were prepared by diluting a 0.2 mg/mL stock solution in THF. The solubility was calculated by dispersing 30 mg of each product in 10 mL of THF for 2 minutes with sonication using a VWR Ultrasonic Bath sonicator (model 75T). Raman spectra of the starting materials and products were obtained from a Bruker RFS 100/S type FT-Raman spectrometer using a Nd-YAG laser excitation source with a wavelength of 1064 nm and a resolution of 8 cm^{-1}. XRD data was collected using a Bruker AXS D8 Advanced diffractometer using CuKα radiation (1.54 Å), with a step size of 0.05° and step time of 1 s/step.

5.3 Results and Discussion

5.3.1 AFM Characterization of Functionalized Graphene Layers

Figure 5.3A shows a representative image of Hexyl-CF_1 graphene nanoplatelets collected in amplitude mode. From a population of over 150 nanoplatelets, it was found that the average lateral size and thickness are 1.6 μm and 0.95 nm, respectively. In Figure 5.3B (height mode AFM), the roughness of the nanoplatelets is clearly visible, as expected for graphene that is highly functionalized in the basal plane.[18] Previous studies from our group have shown smooth surfaces for edge functionalized graphene nanoplatelets,[12] but the surface roughness of the current preparation is clearly depicted in the height cross-section, where maximum heights were found to be 1.7 nm (Figure 5.3A) and 1.2 nm (Figure 5.3B); areas of low functionalization are seen at lower heights with similar color to that of the background. The variability in the height may be attributed to the local degree of functionalization, with high points representing areas of the samples where the functionalization is especially dense and the hexyl groups are standing perpendicular or at a substantial angle to the graphene plane. Another possible contribution to this roughness may be the crumpling of graphene sheets.[20, 21] Also apparent in some images is an increased height in the center of many of the nanoplatelets that also appears as a rough surface and this has been previously reported as solvent trapped between the graphene layer and the substrate.[2, 12, 22]

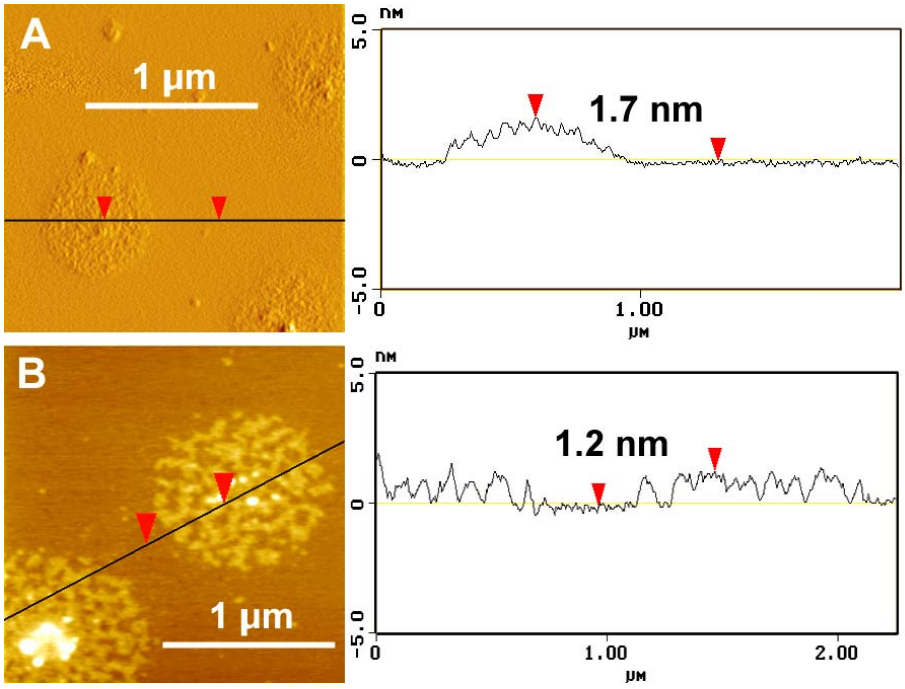

Figure 5.3: Tapping mode AFM images of soluble Hexyl-CF_1 samples on mica. A) A highly resolved image of functionalized graphene nanoplatelets (data collected in amplitude mode with a Z range = 1.5 V) and the corresponding height cross-section. Height difference between red arrows = 1.7 nm. B) A highly resolved image of 2 nanoplatelets (data collected in height mode with a Z range = 10 nm) and the corresponding height cross-section. Height difference between red arrows = 1.2 nm.

5.3.2 FT-IR Spectra of Covalently Functionalized Graphene

Each $(CF_x)_n$ starting reagent and its respective butyl and hexyl-functionalized products were further characterized by FT-IR spectroscopy. Figure 5.4A shows the spectra of $(CF_x)_n$, where x = 1, and the corresponding products: Butyl-CF_1 and Hexyl-CF_1. The strongest band at 1210 cm^{-1} in the spectrum of CF_1 is attributed to the C-F stretching vibration of the tertiary carbon atoms in the basal plane, while the weak bands located on each side of the

dominant peak, at 1340 and 1075 cm^{-1}, are the asymmetric and symmetric stretching vibrations of the peripheral $–CF_2$ groups.[23] In the spectra of the corresponding butyl and hexyl products, the signals of the C-H stretch of the alkyl groups appear in the range of 2850-3000 cm^{-1}, and bands in the 1450-1600 cm^{-1} region can be attributed to C=C stretch. The broad band at approximately 1200 cm^{-1} indicates the possible presence of residual fluorine in the products. As expected, the peaks of the C-H stretching of the hexyl products are more prominent than those of the butyl products.

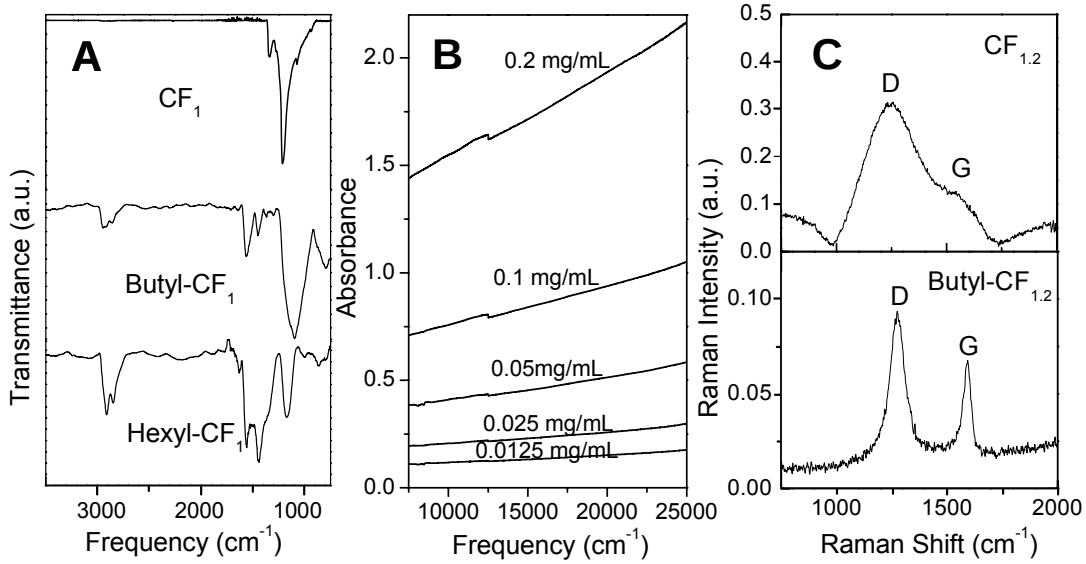

Figure 5.4: A) Baseline corrected mid IR spectra collected from thin films of CF_1 starting material, and butyl and hexyl functionalized products. B) Absorption spectra of Butyl-CF_1 from 7500-25000 cm^{-1} at various concentrations in THF. C) Raman spectra of $CF_{1.2}$ and Butyl-$CF_{1.2}$.

5.3.3 Solution Phase Characterization of Soluble Graphene Layers

In analogy to other Teflon materials, $(CF_x)_n$ is insoluble in all solvents, but the alkylated materials can be dispersed in halogenated solvents such as dichlorobenzene and dichloromethane, and THF. In all cases, solution-phase near-IR absorption spectra show a featureless monotonic spectrum that increases in intensity towards higher frequency, as seen in Figure 5.4B for Butyl-CF_1. By using Beer's law the extinction coefficient was calculated at 10000 cm^{-1} in THF (Table 5.1), and this allowed the determination of the solubility.[24] The extinction coefficient of the products was found to be $\varepsilon \approx 7$ $L.g^{-1}\cdot cm^{-1}$ at 10000 cm^{-1}; slightly higher than the ODA-functionalized graphene (3.3 L/g·cm).[12] After sonication and a 24 hour standing period, the solubility of each product was determined by spectroscopy. The hexyl products were found to be more soluble than the butyl products and the most soluble product was found to be Hexyl-CF_1 (0.54 g/L), having a solubility comparable to that of edge functionalized ODA graphene nanoplatelets (0.5 g/L).[12] The powders were found to disperse readily and were stable in solution for months.

Table 5.1: Solubility and extinction coefficients of the products at 10 000 cm^{-1} in THF.

Sample	Solubility (g/L)	Extinction Coefficient (L/g·cm)
Butyl-$CF_{0.5}$	0.002	8.5
Butyl-CF_1	0.14	7.7
Butyl-$CF_{1.2}$	0.24	6.7
Hexyl-$CF_{0.5}$	0.39	8.2
Hexyl-CF_1	0.54	8.0
Hexyl-$CF_{1.2}$	0.35	6.8

5.3.4 Raman Spectroscopic Characterization of Functionalized Graphene

As in other carbon allotropes, the Raman spectrum of $(CF_x)_n$ contains two characteristic bands: the tangential G-mode and the disorder-induced D-mode. Extensive studies have determined that the positions, intensities and widths of these bands are dependent on the ordering of the sp^2 sites in varying compositions of amorphous and crystalline carbon compounds.[25, 26] As seen in the spectrum of $CF_{1.2}$ (Figure 5.4C), both Raman modes are weak and broad due to a high level of disorder of the graphene layers. All three starting materials gave a similar spectrum, although the peak position of the G band shifted to lower frequencies with increasing fluorine content (from 1586 to 1487 cm^{-1}, Table 5.2).[27] In other work, the G band is observed as two peaks,[27, 28] but this was not observed in our studies, possibly due to the line broadening and overlap of the bands. Upon functionalization, the D and G bands sharpen, and the frequency of

the G band is shifted to 1591-1601 cm^{-1}, indicating the formation of nanocrystalline graphite.[26] A higher sp^2 content would be expected due to the formation of additional unsaturation.

Table 5.2: Raman Shifts of D and G bands.

Sample	D Band	G Band
	Raman Shift (cm^{-1})	Raman Shift (cm^{-1})
$CF_{0.5}$	1265	1568
CF_1	1237	1563
$CF_{1.2}$	1243	1487
Butyl-$CF_{0.5}$	1271	1601
Butyl-CF_1	1279	1595
Butyl-$CF_{1.2}$	1275	1593
Hexyl-$CF_{0.5}$	1266	1593
Hexyl-CF_1	1277	1591
Hexyl-$CF_{1.2}$	1279	1592

5.3.5 Dealkylation of Functionalized Graphene by Annealing

Upon annealing of the functionalized R-CF_x, the G band shifts to higher frequencies, and the ratio of the intensities (I_D/I_G) increases with graphitization (Figure 5.5). This corresponds to a transformation from amorphous to nanocrystalline graphite on the proposed amorphization trajectory.[26] X-ray diffraction patterns of starting materials show a d-spacing of 0.61 nm for the

graphite fluoride; this d_{001} value is typical of a $(CF_x)_n$ covalent stage I compound[27] and the corresponding structure was described in terms of a chair conformation.[29] Upon functionalization no peaks are found in the diffraction pattern indicating that the reaction has fully separated the nanoplatelets; on annealing, a peak corresponding to a d-spacing of 0.34 nm appears, confirming the formation of nanocrystalline graphite (Figure 5.6). Further support is provided in the IR spectra of the annealed samples, where it may be seen that the functionality is lost upon exposure to high temperatures (Figure 5.7).

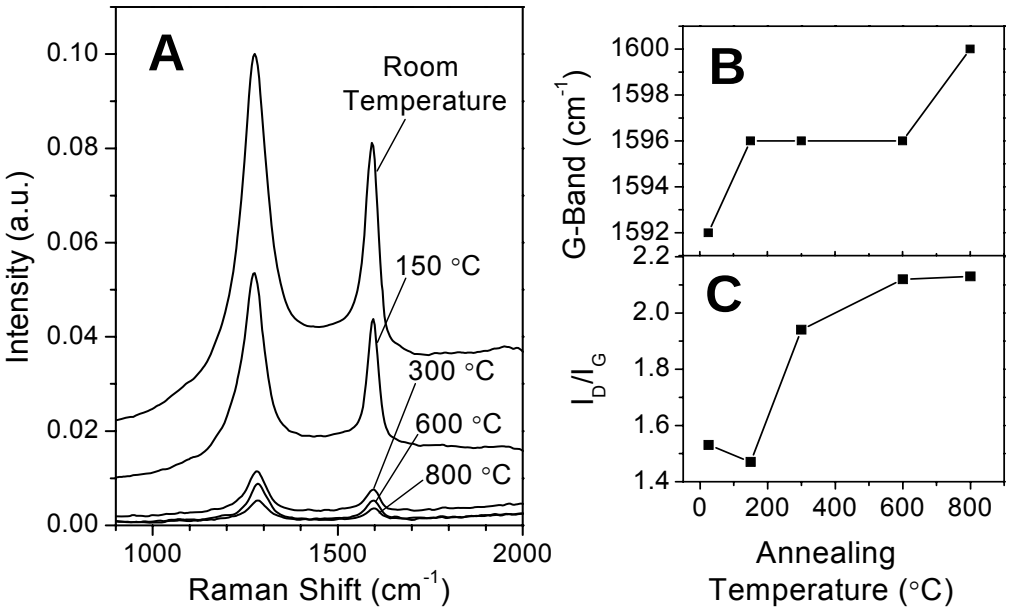

Figure 5.5: A) Raman spectra of bulk samples of Hexyl-CF_1 before and after annealing to 150, 300, 600, and 800 ºC. B) Raman shifts of the G band and, C) I_D/I_G from data collected in A.

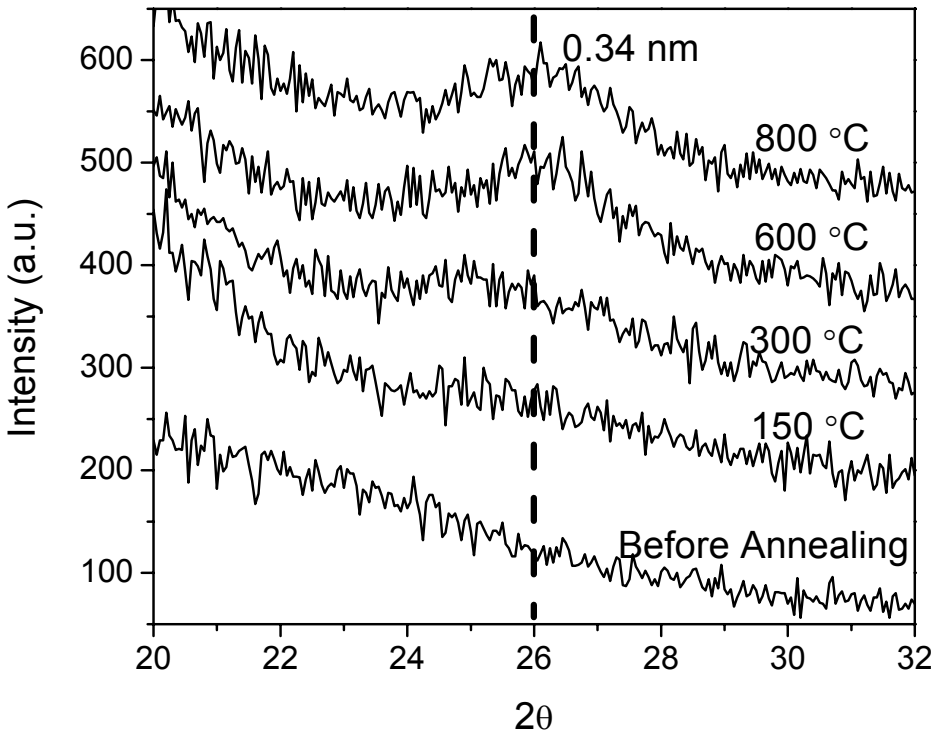

Figure 5.6: XRD patterns of a bulk powder sample of Hexyl-CF_1 before and after annealing to 150, 300, 600, and 800 ºC.

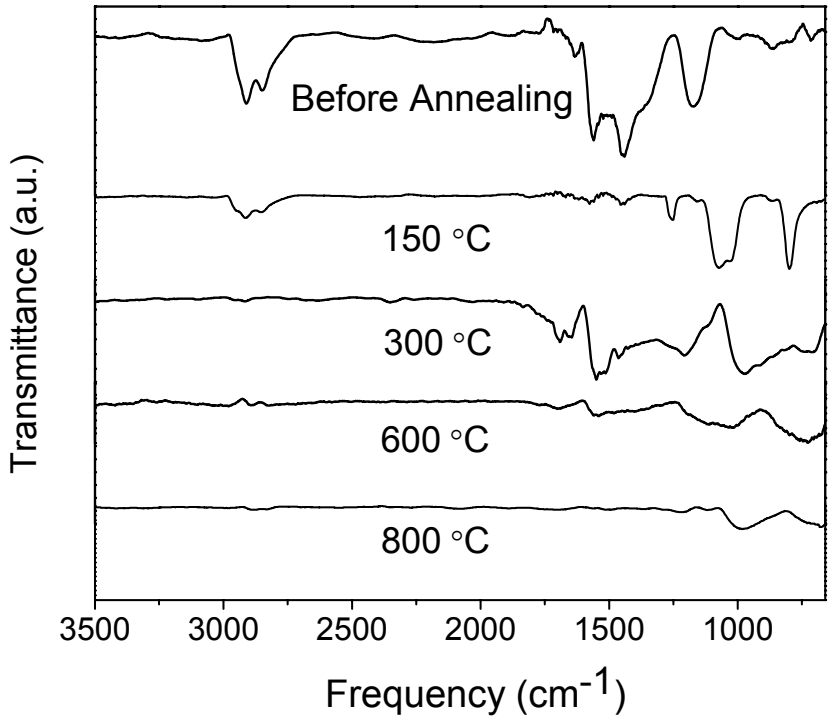

Figure 5.7: Baseline corrected mid IR spectra collected from thin films of the Hexyl-CF_1 before and after annealing to 150, 300, 600, and 800 ºC.

5.4 Conclusions

In a one-step synthesis, soluble graphene layers were formed by subjecting graphite fluoride of various stoichiometries to n-butyl or n-hexyl lithium reagents. The products were characterized using AFM, mid-infrared, UV-vis-near infrared, and Raman spectroscopy. The solubility and extinction coefficient of each product was calculated, and an extension of sp^2 character in the lattice of the products was detected. Dealkylation occurs upon annealing the bulk

samples, further extending the π-system and thus, restoring the electronic properties of the nanocrystalline graphene. Functionalized graphene layers can be readily prepared by this technique and dispersed in organic solvent and upon annealing, the intrinsic properties of the graphene layers can be partially restored.

5.5 References

1. Schadler, L. S.; Giannaris, S. C.; Ajayan, P. M., Load Transfer in Carbon Nanotube Epoxy Composites. *Appl. Phys. Lett.* **1998,** 73, 3842-3844.

2. Novoselov, K. S.; Geim, A. K.; Morozov, S. V.; Jiang, D.; Zhang, Y.; Dubonos, S. V.; Grigorieva, I. V.; Firsov, A. A., Electric Field Effect in Atomically Thin Carbon Films. *Science* **2004,** 306, 666-669.

3. Novoselov, K. S.; Geim, A. K.; Morozov, S. V.; Jiang, D.; Katsnelson, M. I.; Grigorieva, I. V.; Dubonos, S. V.; Firsov, A. A., Two-dimensional Gas of Massless Dirac Fermions in Graphene. *Nature* **2005,** 438, (7065), 197-200.

4. Berger, C.; Song, Z.; Li, T.; Li, X.; Ogbazghi, A. Y.; Feng, R.; Dai, Z.; Marchenkov, A. N.; Conrad, E. H.; First, P. N.; de Heer, W. A., Ultrathin Epitaxial Graphite: 2D Electron Gas Properties and a Route Toward Graphene-Based Nanoelectronics. *J. Phys. Chem. B* **2004,** 108, (52), 19912-19916.

5. Zhang, Y.; Tan, Y. W.; Stormer, H. L.; Kim, P., Experimental Observation of the Quantum Hall effect and Berry's Phase in Graphene. *Nature* **2005,** 438, 201-204.

6. Chen, J.; Hamon, M. A.; Hu, H.; Chen, Y.; Rao, A. M.; Eklund, P. C.; Haddon, R. C., Solution Properties of Single-Walled Carbon Nanotubes. *Science* **1998,** 282, 95-98.

7. Niyogi, S.; Hamon, M. A.; Hu, H.; Zhao, B.; Bhowmik, P.; Sen, R.; Itkis, M. E.; Haddon, R. C., Chemistry of Single-Walled Carbon Nanotubes. *Acc. Chem. Res.* **2002,** 35, 1105-1113.

8. Kelly, K. F.; Chiang, I. W.; Mickelson, E. T.; Hauge, R. H.; Margrave, J. L.; Wang, X.; Scuseria, G. E.; Radloff, C.; Halas, N. J., Insight into the Mechanism of Sidewall Functionalization of Single-Walled Nanotubes: and STM Study. *Chem. Phys. Lett.* **1999,** 313, 445-450.

9. Saini, R. K.; Chiang, I. W.; Peng, H.; Smalley, R. E.; Billups, W. E.; Hauge, R. H.; Margrave, J. L., Covalent Sidewall Functionalization of Single Wall Carbon Nanotubes. *J. Am. Chem. Soc.* **2003,** 125, 3617-3621.

10. Chen, J.; Rao, A. M.; Lyuksyutov, S.; Itkis, M. E.; Hamon, M. A.; Hu, H.; Cohn, R. W.; Eklund, P. W.; Colbert, D. T.; Smalley, R. E.; Haddon, R. C., Dissolution of Full-Length Single-Walled Carbon Nanotubes. *J. Phys. Chem. B* **2001,** 105, 2525-2528.

11. Bekyarova, E.; Davis, M.; Burch, T.; Itkis, M. E.; Zhao, B.; Sunshine, S.; Haddon, R. C., Chemically Functionalized Single-Walled Carbon Nanotubes for Ammonia Sensors. *J. Phys. Chem. B* **2004,** 108, 19717-19720.

12. Niyogi, S.; Bekyarova, E.; Itkis, M. E.; McWilliams, J. L.; Hamon, M. A.; Haddon, R. C., Solution Properties of Graphite and Graphene. *J. Am. Chem. Soc.* **2006,** 128, (24), 7720-7721.

13. Stankovich, S.; Dikin, D. A.; Dommett, G. H. B.; Kohlhaas, K. M.; Zimney, E. J.; Stach, E. A.; Piner, R. D.; Nguyen, S. T.; Ruoff, R. S., Graphene-based Composite Materials. *Nature* **2006,** 442, (7100), 282-286.

14. Ramesh, P.; Sampath, S., Electrochemical Characterization of Binderless, Recompressed Exfoliated Graphite Electrodes: Electron-transfer Kinetics and Diffusion Characteristics. *Anal. Chem.* **2003,** 75, (24), 6949-6957.

15. Viculis, L. M.; Mack, J. J.; Kaner, R. B., A Chemical Route to Carbon Nanoscrolls. *Science* **2003,** 299, (5611), 1361-1361.

16. Du, X. S.; Xiao, M.; Meng, Y. Z.; Hay, A. S., Direct synthesis of poly(arylenedisulfide)/carbon nanosheet composites via the oxidation with graphite oxide. *Carbon* **2005,** 43, (1), 195-197.

17. Stankovich, S.; Piner, R. D.; Chen, X. Q.; Wu, N. Q.; Nguyen, S. T.; Ruoff, R. S., Stable Aqueous Dispersions of Graphitic Nanoplatelets via the Reduction of Exfoliated Graphite Oxide in the Presence of Poly(sodium 4-styrenesulfonate). *J. Mater. Chem.* **2006,** 16, (2), 155-158.

18. Schniepp, H. C.; Li, J. L.; McAllister, M. J.; Sai, H.; Herrera-Alonso, M.; Adamson, D. H.; Prud'homme, R. K.; Car, R.; Saville, D. A.; Aksay, I. A., Functionalized Single Graphene Sheets Derived from Splitting Graphite Oxide. *J. Phys. Chem. B* **2006,** 110, (17), 8535-8539.

19. Mickelson, E. T.; Chiang, I. W.; Zimmerman, J. L.; Boul, P. J.; Lozano, J.; Liu, J.; Smalley, R. E.; Hauge, R. H.; Margrave, J. L., Solvation of Fluorinated Single-Wall Carbon Nanotubes in Alcohol Solvents. *J. Phys. Chem. B* **1999,** 103, 4318-4322.

20. Beckett, R. J.; Croft, R. C., The Structure of Graphite Oxide. *J. Phys. Chem.* **1952,** 56, (8), 929-935.

21. Wen, X.; Garland, C. W.; Hwa, T.; Kardar, M.; Kokufuta, E.; Li, Y.; Orkisz, M.; Tanaka, T., Crumpled and Collapsed Conformations in Graphite Oxide Membranes. *Nature* **1992,** 355, (6359), 426-428.

22. Jeong, S. K.; Inaba, M.; Iriyama, Y.; Abe, T.; Ogumi, Z., AFM Study of Surface Film Formation on a Composite Graphite Electrode in Lithium-Ion Batteries. *J. Power Sources* **2003,** 119, 555-560.

23. Kita, Y.; Watanabe, N.; Fujii, Y., Chemical Composition and Crystal Structure of Graphite Fluoride. *J. Am. Chem. Soc.* **1979,** 101, (14), 3832-3841.

24. Zhao, B.; Itkis, M. E.; Niyogi, S.; Hu, H.; Zhang, J.; Haddon, R. C., Study of the Extinction Coefficients of Single-Walled Carbon Nanotubes and Related Carbon Materials. *J. Phys. Chem. B* **2004,** 108, 8136-8141.

25. Tuinstra, F.; Koenig, J. L., Raman Spectrum of Graphite. *J. Chem. Phys.* **1970,** 53, (3), 1126-1130.

26. Ferrari, A. C.; Robertson, J., Interpretation of Raman spectra of disordered and amorphous carbon. *Phys. Rev. B* **2000,** 61, (20), 14095-14107.

27. Rao, A. M.; Fung, A. W. P.; Divittorio, S. L.; Dresselhaus, M. S.; Dresselhaus, G.; Endo, M.; Oshida, K.; Nakajima, T., Raman-Scattering and Transmission-Electron-Microscopy Studies of Fluorine-Intercalated Graphite Fibers CxF (7.8 ≥ x ≥ 2.9). *Phys. Rev. B* **1992,** 45, (12), 6883-6892.

28. Gupta, V.; Nakajima, T.; Ohzawa, Y.; Zemva, B., A Study on the Formation Mechanism of Graphite Fluorides by Raman Spectroscopy. *J. Fluorine Chem.* **2003,** 120, (2), 143-150.

29. Rudorff, W.; Rudorff, G., Zur Konstitution Des Kohlenstoff-Monofluorids. *Z. Anorg. Allg. Chem.* **1947,** 253, (5-6), 281-296.

Chapter 6

Conclusions

Graphitic carbon materials such as SWNTs and graphene exhibit exceptional properties. Their sp^2 hybridized framework, can be modified by functionalization, which can render the material soluble in aqueous or organic solvents leading to their exploitation in various applications. This dissertation has focused on the preparation and processing of these materials in order to optimize their performance.

Nitric acid purification of SWNTs results in the generation of oxygen functionality and carboxylated carbons (CCs). A mild base treatment using dilute NH_4OH is an effective technique for the removal of CCs. Upon their isolation, they could be characterized as a bulk material and were discovered to be composed of highly functionalized polycyclic material.

The extracted CCs of low molecular weights were identified after converting them to their methylated form. They were determined to be comprised of small benzopolycarboxylic acids and organic nitro compounds. The majority of the identified material has been seen in previous literature for oxidized

coal, and the yield of each compound was roughly estimated although this result is highly dependent on the starting SWNT sample, the nitric acid reaction conditions and overall processing of the material.

After exhaustive base washing and the removal of the CCs, the remaining SWNTs were observed to contain detectable amounts of acid functionality which are available for covalent chemical functionalization. Functionalization with octadecylamine was shown to produce material that is soluble in organic solvents.

In a one-step synthesis, soluble graphene layers were formed by subjecting graphite fluoride to alkyl lithium reagents. The products were fully characterized and the solubility was determined. Dealkylation occurs upon annealing, further extending the π-system and partially restoring the electronic properties of the nanocrystalline graphene. Functionalized graphene layers can be readily prepared by this technique.

Future work would involve the testing of these materials as thin films or composites in applications such as sensors, fuel cells or other devices and comparing them to other materials.